6th International PhD Symposium in Civil Engineering

23-26 August 2006, Institute of Structural Engineering ETH Zurich

Originally published in:
IBK Publikation SP 15

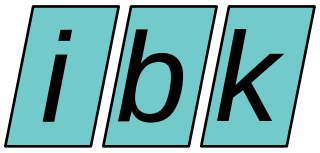

6th International PhD Symposium in Civil Engineering

23-26 August 2006

Institute of Structural Engineering ETH Zurich

Edited by

Thomas Vogel
Nebojša Mojsilović
Peter Marti

Table of Contents

Preface

The International PhD Symposium exists now for a decade and has become a milestone in both the agenda of the civil engineering community and the curricula of many PhD students. It is an honour to be the host of this distinguished event, and we shall do our best to assure its continued success. Compared to the last Symposium in Delft, we are focussing the covered areas on structural engineering, including the three sub themes *structural analysis and design*, *concrete and masonry structures*, and *steel, timber and composite structures*, and its neighbouring disciplines, *building materials* and *geotechnical engineering*.

The PhD Symposium serves as a forum for international scientific discussion in civil engineering. PhD students have the opportunity to present their work either at the beginning of their thesis, discussing the research plan, or at a later stage, showing preliminary or final results. By a tough review of both the abstracts and the full papers a high quality level could be set and useful hints were given to improve the legibility and accuracy of the contributions. The efforts of the members of the Scientific Committee who completed these tasks are gratefully acknowledged.

The Scientific Committee selected 121 contributions out of 140 abstracts to be presented. Finally, 81 of them were submitted as a final paper of up to 8 pages and 75 of those have been accepted for printing and oral presentation. Following the general trend of reducing paper consumption and printing costs only extended abstracts have been published as printed proceedings. The full length papers have been stored on a CD-ROM, being an integral part of the proceedings. Compared to previous symposia, the attendance is considerably smaller. We see this positively as an indication that in the meantime, many other congress organisers encourage young researchers to participate and to present their work on their own, even if they have a senior co-author. For the organisation the smaller number of participants also has advantages. By keeping the planned five half days of presentations, only two parallel sessions are needed. This facilitates the overview on all presentations and a fair rating for the awards.

To host this symposium would not have been possible without the generous support of ETH Zurich. The entire necessary infrastructure is at our disposal for free and two funds supervised by the rector of ETH Zurich donated considerable sums. Our main sponsor, the Civil Engineering Group of the Swiss Society of Engineers and Architects (SIA), donated the whole prize money for the awards and the other sponsors (see page 17) helped to cover other expenses. In this way, we succeeded in reducing the conference fee to a moderate level.

Many thanks to all other persons and institutions not mentioned individually and to the Organising Committee that helped to make this event a success.

Zurich, August 2006

The Editors:
Thomas Vogel
Nebojša Mojsilović
Peter Marti

International PhD Symposia in Civil Engineering

28-31 May 1996
Budapest University of Technology and Economics – Budapest
G.L. Balázs (editor)

26-28 August 1998
Budapest University of Technology and Economics – Budapest
G.L. Balázs (editor)

5-7 October 2000
University of Natural Resources and Applied Life Sciences, Vienna
K. Bergmeister (editor)

19-21 September 2002
Technische Universität München – Munich
P. Schießl, N. Gebbeke, W. Kreuser, K. Zilch (editors)

16-19 June 2004
Delft University of Technology – Delft
J. Walraven, J. Blaauwendraad, T. Scarpas, B. Snijder (editors)

23-26 August 2006
ETH Zurich – Zurich
T. Vogel, N. Mojsilović, P. Marti (editors)

Universities/Institutions and Countries

University of New South Wales	Australia
The University of Technology Sydney	Australia
Vienna University of Technology	Austria
Ghent University	Belgium
Hohai University	China
Brno University of Technology	Czech Republic
Technical University of Denmark (DTU)	Denmark
University of Stuttgart	Germany
Technical University of Munich	Germany
University of Karlsruhe	Germany
RWTH Aachen University	Germany
Technical University of Hamburg-Harburg	Germany
University of Patras	Greece
Budapest University of Technology and Economics	Hungary
University of Pécs	Hungary
Università IUAV Venezia	Italy
Politecnico di Torino	Italy
University of Brescia	Italy
University of Catania	Italy
University of Tokyo	Japan
Poznan University of Technology	Poland
Silesian University of Technology	Poland
Technical University of Lisboa	Portugal
University of Porto	Portugal
Royal Institute of Technology in Stockholm	Sweden
ETH Zurich	Switzerland
École Polytechnique Fédérale de Lausanne (EPFL)	Switzerland
Delft University of Technology	The Netherlands
Loughborough University	United Kingdom

Organisation

Scientific Committee

Chairman: Peter Marti, Switzerland

Secretary: Nebojša Mojsilović, Switzerland

Andrzej B. Ajdukiewicz, Poland
György L. Balázs, Hungary
Michael F. Bartlett, Canada
Konrad Bergmeister, Austria
Fernando A. Branco, Portugal
Eugen Brühwiler, Switzerland
Chris J. Burgoyne, United Kingdom
Gian Michele Calvi, Italy
Joan R. Casas, Spain
Hugo Corres Peiretti, Spain
Alessandro Dazio, Switzerland
Rolf Eligehausen, Germany
Michael H. Faber, Switzerland
Michael N. Fardis, Greece
Jürgen Feix, Austria
Josef Fink, Austria
Mario Fontana, Switzerland
Stephen J. Foster, Australia
Thomas Keller, Switzerland
Johann Kollegger, Austria
Ulrike Kuhlmann, Germany
Massimo Laffranchi, Switzerland
Koichi Maekawa, Japan
Giuseppe Mancini, Italy
Marco Menegotto, Italy
Jan G.M. van Mier, Switzerland
Harald S. Müller, Germany
Aurelio Muttoni, Switzerland
David A. Nethercot, United Kingdom
Hans-Wolf Reinhardt, Germany
Viktor B. Sigrist, Germany
Johan Silfwerbrand, Sweden
Enzo Siviero, Italy
Sarah M. Springman, Switzerland
Luc Taerwe, Belgium
Miha Tomazevic, Slovenia
Frank J. Vecchio, Canada
Jan L. Vitek, Czech Republic
Thomas Vogel, Switzerland
Laurent Vulliet, Switzerland
Joost C. Walraven, The Netherlands

Organising Committee

Chairman: Thomas Vogel, Switzerland

Secretary: Nebojša Mojsilović, Switzerland

Renate Amatore, Switzerland
Natalie Ammann, Switzerland
Markus Baumann, Switzerland
Alessandro Dazio, Switzerland
Emil Honegger, Switzerland
Peter Marti, Switzerland
Orlando Monsch, Switzerland
Regina C. Nöthiger, Switzerland
Roberto Pascolo, Switzerland
Hans Seelhofer, Switzerland

Sponsors

Main Sponsor

berufsgruppe ingenieurbau
groupe professionnel génie civil
sia

Swiss Society of Engineers and Architects (SIA), Civil Engineering Group (BGI)

Sponsors

Ernst & Sohn
A Wiley Company
www.ernst-und-sohn.de

Ernst & Sohn Verlag für Architektur und technische Wissenschaften GmbH

cubus
ENGINEERING SOFTWARE

CUBUS AG, Engineering Software

fbh/gpc
Fachgruppe für Brückenbau und Hochbau
Groupe spécialisé des ponts et charpentes

Swiss Society of Engineers and Architects (SIA), Structural group (FBH)

Proceedings-CD file name:
238_Aberspach.pdf

CRACK MODELLING FOR LARGE REINFORCED CONCRETE STRUCTURES

Lars Aberspach
Hamburg University of Technology, Hamburg, Germany
Viktor Sigrist, Supervisor

In recent years pier walls and foundation beams of container cranes of ports are increasingly built without expansion joints. This is due to the fact that construction and maintenance of the joints are costly and the deformation behaviour of the structures is often unsatisfactory.
It has to be admitted that structures without expansion joints are sensitive to temperature variations and settlements. Concrete technology, detailing and the construction process play an important role in building such structures successfully.

Large dimensions and complex structural geometries along with nonlinear material and soil behaviour and variable loads, such as temperature-induced strains and live loads from cranes and tidal changes, necessitate the use of computer based methods.
Models for prediction of cracking of concrete structures have to account for deformation behaviour of the structure and soil-structure interaction. This requires to take the behaviour of cracked concrete as accurately as possible into account. In this research a finite element approach is used.

As a basis for modelling reinforced concrete, the tension chord model, which incorporates an idealisation of the rather complex bond effects between reinforcing bars and concrete, is chosen. The tension chord model uses a rigid, perfectly plastic bond-stress steel-stress relationship. A stepped diagramm with a high level of bond stress in linear elastic range of reinforcement and a lower level of bond stress after the onset of yielding of reinforcement, is used. With this model problems of cracking, minimum reinforcement and deformation capacity of structural concrete members can be treated with reasonable accuracy.

Traditionally, reinforced concrete is modelled as elements with either smeared reinforcement, where concrete and steel share the same strains, or with discrete rebars, which are connected to the concrete with interface elements. The latter requires high computational effort. In this contribution a composite material element approach is introduced, consisting of solid (cracked) concrete and one ore more reinforcing bars, which do not necessarily have the same strains as the concrete.

To consider the bond effects between concrete and rebars, information about crack spacing and crack width must be provided for calculation of the relative displacement between concrete and steel bars. For this purpose, the crack width is added as a degree of freedom to the element nodes, additionally, crack spacing and crack directions are defined as nodal status variables. By knowing the crack widths, average concrete strains and steel strains in and between the cracks can be calculated with help of the basic equations of the tension chord model. The contribution of plain concrete to the element stiffness matrix is calculated with the principle of virtual work using the concrete strains. The reinforcing bars contribute to the stiffness in accordance to their position in the element.

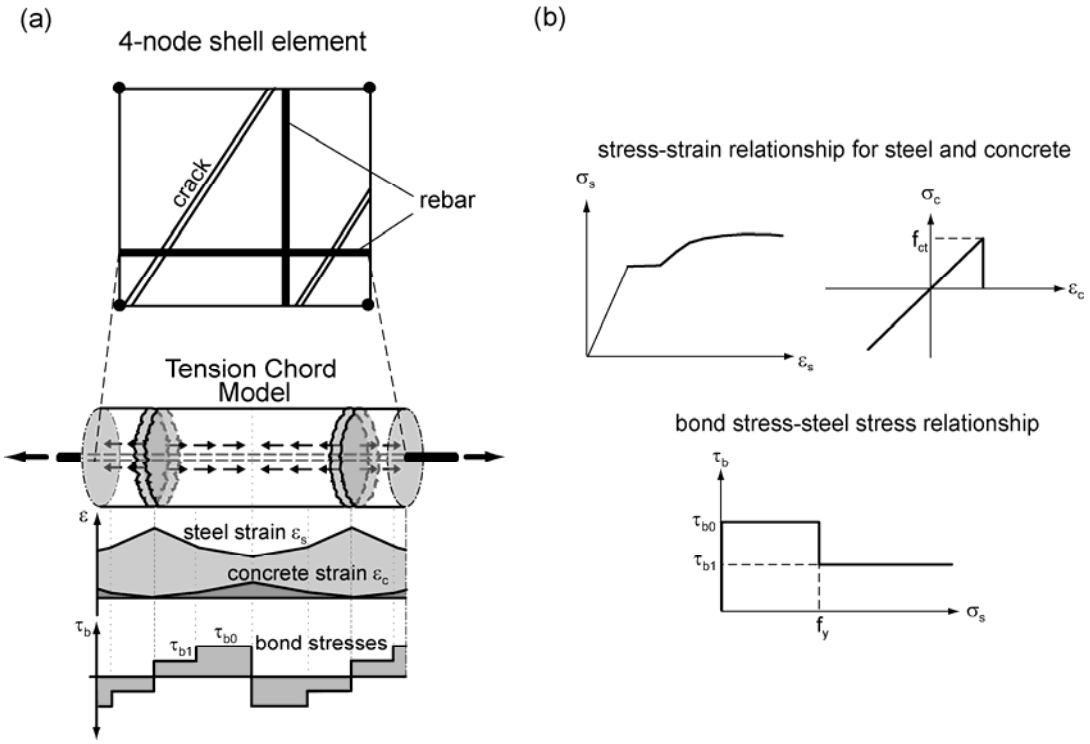

Figure 1: a) Shell element with discontinuities, tension chord model; b) Material properties

Up to now, the model has been adopted to a linear 4-node rectangular shell element, with orthogonal aligned rebars and a linear elastic behaviour of concrete between the cracks. In comparison to uniaxial tension tests sufficiently accurate results are achieved.
For the aim of treating thick-walled concrete structures such as quay constructions, a three dimensional solid element has to be developed, the soil-structure interaction as well as effects like shrinkage, creep and temperature-induced strains shall be considered.

Lars Aberspach
Hamburg University of Technology
Institute of Concrete Structures
Denickestr. 17
21071 Hamburg, Germany
lars.aberspach@tu-harburg.de

Prof. Dr. Viktor Sigrist
Hamburg University of Technology
Institute of Concrete Structures
Denickestr. 17
21071 Hamburg, Germany
sigrist@tu-harburg.de

CONCRETE CONSISTING OF HIGH STRENGTH ELEMENTS AND HARDENED CEMENT PASTE

Sebastian Zoran Ambro
Vienna University of Technology- Institute for Structural Engineering, Vienna, Austria
Johann Kollegger, Supervisor

Concrete is a material that is very strong in compression. When concrete is used in a structure to carry loads, the tensile regions are expected to crack. Compared to the compressive strength, the tensile strength is very low, the failure is strongly localized, brittle and without prior indication. Statically determinate concrete structures under bending or tensile loading fail at the initiation of the first crack. The concrete member cracks at the location with the lowest strength. The usual methods to improve the behaviour of concrete in tension are steel bar reinforcements or prestressing using steel cables. Another way of improving the tensile properties is to add fibers to the concrete mix. Steel fibers are most commonly used. The fibers are uniformly dispersed, but not oriented in the concrete. Thus only part of the fibers can be activated to carry load.
The high strength element presented in this paper is an aggregate that acts simultaneously as a reinforcing element. The shape of the element is such, that the load can be transferred from the matrix material into the reinforcing element by compressive and shear stresses. Thus, the low tensile strength in that interface is no longer relevant. It will be shown that the concrete with high strength elements has a post-cracking strength which is higher that the cracking strength.
Three different types of materials were investigated, namely epoxy resin, UHPFRC (ultra-high-performance fiber-reinforced concrete) and GFRC (glass fiber reinforced concrete). The elements made of epoxy resin have a circular cross section and a widening on both ends. The length of the element was 80 mm and the diameter in the center was 16 mm. The elements made of UHPFRC were cast in the same formwork and had therefore the same shape. The dimensions of the elements made of GFRC were slightly different from the other two elements. The cross section was square with dimensions 13x13 mm. The length was 80 mm, the same as for the other elements.
Three different types of specimens were produced and tested under four-point bending, which means that the central part is subjected to a constant moment. First, the high strength elements were put into the formwork and the cement paste was inserted afterwards. After one day the formwork was removed. At an age of 9 days the specimens were tested. The specimen dimensions were 15x15x60 cm and the span was 45 cm. The specimen dimensions and the test procedure were according to recommendations (Austrian Society for Concrete and Construction Technology, 2002).
The load was applied using a hydraulic jack and measured using a load cell. The deflection was determined in the middle of the specimen with one displacement transducer on each side. The deformation rate was 0,2 mm/min.
The load-displacement diagrams for the specimens with epoxy elements and reinforcement bars are plotted in figure 1. Before cracking the behavior is roughly the same for all specimen types. Furthermore, the load at initiation of the first crack was in a narrow range. After cracking the behavior is vastly different. For all specimens the load increased after cracking, as well as the displacement. The highest load was attained with the oriented, densely packed epoxy elements, specimen PK4. The highest displacement at maximum load was reached by the steel reinforced specimens PK5 and PK6. The lowest displacement at maximum load

was reached for the disordered specimens, specimen PK1, PK2. However, the specimens failed by a smooth softening. The curve does not show sudden stress drops, which is usual for steel fiber reinforced concrete. Additionally, during softening, several cracks were formed. The load-displacement curve of specimen PK3 (oriented, not densely packed, epoxy elements) is between PK1, PK2 and PK4.

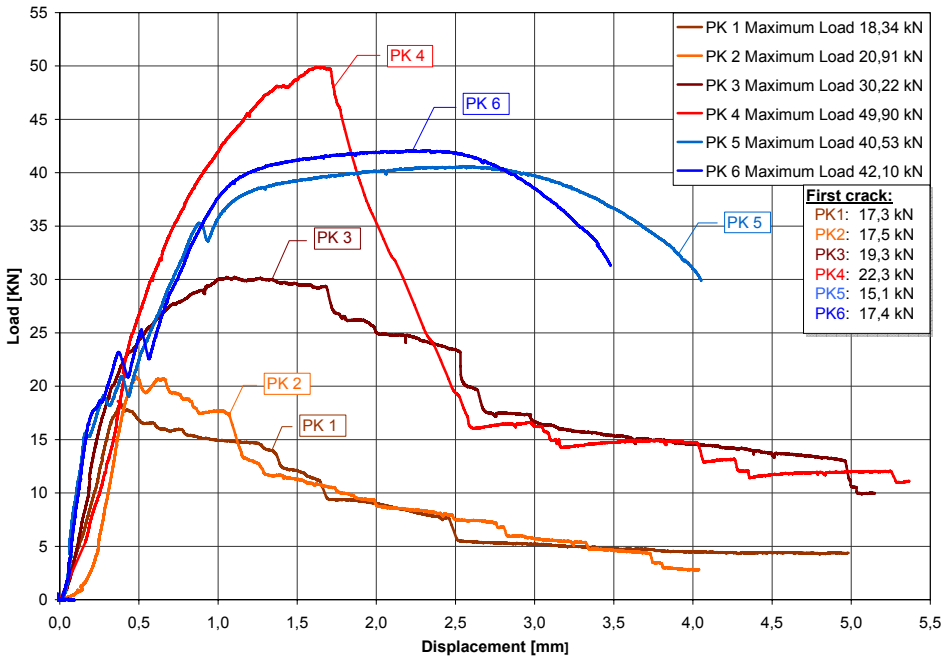

Figure 1 The load-displacement curves of all tested specimens made with epoxy elements and reinforcement bars

The experimental results confirmed the assumption that it is possible to increase strength and ductility by applying high strength elements. The orientation and the ductility of the high strength elements have a major influence on specimen behavior in bending. The specimens with disordered elements showed a good ductility, while the oriented, densely packed elements showed a very high ultimate load. The stresses by the maximum load reached values up to 6.7 N/mm².

Sebastian Zoran Ambro
Vienna University of Technology
Institute for Structural Engineering
Karlsplatz 13/ E212 - Betonbau
1040 Vienna, Austria
szambro@mail.tuwien.ac.at

Johann Kollegger
Vienna University of Technology
Institute for Structural Engineering
Karlsplatz 13/ E212 - Betonbau
1040 Vienna, Austria
johann.kollegger+e212@tuwien.ac.at

NUMERICAL SIMULATION OF CONCRETE STRUCTURAL BEHAVIOUR AT EARLY AGES

Miguel Azenha
Faculty of Engineering of the University of Porto, Porto, Portugal
Rui Faria, Supervisor
Koichi Maekawa, Co-Supervisor

The importance of early age structural behaviour has been widely recognized in concrete science. The initially developed stresses (of thermal or shrinkage origin) which are usually not accurately considered in design can be responsible for the occurrence of cracks at early ages or during service conditions. These cracks can represent serious problems in terms of both structural performance (live loads) and durability (open doorways for the entrance of external aggressive agents).

Nowadays, many approaches exist for the numerical simulation of concrete structural behaviour at early ages. Within this research, an integrated approach of coupled thermal, moisture and stress fields of real sized concrete structures is intended. For such purpose, investigation is being conducted for numerical implementation and experimental validation. In this paper, focus is pointed towards one specific task of the doctoral programme that is currently under development: numerical simulation of boundary conditions for moisture fields under arbitrary environment.

A part of the conducted research consisted in an experimental campaign regarding the sensitivity of evaporation from mortar when exposed to several environmental conditions (in terms of temperature, relative humidity and wind speed) at variable ages (0 ,1 ,3 and 7 days). Two specimen geometries were used: prismatic (7.3 m×5.1 cm×3.0 cm) and cylindrical (5 cm diameter and 5 cm tall). In all experiments there was only one exposed surface during the test. Regarding the composition of the specimens, two mixes of mortar were used: one with a w/c = 55%, and another with w/c = 35%. During the experiments water loss was monitored by performing weight measurements of the samples in a high precision scale. Several combinations of mortar compositions, environmental conditions and ages of exposure were tested. The results of the experiments were analyzed in view of the three stages of drying from porous media - evaporation controlled, transition and diffusion controlled phases - , as well as of the evolving pore structure of mortar, and the autogenous water consumption by cement hydration.

A formulation for moisture boundary conditions in numerical modelling of moisture fields, based on water vapour pressure potentials and experimentally determined moisture emissivity coefficients, is put forward and implemented in DuCOM – the currently existing numerical framework at the University of Tokyo - , and the feasibility of its predictions is confirmed by comparison with experimental results. An example of a typical finite element mesh reproducing a prismatic mortar sample, as well as a comparison between experimental and numerical results are depicted in Figure 1.

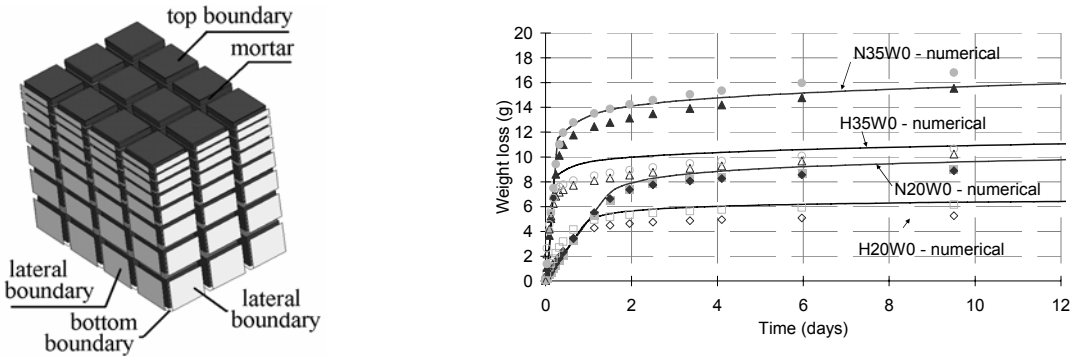

Figure 1 – a) FE mesh adopted for a prismatic specimen; b) Weight losses under 20°C and 35°C environments (experimental versus numerical)

The overall coherence between the numerical and the experimental results was quite satisfactory, and a fairly good prediction of the transitions between the three stages of drying was obtained. This demonstrates the feasibility of the novel moisture boundary conditions here proposed, as well as the ability of DuCOM to simulate the moisture movements inside the evolving pore structure of cementitious materials and the autogenous water consumption by the hydration reactions.

Miguel Azenha
Faculty of Engineering of the University of Porto
Department of Civil Engineering
Structural Division
R. Roberto Frias, s/n
4200-465 Porto, Portugal
mazenha@fe.up.pt

Rui Faria
Faculty of Engineering of the University of Porto
Department of Civil Engineering
Structural Division
R. Roberto Frias, s/n
4200-465 Porto, Portugal
rfaria@fe.up.pt

Koichi Maekawa
The University of Tokyo
Department of Civil Engineering
Faculty of Engineering
7-3-1 Hongo, Bunkyo-ku,
Tokyo, Japan
maekawa@concrete.t.u-tokyo.ac.jp

MODELLING AND INELASTIC SEISMIC RESPONSE ANALYSIS IN 3D OF CONCRETE BRIDGES HAVING MONOLITHIC CONNECTION BETWEEN DECK AND PIERS

Vasilios G. Bardakis
University of Patras, Patras, Greece
Michael N. Fardis, Supervisor

Non-linear seismic response analysis procedures, static (pushover) or dynamic, are currently entering seismic design practice, either as means of checking the design of a bridge designed through linear elastic analysis and on the basis of a global behaviour factor, q, for the reduction of elastic force demands, or as a means for design of a new bridge iteratively, without recourse to a behaviour factor, q. Moreover, nonlinear seismic response analysis is the backbone for the development of reliable displacement-based seismic design procedures for bridges, in which seismic displacements are the primary response variable for the design: design criteria are in terms of displacements and hence member displacement demands need to be directly estimated, to be compared to member capacities.
In this paper, a nonlinear modeling capability is developed for the seismic response analysis of concrete bridges with continuous deck, consisting of a prestressed concrete box girder monolithically connected to the piers. It covers nonlinear dynamic (response-history) analysis under one or two horizontal ground motion components (transverse or parallel to the bridge), and nonlinear static analysis (pushover) under increasing lateral forces proportional to a specified force pattern. Piers of circular or rectangular cross-section, solid or hollow, are modelled as single elements with inelasticity lumped at their ends and effective elastic stiffness equal to the secant stiffness of the pier at yielding of its end section(s). Modelling of the nonlinear force-deformation relations of the pier and assessment of its performance (failure or not) under seismic loading is based on expressions for:

- the pier yield moment;
- the deflection of the pier at yielding of its end section(s) – including effects of shear and pull-out of vertical bars from their anchorage beyond the pier end;
- the shear capacity of the pier – including its reduction after flexural yielding with the magnitude of cyclic inelastic deformation; and
- the ultimate chord-rotation capacity at the pier end under cyclic loading,

all in terms of the pier cross-sectional geometry and reinforcement.
The computational capability is developed in a user-friendly graphical environment. The program possesses a post-processor that allows a fully graphical display of plots of force, displacement, or deformation from the analysis, and of performance (demand-capacity ratio in flexure, or in shear). In the case of nonlinear dynamic analyses for a set of strong motion components, minimum, maximum or mean values and coefficients-of-variation are displayed for the suite of the motions.
The computational capability is applied to a real free-cantilever bridge having a central span and two equal side spans, two piers of unequal height, sliding supports at the abutments in the longitudinal direction and full transverse restraint there. The (curved-in-plan) deck is discretized longitudinally into a series of nonlinear elements, with yield moment and effective stiffness given separately for the two main directions of bending of the box girder (about the horizontal cross-sectional axis for the response within a vertical plane through the longitudinal axis, about the vertical axis for the response within a horizontal plane in the transverse direction of the bridge). The yield moment and the effective stiffness are obtained

through an algorithm that takes into account the cross-sectional geometry, the longitudinal reinforcement and the prestressing of the box-girder.

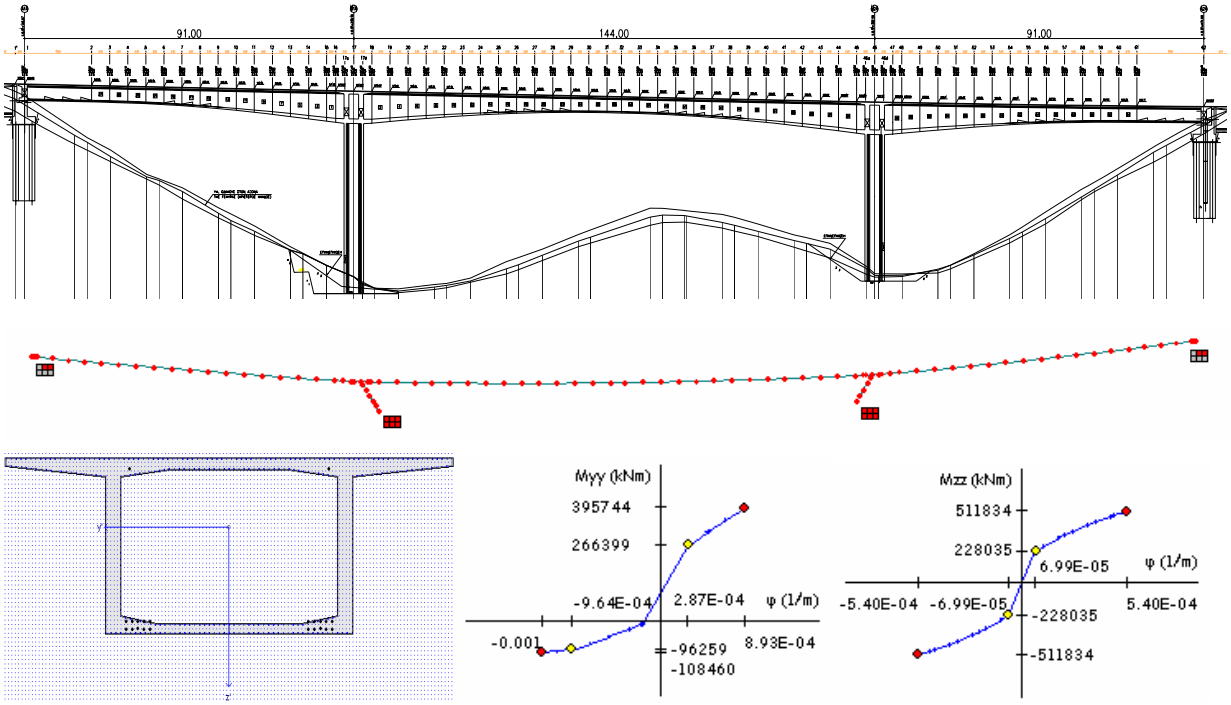

As the analysis capability is meant to be used for the development and calibration of a Displacement-Based seismic design procedure in which inelastic deformation demands in the piers are estimated through appropriate linear-elastic seismic response analyses, results reported in the paper focus on comparisons of chord-rotation demands in the piers and the deck obtained by nonlinear dynamic (response-history) analyses, to appropriate linear-elastic predictions. Under ground motions about twice as strong as the design seismic action, elastic chord rotation demands from elastic modal response spectrum analysis are very close, on average, to those predicted from nonlinear dynamic analysis. This is despite the inelasticity that develops both in the deck and in the piers under seismic motions of such magnitude. Further analyses of different bridge configurations are necessary, to confirm the conclusion that the “equal displacement rule” applies in approximation to the local deformations (chord rotations and curvatures) of the bridge deck and the piers.

Vasilios G. Bardakis
University of Patras
Dept. of Civil Engineering
Patras GR 26500
Greece
vbarda@upatras.gr

Michael N. Fardis
University of Patras
Dept. of Civil Engineering
Patras GR 26500
Greece
fardis@upatras.gr

DESIGN AND INSTALLATION OF BORED DISPLACEMENT PILES AND THEIR EFFECTS ON THE SOILS

David Baxter
Centre for Innovative and Collaborative Engineering, Loughborough University, UK
Neil Dixon, Paul Fleming, Steve Hadley, Supervisors

Introduction

A bored displacement (bd) pile is a type of piled foundation formed using a shaped auger to cause lateral displacement of the earth to form a void. A reinforced concrete pile is then formed *in-situ* in the void that has been formed. The use of bd piles in the UK is increasing, largely due to the requirement to develop brownfield sites and to avoid the rising cost of spoil disposal. As their use increases, the need to understand their behaviour becomes more important as does the development of accurate, efficient design techniques, which allow for the complex processes undergone by the soil during construction.

Research Context

The research described here forms part of an Engineering Doctorate (EngD), an alternative to the traditional PhD which provides industrial context to the research through collaboration with an industrial partner.

Pile Classification

Piles have traditionally been classified as either displacement or non-displacement types, according to their method of construction. A bd pile shares some properties within both pile classification divisions.

The term ‘bored displacement’ covers a surprisingly broad variety of pile types. This paper proposes a uniform classification system for bd piles, which is summarised in Figure 1.

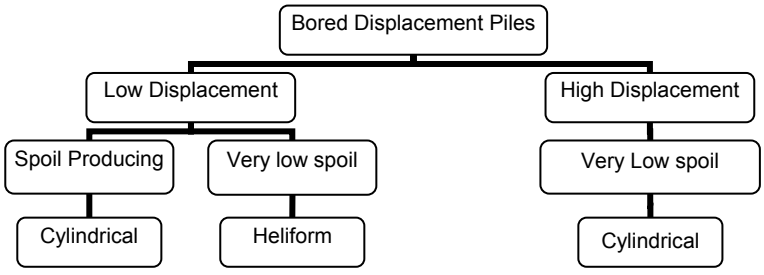

Figure 1. Bored Displacement Pile Classification

In order to understand the load carrying behaviour of a pile constructed using bd techniques, it is essential to understand the mechanism of the displacement of the soil during the construction process, its effects and changes in the behaviour of the soil. For a modern bd pile, it is necessary to consider the installation phase as three discrete stages. The first stage is the insertion of the auger; this is followed by stress relief after the displacing auger head has passed. Finally, the auger head will pass a second time upon extraction to be followed by an injection of concrete.

Conclusions

It is concluded that complex changes occur in the stress states of the surrounding soil. Such effect of the pile installation on the soil should be accounted for and there is a need, therefore, to refine the design process for these piles further.

The effect of the displacement on the soil should be considered in design calculations. Where empirical correlations are used, further work is required to determine the value of coefficients specific to the pile type and soil condition. Information is particularly lacking for the total stress approach often adopted within the UK for fine-grained soils. A series of pile load testing, analysis and comparison with other pile types is planned to extend this research.

David Baxter
Centre for Innovative and Collaborative Engineering,
Department of Civil and Building Engineering,
Loughborough University
Loughborough,
Leicestershire, UK.
d.j.baxter@lboro.ac.uk

Dr Neil Dixon
Department of Civil and Building Engineering,
Loughborough University
Loughborough,
Leicestershire, UK.
n.dixon@lboro.ac.uk

Dr Paul Fleming
Department of Civil and Building Engineering,
Loughborough University
Loughborough,
Leicestershire, UK.
p.r.fleming@lboro.ac.uk

Steve Hadley
Rock and Alluvium Limited,
SBC House,
Restmor Way,
Wallington,
Surrey, UK.
steve.hadley@rockal.com

APPLICATION OF BAYESIAN PROBABILISTIC NETWORKS FOR LIQUEFACTION OF SOIL

Yahya Y. Bayraktarli
ETH Zurich, Institute of Structural Engineering (IBK), Switzerland
Michael Havbro Faber, Supervisor

Earthquake risk management constitutes a very complex problem framework. It requires a realistic and reliable modelling of the seismic hazard, the soil response including soil failures like liquefaction, the structural response, the damage assessment and all possible consequences. The tools for the structuring and modelling of such large complex problems are fault and event trees. The entire decision problem structure can be modelled by these two supplementary analysis tools. The main drawback of these tools however is the exponentially growing size of the branches of the trees with increasing number of variables. This makes the model awkward and very difficult to communicate to third parties for validation purposes. Bayesian probabilistic networks (BPN's) provide a remedy for these drawbacks, as they map the problem framework by a graphical representation of nodes and directed links explicitly showing the probabilistic dependence between the nodes and the information flow in the model; nodes characterising the uncertain quantities of the problem, arrows the causal interrelation between these quantities.
In the present paper the evaluation of one type of soil response, the earthquake induced liquefaction, by a BPN will be discussed. During an earthquake, loosely packed water-saturated sediments near the ground surface may lose their strength and stiffness as a result of pore water pressure increase. This phenomenon, known as liquefaction may cause serious damage to the built environment as experienced during the earthquakes in Niigata (1964), Loma Prieta (1989) and Kocaeli (1999). The soil liquefaction is quantified using deterministic and probabilistic techniques either based on laboratory tests or empirical correlations of in-situ index tests with field case performance data. The deterministic empirical correlation in using Standard Penetration Test (SPT) proposed by Seed and Idriss (1971) is widely used in practice to evaluate the potential for soil liquefaction. A revised version of this so-called simplified procedure (Youd et al. 2001) will be applied in this paper to illustrate the application of BPN in liquefaction analysis.

A BPN may be formulated by the following steps, see also Figure 1:

- Variables necessary and sufficient to model the problem framework of interest are identified.
- Causal interrelations existing between the nodes are formulated. They are graphically shown in terms of arrows connecting variables.
- A number of discrete mutually exclusive states are assigned to each variable.
- Probability tables are assigned for the states of each of the variables.

Figure 1 illustrates the BPN considered for the example application in the paper. The annual probabilities for each moment magnitude Mw (Mw = 5.5, 6.5, 7.0, 7.5) are calculated using the Gutenberg-Richter magnitude reoccurrence relationship. The seismic source zone is considered as a point source and the occurrence of strong earthquakes is assumed to follow a stationary Poisson process. These probabilities form the probability tables for 'Earthquake magnitude'. The epicentre distances are assumed to be R = 10 km, 20 km, 40 km and

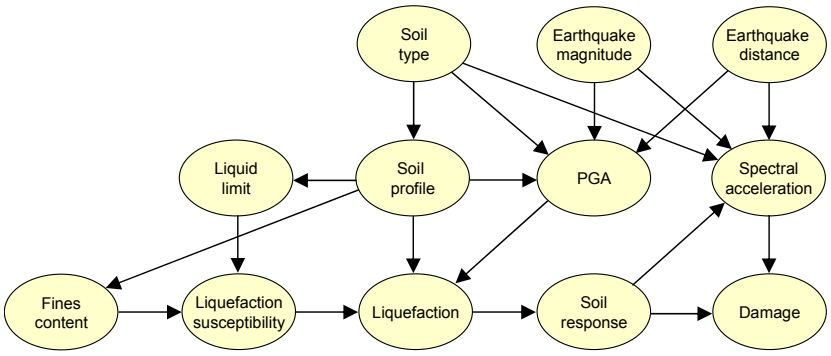

Figure 1: Bayesian probabilistic network for assessing liquefaction of soil.

80 km to the site and are presented by 'Earthquake distance'. 'Soil type' constitutes the states rock, gravel, sand, silt and clay. 'Spectral acceleration' is conditioned on these three nodes and on 'Soil response'. 'Soil profile' constitutes the different layers of the considered bore profile. 'PGA (Peak Ground Acceleration)' is assumed to be independent of 'Spectral acceleration' but dependent on the 'Earthquake magnitude', 'Earthquake distance', 'Soil type' and 'Soil profile'. The 'Modified Chinese Criteria' is implemented as a logical connection in 'Liquefaction susceptibility'. Its conditional probability table depends on 'Liquid limit (LL)' with the two states LL < 32, LL ≥ 32 and on 'Fines content (FC)' with the two states FC < 10%, FC ≥ 10%. The node 'Liquefaction' comprises the conditional probabilities for liquefaction computed based on the revised version of the simplified procedure, whereby the states of 'PGA' are taken from the simulated acceleration time histories. 'Soil response' has two states 'Ground amplification' and 'Liquefaction'. Conditional on the 'Spectral acceleration' and 'Soil response', the probabilities of being in a predefined damage state form the conditional probability tables in the 'Damage' node.

For the BPN analysis the software package Hugin Researcher is used. The analysis is performed for each layer of the considered soil profile resulting in the probability of liquefaction in the node 'Liquefaction'. The information flows from this node to the distribution of damage on the structure on the site. With observations of one or more of the variables the updated probabilities can be calculated easily using the BPN.

Yahya Y. Bayraktarli
Institute of Structural Engineering IBK
ETH Zurich
8093 Zürich, Switzerland
bayraktarli@ibk.baug.ethz.ch

Prof. Dr. Michael Havbro Faber
Institute of Structural Engineering IBK
ETH Zurich
8093 Zürich, Switzerland
faber@ibk.baug.ethz.ch

NONLINEAR FINITE ELEMENT FOR REINFORCED CONCRETE STRUCTURES IN PLANE STRESS

Gabriele Bertagnoli
Politecnico di Torino, Torino, Italy
Giuseppe Mancini, Supervisor

In this paper a very compact material formulation for reinforced concrete is presented. It's implemented in a finite element program, able to describe the behaviour of 2D structures, subjected to plane stress actions, from serviceability conditions up to the collapse.
The method is based on a smeared crack and smeared embedded reinforcement approach.
The crack direction is fixed, once the crack is opened, but the compressive field rotates in concrete after crack formation.
Three different resistant criteria for concrete in compression-compression, compression-tension tension-tension are adopted. Several different layers of reinforcement, no matter how oriented within the concrete matrix, can be taken into account.

Sargin law has been adopted as the uniaxial constitutive equation for concrete in compression. The ultimate compressive strain and the tensile strength have been taken according to EC2. A tri-linear tension softening branch follows after cracking.
When both the principal stresses in the concrete matrix are negative, the incremental constitutive law is similar to the behaviour of an orthotropic material, according to the theory of Darwin and Pecknold, and the failure curve given by Kupfer and Gerstle is adopted.
In tension-compression an innovative procedure has been implemented to describe the whole stress path the structure goes through along its load history. As described by Carbone, if the element is cracked, two main causes of the compressive strength decrease in concrete are detected. The fist one is related to the presence of tangential stresses along the cracks. This phenomenon is taken into account by the deviation angle $\Delta\theta$ between the direction of the compressed field at first cracking and its direction at the load level at which the analysis is performed. The second cause is the presence of tensile stresses induced in the compressed concrete struts by the crossing tensed reinforcement.
When both the principal stresses in concrete are positive, a bilinear failure surface is used coupled with the uniaxial tension softening branch.
Reinforcement bars are seen by the code as layers of a virtual material with stiffness and resistance only in the longitudinal direction of the bars. Reinforcement is therefore not introduced with additional finite elements (i.e. trusses), but as a contribute to the stiffness of the concrete matrix.
The proposed model has been first tested on simple shear panels well known in literature. Two different experimental campaigns have been chosen.
The first one was accomplished by L. Vecchio e M. P. Collins in 1982 whereas the second one was carried out by A. Belarbi and T. T. C. Hsu in 1991.
The model has been also tested on more complex structures such as deep beams. Two different experimental campaigns have been again chosen as test cases.
The first one is a classic study, published in 1966 by F. Leonhardt and R. Walther, while the second one is a study published in 1993 by J. Foster and R. Ian Gilbert.
Figure 1 shows the comparison between experimental and numerical load-displacement curves for the vertical displacement of three Leonhardt and R. Walther beams.

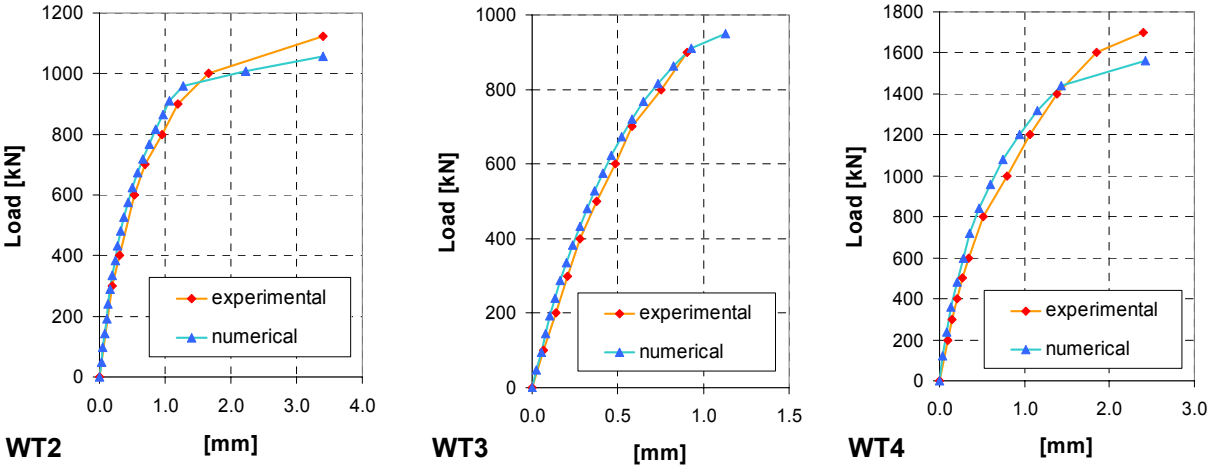

Figure 1 Comparison between experimental and numerical load-deformation curves for Leonhardt and Walter deep beams

As a conclusion it can be said that a new resisting criterion for concrete in tension-compression has been used. An innovative compression softening rule has been derived from this criterion and implemented in the model. These innovations greatly helped the model in describing reinforced concrete subjected to compression and shear actions.
The element has been largely tested on well known and recognized experimental tests available in literature, also covering a very large field of concrete compressive strengths (15÷88 MPa). It fits very well the experimental results of real structures like deep beams, and show moderate deviations when it's asked to reproduce the behaviour of panels subjected to uniform state of stress.
In addition to the good performance of the results, the main advantage of this finite element, relies on the small number of input parameters required to describe the materials (five for steel bars and one for concrete) and on its versatility of use.
The future evolution of this element may consider its extension to non monotonic load histories and the development of a multi-layered shell element.

Gabriele Bertagnoli
Politecnico di Torino
Dipartimento di Ingegneria Strutturale e Geotecnica
C.so Duca degli Abruzzi, 24
Torino, Italy
gabriele.bertagnoli@polito.it

Giuseppe Mancini
Politecnico di Torino
Dipartimento di Ingegneria Strutturale e Geotecnica
C.so Duca degli Abruzzi, 24
Torino, Italy
giuseppe.mancini@polito.it

SEISMIC SAFETY OF EXISTING BRIDGES IN REGIONS OF MODERATE SEISMICITY

Martin Bimschas
ETH Zurich, Switzerland
Alessandro Dazio, Supervisor

The seismicity of Switzerland can be considered as moderate, but the seismic hazard has been underestimated for a long time. Based on extensive research the code provisions concerning seismic demand have become more restrictive during the last decades. Therefore, it can be assumed that the safety of new bridges designed according to current codes is sufficient for the expected seismic events. However, the large majority of Swiss bridges has been built according to previous generations of codes which either prescribed lower seismic actions or did not include any seismic provisions at all. Those bridges usually do not comply with the current codes and shall be assessed in order to determine their seismic safety and the possible need for retrofitting.
In this paper a multi-span bridge with simply supported superstructure and characteristics typical for existing Swiss bridges built in the late 1960s is being analysed for excitation in the transverse direction. The study focuses on the response of the piers, because these have shown to be potentially critical in previous earthquakes. The goal is to find out how vulnerable the existing bridge stock in Switzerland is and to highlight problem cases. Different displacement based analysis techniques as well as nonlinear time history analyses are being applied. The computed displacement demands are compared to the displacement capacities taking typical weak spots of existing bridges into account.

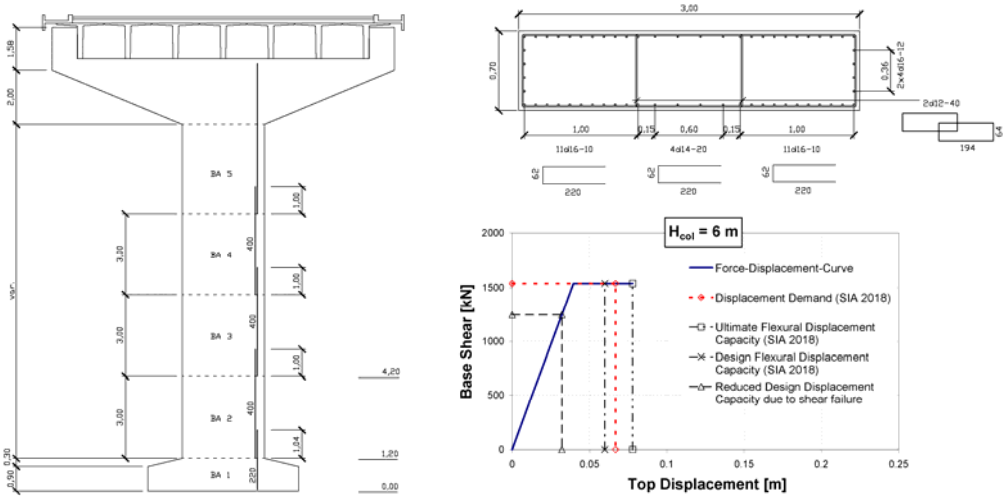

Since the individual spans of the superstructure are simply supported, the piers mainly respond independently and can therefore be modelled as single-degree-of-freedom systems. In the figure above the layout of the piers is shown in elevation and cross-section. It can be seen that the piers have a very low ratio of transverse reinforcement as well as a rather unfavourable lap-splice at the column base. The low transverse reinforcement ratio does not provide any confinement and ensures only a low shear strength that can lead to a brittle shear failure, especially for short piers. In that case they cannot develop their full flexural

displacement capacity. The lap-splice at the column base is unfavourable because it can fail due to large cyclic deformations that are expected in this plastic region during an earthquake. The diagram presented above shows the bilinear approximation of the force-displacement relationship of a pier with 6 m clear height. The displacement demand due to the Swiss design earthquake is compared to the corresponding displacement capacity. It can be seen that the demand exceeds the flexural design capacity by roughly 15%. However, because of the expected premature shear failure, this flexural displacement capacity cannot develop, so that the real displacement capacity is greatly reduced. Taking this into account, the demand exceeds the reduced displacement capacity by 120%, which might represent an unacceptable situation.

Finally, it can be summarized that even in Switzerland, with its moderate seismicity, the response of existing bridge piers, not designed according to modern seismic provisions, can become critical during the design earthquake. This is particularly the case for short and squat piers whose flexural displacement capacity is low and which are additionally susceptible to premature shear failure. Other potential weak-spots, like e.g. lap-splices in the plastic hinge regions, may have a further unfavourable influence on the seismic behaviour of bridge piers and also need to be taken into account.

In conclusion, this study shows that there exists an urgent need to assess the seismic safety of the Swiss bridge stock.

Martin Bimschas
ETH Zurich
Institute of Structural Engineering
Wolfgang-Pauli-Str. 15
8093 Zürich, Switzerland
bimschas@ibk.baug.ethz.ch

Prof. Dr. Alessandro Dazio
ETH Zurich
Institute of Structural Engineering
Wolfgang-Pauli-Str. 15
8093 Zürich, Switzerland
dazio@ibk.baug.ethz.ch

AFFECT-BASED APPROACH: QUANTIFYING USER COSTS RELATED TO INFRASTRUCTURE

James D. Birdsall
Ecole Polytechnique Fédérale de Lausanne, Lausanne, Switzerland
Eugen Brühwiler, Supervisor

Introduction

A key component of civil engineering life-cycle analysis is the consideration and inclusion of user costs. Currently traffic delay user costs are assessed by formulating a constant valuation of the user's time. This approach fails to consider the evolution and reformation of society's expected performance throughout a given construction period.

Constructive evaluation

From a psychological perspective, one can observe that as a person experiences a set of interactions, the individual compares and evaluates the current sensorial data against their previous experiences. Where environmental changes occur, the person is unconsciously spurred to determine if the given change correlates with the pre-existing experience, whether the change is positive or negative, and if any unconscious or conscious action is warranted (Bargh and Chartrand 1999). The individual then employs these subsequent interactions, assessments and evaluations to refine or redefine, where warranted, their constructs to more accurately represent their experienced reality (Kelly 1955). The end result is an evaluation measure unique to each individual – a product of the quantity, range, and sequence of the individual's environmental interactions (Glasersfeld 1996).

Quantifying constructive evaluation – affective assessment

These psychological findings are employed to develop an *affect-based evaluation approach* to quantify the impact of a sequence of interactions. The key component of this affective assessment is the evaluation of the current interaction against the individual's previous perceived experience. This is done by calculating the offset between the current interaction the perceived mean experience for all previous interactions. This evaluation is then incorporated into the perceived mean experience which will be in turn used to evaluate a subsequent experience. This is graphically shown in Figure 1a.

Construction delay affective assessment

This affective assessment approach is then employed to evaluate a 42-day traffic sequence followed by a 15-day theoretical construction intervention. This assessment approach shows that the initial 42-day period establishes an evaluative measure which frames the subsequent three-week construction period. Therefore when the construction induced 20 km/hr speed reduction is introduced, the response is initially significant, but as the individual experiences this speed reduction, their evaluative measures adjust to this new condition and the affective valuation reduces. By the end of the 3-week construction period, the individual's evaluative measures have adjusted to and compensated for the construction conditions and therefore the affective valuation is substantially reduced.

This affective assessment is applied to weight and redistribute the standard traffic delay user costs Figure 1b. By affectively weighting the user costs, 16% of the total user costs are redistributed over the first three days, the first 20%, of the construction period. These aligned and redistributed construction user costs more-closely model the dynamic and evolutionary nature of user valuation as compared to the standard static user cost assessment approach.

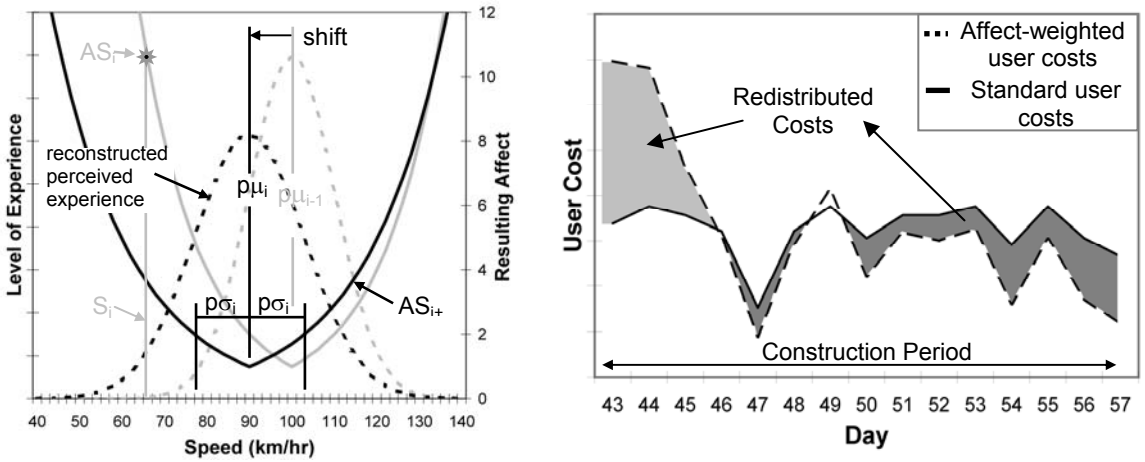

Figure 1a) Interaction i to interaction i+i, the reconstruction of the perceived experience, Figure 1b) Standard and affect-weighted user costs during the construction period.

References

Bargh, J.A., Chartrand, T.A., 1999, The unbearable automaticity of being, American Psychologist, 54, 462-479.

Glasersfeld, E., 1996, The conceptual construction of time, International Symposium on Mind and Time, Neuchâtel, Switzerland.

Kelly, G., 1955, The psychology of personal constructs, New York, United States of America.

James D. Birdsall
Ecole Polytechnique
Fédérale de Lausanne
(EPFL)
Structural Institute - MCS
Station 18
Lausanne, Switzerland
james.birdsall@epfl.ch

Prof. Eugen Brühwiler
Ecole Polytechnique
Fédérale de Lausanne
(EPFL)
Structural Institute - MCS
Station 18
Lausanne, Switzerland
eugen.bruehwiler@epfl.ch

PLASTIC REDISTRIBUTION CAPACITY OF TRADITIONALLY DESIGNED ECCENTRICALLY BRACED FRAMES

Melina Bosco
University of Catania, Catania, Italy
Aurelio Ghersi, Supervisor

Eccentrically Braced Frames (EBFs) are steel structural systems in which the presence of bracings, although not converging to the same point, provides the scheme with enough stiffness while the beam segment between the braces, named *link*, is able to undergo large plastic deformations and to dissipate a large amount of energy. Some studies have pointed out that seismic behaviour of EBFs, evaluated by means of non-linear dynamic analysis, in some cases (mostly in buildings having a large number of stories) is characterised by storey collapse mechanisms which do not allow the full development of the high energy dissipation expected for such systems. Other researchers affirm that an unsatisfactory seismic behaviour of EBFs can be caused by ill proportioning of links and that a correct heightwise distribution of link strength produces collapse mechanisms characterized by almost uniform distribution of link inelastic deformations.
Attention has been here particularly focused on the seismic behaviour at collapse of a congruous set of EBFs characterised by different dynamic and mechanical properties. EBFs have been designed according to capacity design criteria: consequently, links have been dimensioned on the basis of internal actions deriving from design computational analyses (static or modal) while other elements have been designed with reference to the maximum internal actions sustainable by links. Frames designed by means of modal analysis are characterised by quite uniform distribution of overstrength (O_s), defined as the ratio of shear resistance of links and shear forces evaluated by means of modal analysis. On the contrary frames designed by means of static analysis present high scattering in the overstrength especially in the case of high-rise systems where contribution of higher modes is more significant.
The inelastic response of the analysed systems has been evaluated by means of non-linear dynamic analyses. Collapse mechanisms are global as links of each storey are yielded. Nevertheless behaviour is not ductile because the distribution of plastic rotations is not uniform. Particularly in EBFs designed by static analysis, collapse configuration is characterised by moderate plastic deformations of only few links.
With the aim of defining a relationship between the uniformity of normalised plastic deformations in links and a parameter able to measure the heightwise uniformity of overstrength, in Figure 1a EBFs are represented by means of white (4 storey), grey (8 storey) and black (12 storey) points having abscissa equal to the ratio of the maximum and minimum overstrength and ordinate equal to the average value R_m of plastic rotations of links normalised with respect to their plastic capacity. Results show that frames characterised by similar scattering in overstrength present seismic behaviour very different and that also frames with an almost correct strength distribution can exhibit poor collapse mechanisms. On the basis of such a consideration the uniformity of overstrength is not sufficient to guarantee a good seismic response of EBFs.
In order to define a simple parameter able to predict and explain the poor performance of some EBFs, attention has been focused on the plastic redistribution capacity, which is intended as the ability of structures to favour spreading of plastic deformations in links before the attainment of their ultimate plastic rotations. A numerical value of the plastic redistribution capacity factor (*PRC* factor) is evaluated, with reference to each storey where link is supposed to be yielded, as a function of the interstorey drifts which develop at all storeys

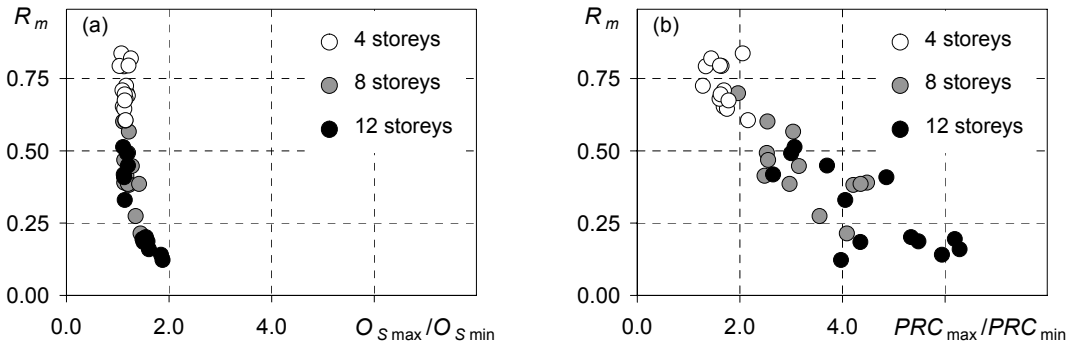

Figure 1 Seismic performance of EBFs in function of the scattering of: (a) Overstrength; (b) PRC *factor*

after yielding of link. Interstorey drifts will be defined as either elastic or plastic with the aim of distinguish displacements of storeys in which links are considered to be elastic or yielded. Both displacements are evaluated by modal analysis of the structure in which the link stiffness at the storey under investigation (i.e. in which the *PRC* is calculated) is reduced with respect to that corresponding to the elastic behaviour in order to simulate yielding and are divided by the maximum interstorey drift allowed at the same storey by the inelastic rotational capacity of links.

On the basis of the analysis of the seismic response of the above-mentioned systems, the seismic performance of EBFs seems to be strongly dependent on the minimum value of the *PRC* factor. In order to verify if the *PRC* factor is reliable in predicting the tendency of EBFs to collapse with non-ductile mechanisms, the average value of the normalised plastic link rotations R_m has been plotted as a function of the variability of *PRC* along the height (Fig. 1b), conventionally measured as the ratio of the maximum and minimum values of *PRC*. Also in this case EBFs of 12, 8 and 4 storeys are represented by means of black, grey and white points, respectively. Results confirm that seismic performances of eccentrically braced frames are negatively influenced by non-uniform distributions of the *PRC* factor and that the evaluation of such a factor seems to be a design tool able to predict, by means of simple analyses, the seismic performance of EBFs.

A more accurate prediction could be gained defining a parameter able to take into account the effects produced by simultaneous scattering in overstrength and in plastic redistribution capacity.

Melina Bosco
University of Catania
Department of Civil and Environmental Engineering
Institute of Structural Engineering
Viale Andrea Doria 6
Catania, Italy
mbosco@dica.unict.it

Aurelio Ghersi
University of Catania
Department of Civil and Environmental Engineering
Institute of Structural Engineering
Viale Andrea Doria 6
Catania, Italy
aghersi@dica.unict.it

CREEP AND RELAXATION CHARACTERISTICS OF YOUNG CONCRETES

Isabel Burkart
University of Karlsruhe (TH), Karlsruhe, Germany
Harald S. Müller, Supervisor

Within the last decades various approaches have been developed in order to describe the load dependent deformation of common structural concretes. These generally provide – within their range of application – sufficient prediction accuracy for practice. The concrete behaviour is usually characterized by a creep function, which is based either on a summation or a product model. Dependent on the mathematical approach these models are either developed from empirical formulas or based on rheological models consisting of spring and dashpot elements with constant or aging parameters.

Within the range of service stresses, the prediction of creep and relaxation is generally based on the assumption of a linear relation between creep and creep inducing stress, which is a major precondition for the validity of the principle of superposition. However, a comparison of the prediction applying the principle of superposition with the results of corresponding creep experiments with variable stress histories revealed a distinctive nonlinear deformation behaviour of concrete. Dependent on the stress history and the stress level, the prediction either under- or overestimates the creep deformation even within the range of service stresses.

Besides the inadequate consideration of the nonlinear deformation behaviour, both linear product and summation approaches show characteristic disadvantages. Especially at very early ages at loading, product models, for example, may predict a strain reversal after a complete unloading of a creep specimen (Fig. 1, left) or, in case of relaxation, a change of sign in the related stress function (Fig. 1, right).

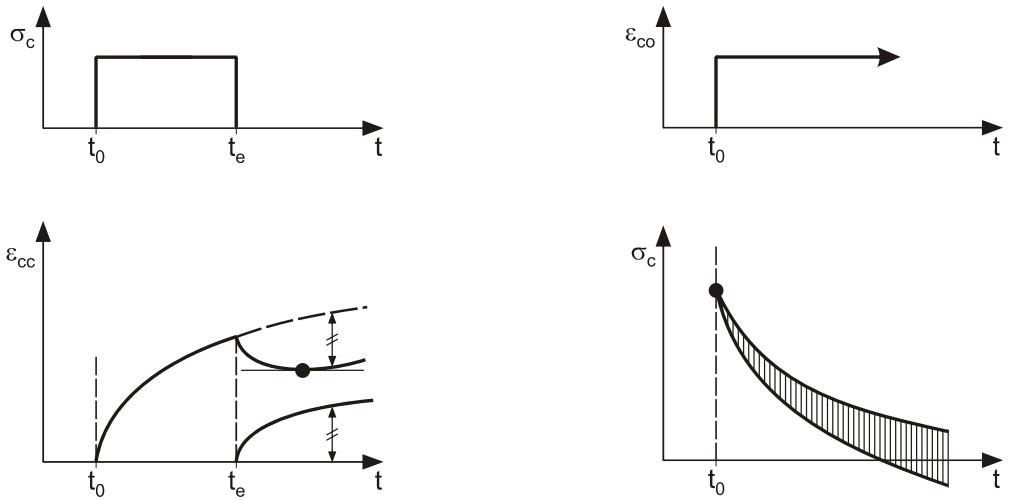

Figure 1 Prediction errors of linear product models

The major purpose of this research project is therefore to develop a new nonlinear rheological material law, which accurately and thermodynamically sound describes the creep and relaxation characteristics of very young concretes. The calibration of the material law will

be based on an extensive experimental programme, including both creep and relaxation tests, performed on normal strength and high-strength concretes. In order to determine the nonlinearity of the stress-deformation characteristics of concrete, both constant and variable stresses will be applied to the creep specimens. The ages at loading will be less or equal to 24 hours. In addition, the creep recovery will be recorded subsequent to selected creep experiments.

The first analysis of the experiments on high-strength concrete shows a large scatter of the mechanical properties, especially at early concrete ages. This results from variable fresh concrete temperatures which cannot be controlled sufficiently in a manner to prevent strong influences on the hydration rate within the first hours after casting.

Furthermore, the experiments have confirmed a distinctive creep capability of young concretes. Fig. 2 shows the creep and shrinkage strains of a high-strength concrete loaded at the age of 24 h. It can be observed that the major part of the creep strains develop within the first 10 days after loading. This results from the rapid hydration progress after loading which strongly reduces the effective stress level during the creep experiment.

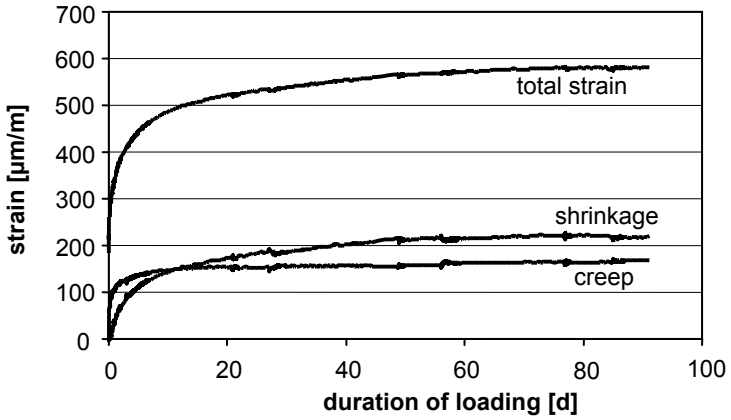

Figure 2 Time-dependent deformation of a high-strength concrete (C90/105, t_0 = 24 h, $\bar{\sigma} = 20\,\%$)

Dipl.-Ing. Isabel Burkart
University of Karlsruhe
Institute of Concrete Structures
and Building Materials
Gotthard-Franz-Str. 3
76131 Karlsruhe, Germany
burkart@ifmb.uka.de

Prof. Dr.-Ing. Harald S. Müller
University of Karlsruhe
Institute of Concrete Structures
and Building Materials
Gotthard-Franz-Str. 3
76131 Karlsruhe, Germany

TIME-DEPENDENT SIMULATION OF REINFORCED CONCRETE SUBJECTED TO COUPLED MECHANISTIC AND ENVIRONMENTAL ACTIONS

Nobuhiro Chijiwa
University of Tokyo, Tokyo, Japan
Koichi Maekawa, Supervisor

Objective

For clear understanding of remaining capacity and rational repair of existing structures, the coupling effects of each chemo-physical event and mechanical damages of structural concrete shall be tackled for strategic maintenance of vast variety. The knowledge basis of structural concrete and hygro-physical natures of cementitious composites is required as the durability design and maintenance tools.
The author utilizes two computational systems as the basis of study, i.e., thermodynamics oriented computational system named DuCOM, and nonlinear structural analysis program for reinforced concrete coded by WCOMD/COM3. The objective of this research is to establish the unified simulation system to predict the deterioration process and following behavioural responses from casting to the end of service life.

Analytical system

The sea-saw iterative computation with *DuCOM* and WCOMD/*COM3* is applied as the computational platform. The growth of micro structures of concrete and volumetric change are conveyed during the small increment of time to the structural analysis system for computing inherently induced damages like cracking and yielding of steel. The rate of corrosion is also brought to the structural analysis. Here, the transient stiffness and strength of concrete are also transferred from *DuCOM* to WCOMD/*COM3*. The nonlinear structural analysis in turn brings the progressive damaging and crack deformation to the micro-scale analysis, i.e., this information is commonly shared with the thermo-hygro computation platform *DuCOM* and the mass-transport simulation is driven with the information of mechanistic states of large scale in a short time increment.

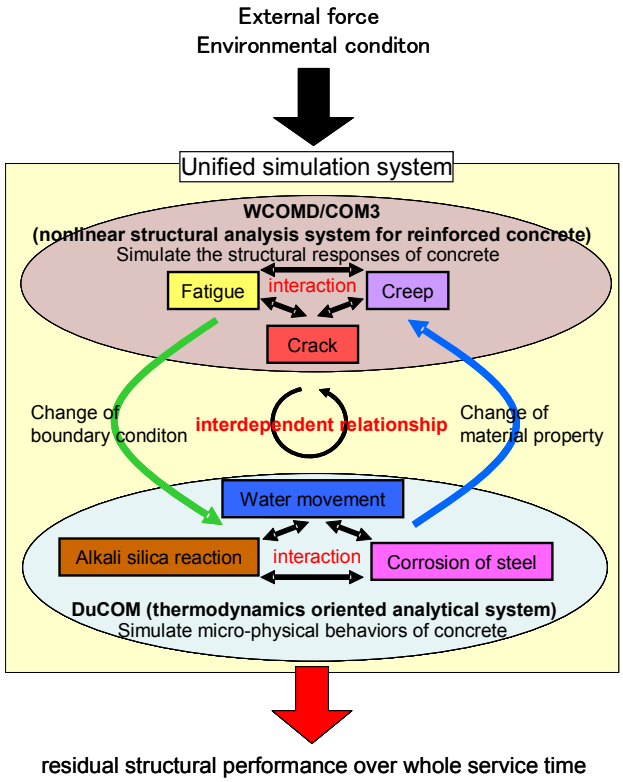

Fig.1 Integration of WCOMD/COM3 and DuCOM

Application to real structure

Seriously damaged bridge (partial pre-stressed concrete) with high density of cracking was found, and accurately recorded and investigated by the Concrete Committee in Japan Society of Civil Engineers (JSCE). As the bridge concerned is still not in service, almost all necessary data for cause investigation are available. Then, this incident can be also used for system verification at the real scale. Large

amount of reinforcement with great shrinkage of concrete is thought to be the chief cause of this incident.
In order to identify the mechanism occurring in this actual structure, investigation is conducted by the unified simulation system. The approximate climate data is assumed from meteorological records as ambient boundary conditions, and the analytical result is compared with the site-data. The key is the enlarged deflection and horizontal displacement of supports, which correspond to coupling action by remaining pre-stress and shrinkage of concrete. The loss of pre-stress and shrinkage are investigated to have different sensitivity to span deflection and displacement of the supports, respectively. Through the discussion based on the analytical result, the remaining pre-strain is estimated to be 5000 μ which is almost the same as the designed value, and the mean shrinkage over the web and slab members is estimated to be 750 μ or more. The remaining fatigue life is required to be estimated for planning of future maintenance and cost estimation.

Experimental study taking into account corrosion of steel
For verification of the coupled computational system used under any ambient conditions and pre-induced mechanical damages, a new series of experiment is scheduled in April, 2006. The aim of this experiment is to assess the capacity of deteriorated beams with different detailing at anchorage to strengthening the analysis stated above in practice. Against shear, the truss system is formed in the beam. If the anchorage zone is strong enough, the structure system may turn to the tied-arch with improved shear capacity. Another scenario is failure of anchorage zone which brings about entire collapse of the structural concrete. In this study, academic attention is directed to the anchorage zone with corrosive damage as of importance to the entire structural concrete system. The comparison of the analysis and experimental results and their detailed discussion will be made in Zürich Ph.D. conference.

Conclusions
Unification of two computational platforms of different multi-scales, that is to say, *DuCOM* and *WCOMD/COM3*, enables us to trace deteriorating process of structural concrete and to estimate remaining functions, but further detailed verification and improvement are essential to meet the challenge of engineering practice. To date, damaged structural performance of laboratory and real scales has been investigated. Amalgamation of knowledge on two scales is aimed in near future.

Nobuhiro Chijiwa
The University of Tokyo
Department of Civil Engineering
School of Engineering
7-3-1 Hongo, Bunkyo-ku,
Tokyo, Japan
chijiwa@concrete.t.u-tokyo.ac.jp

Prof. Koichi Maekawa
The University of Tokyo
Department of Civil Engineering
School of Engineering
7-3-1 Hongo, Bunkyo-ku,
Tokyo, Japan
maekawa@concrete.t.u-tokyo.ac.jp

NUMERICAL ANALYSIS OF THE EFFECT OF HORIZONTAL DEFORMATION OF THE GROUND DUE TO MINING ACTIVITY ON FOUNDATIONS

Szymon Dawczyński
Silesian University of Technology, Gliwice, Poland
Marian Kawulok, Supervisor

Description, analysis and assessment of the interaction of the structure and subsoil are very complex and relatively complicated constructional issues. It results mainly from the fact that both concrete as well as soil are to great extent composite and multiphase materials. The problem of the interaction is even much more difficult when the structure is footed in the mining area. Each kind of underground mining causes invasive disturbance of rock formation balance. Alteration to forces and stresses system takes place having negative influence on buildings. Therefore all mining interactions should be considered as additional loads while designing new structures or protecting the existing ones.
The paper presents FEM numerical model of concrete foundation footed on the mining subsoil. Impact of the horizontal deformations changing in time, on stress state and deformations in the foundation, has been analysed in detail. Calculations have been done with ANSYS software with the use of two different elastic-plastic material models. Five-parameter Willama-Warnke model was employed to model concrete continuous footing. Subsequent model, elastic perfectly plastic Drucker-Prager model, of conical plasticity surface and circular deviatoric section, was used to determine mining subsoil. Employed computational arrangement included 10530 volume elements and 164 pairs of contact elements. Eight-nodes volume elements of three degrees of freedom in each node (displacements in main directions UX, UY and UZ) were used to model subsoil (elements SOLID45) as well as concrete continuous footing (elements SOLID65). Due to significant discrepancies in concrete and soil rigidity, employed surface-to-surface contact elements were corresponding, inseparable pairs: target surface was defined with the use of elements TARGE170 on more rigid material (concrete) and contact surface made of CONTA174 elements was fixed on less rigid material (soil). Lagrange multiplier method applied on the contact normal and the penalty method on the frictional plane were used as a contact algorithm which prevents penetration of the adjacent materials in the contact plane.
Continuous footing of typical dimensions was used in calculations: length 20,0 m, total height 2,5 m, width of the footing base 1,2 m and width of the foundation wall 0,4 m. Concrete with parameters corresponding with standard concrete of C12/15 class, according to Eurocode 2, has been used for calculations. Dimensions of the modeled, interactive soil plate structure are as follows: length 80,0 m, height 40,0 m. It is composed of four layers, 10,0m each (sand clay, firm clay, gravels and clay aggregates and silt). Each layer has different elastic properties (module of elasticity and Poisson coefficient) and plastic properties (cohesion, friction angle and flow angle).
In the first step of loading when the structure was out of the mining impacts range, impacts from dead load and useful load were determined. The next loading steps (each divided into smaller substeps) showed additional loadings acting on foundation as a result of horizontal area movements occurring when full mining subsidence basin goes under the building. Hereby paper does not give consideration to additional impact of the area curvature on the construction, whereas an impact of the horizontal deformations of the area surface on the foundation has been examined in detail. The following equation describes these deformations in accordance with the Knothe's theory:

$$\varepsilon(x) = \frac{du}{dx} = -w_{\max} \cdot \sqrt{2 \cdot \pi} \cdot \frac{x}{r^2} \cdot e^{-\frac{\pi \cdot x^2}{r^2}} \quad (1)$$

Received values of horizontal deformations were applied in adequate loading steps in the form of corresponding displacements to the model, in particular nodes of finite elements mesh.
The full paper presents some of the results obtained in different loading steps. Especially the loading steps corresponding with the occurrence of extreme loosing and extreme compressing subsoil deformations under the footing were emphasized. The maps of the horizontal displacements, stress intensity, elastic and plastic strain intensity of whole interactive system or only continuous footing itself are also presented.

The subject of the analysis is very difficult or even impossible to test in traditional laboratory due to the large number of random parameters identifying structure, as well as the mining subsoil. Models featuring only linear-elastic material properties dominated analyses which have been carried out to date. However, due to appropriate protection of both existing and designed structures, process of subsidence basin creation and its impact on the building requires much more precise approach. Taking into account loading history as well as plastic properties of particular materials results in the fact that such approach shows, to great extent, actual nature of the interaction between a building and subsoil. Therefore, one of the main advantage of the above referred model is possibility to obtain full and accurate results for each finite element. Moreover, possibility to analyse construction effort at any substep of loading is great convenience for the construction designer. Proposed model can be adjusted to changing boundary conditions. Calculations can be repeated at every stage of analysis for different material and geometrical properties of the structure-subsoil interactive system. One of the assumptions of the work is the use of the model in the engineering issues which is why further efforts will be made to extend analysed system by reinforced concrete and masonry foundations.

Szymon Dawczyński
Silesian University of Technology
Faculty of Civil Engineering
Department of Structural Engineering
Akademicka 5
Gliwice, Poland
szymon.dawczynski@polsl.pl

Marian Kawulok
Silesian University of Technology
Faculty of Civil Engineering
Department of Structural Engineering
Akademicka 5
Gliwice, Poland
itb_kawulok@pro.onet.pl

MODELING OF ECC MATERIALS USING NUMERICAL FORMULATIONS BASED ON PLASTICITY

Lars Dick-Nielsen
Technical University of Denmark (DTU), Kgs. Lyngby, Denmark
Henrik Stang and Peter Noe Poulsen, Supervisors

This paper discusses the considerations for the establishment of a damage model for Engineered Cementitious Composite (ECC). ECC is a short fiber reinforced cement composite with moderate fiber volume fractions (approximately 2 vol.%). ECC materials are characterized by their strain-hardening capability when loaded in tension. It is critical for the application of ECC materials that proper material models exist for implementation in numerical structural analysis programs. Three different length scales are used in the approach for deriving the damage model. On each length scale important phenomena are investigated by use of numerical and analytical calculations. The lowest scale discussed here is the micro scale. The phenomena dealt with on this scale are initial matrix flaws and the debonding, bridging and pull-out of a single fiber. The next scale is the meso scale. On meso scale I phenomena involving the propagation of a single crack bridged by many randomly oriented fibers is looked upon. On meso scale II a part of the material undergoing multiple cracking is investigated. The macro scale is the scale of the structural element.

On the micro scale modeling of the fiber bridging and debonding appearing in the ECC during crack propagation has been performed. This was done in order to examine the assumptions typically used in modeling cohesive laws in ECC. Often a superposition scheme for the average fiber bridging stresses and the matrix cohesive law (the fictitious crack model) is employed in order to arrive at an average cohesive law for the composite material. The primary purpose of the modeling was to validate this superposition scheme. A 3D FEM model of a Representative Volume Element (RVE) was set up. The three basic cases: debonding and pull-out of a straight fiber perpendicular to the crack face, crack propagation in pure mortar and crack propagation in a RVE with mortar and fiber were analyzed. It was shown that the cohesive law for a unidirectional fiber reinforced cementitious composite can be found through superposition of the cohesive law for mortar and the fiber bridging curve.

On the meso scale I an investigation is performed by use of a semi-analytical model. The investigation is concerned with one crack propagating in a fiber reinforced, infinite sheet under uniaxial tension. The crack is assumed to be cohesive and the cohesive law applied takes into account fiber as well as mortar properties. A series of calculations has been conducted in order to investigate the influence of tensile strength of the mortar for crack propagation in an infinite sheet.
For a mortar with high tensile strength the crack propagation becomes unstable for relatively small crack lengths (less than 23 mm), while the crack propagation remains stable up to relative large crack lengths for a small tensile strength of the mortar.

On the meso scale II two simulations of the same sheet loaded in uniaxial stress are performed. The sheet has a length of 80 mm and a width of 30 mm and the load is applied as a displacement load. The sheet contains 40 initial stress free flaws with a length of 4 mm. The initial flaws are randomly distributed over the width with a fixed spacing in the load direction. The sheet was modeled using FEM using an interface and smeared approach in the two simulations respectively. In figure 1 a contour plot of the largest principal strains are

plotted for the two simulations at a total deformation of 50 μm. Even though the material was homogeneous and the initial flaws all had the same length the micro cracks did not propagate simultaneously and they did not run through the specimens at once. In both models interaction between initial flaws and micro cracks was observed in areas where the concentration of initial flaws weakened the material.

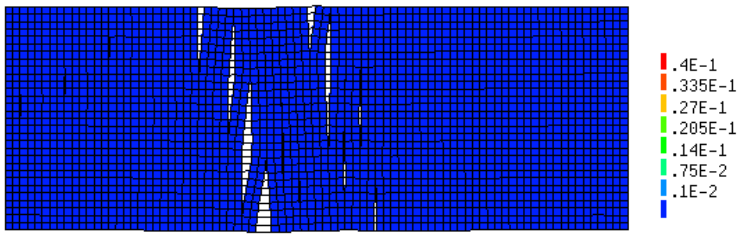

(a) Interface model.

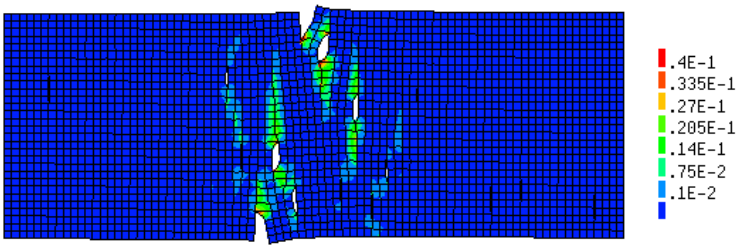

(b) Smeared model.

Figure 1 Principal strains at a total deformation of 50 μm (scale factor 50).

The final step is to develop a material model. The material model should take account of the phenomena observed on the different scales. The material model will be based on smeared cracking and combined with generalized plasticity. In order to get information about the crack opening, spacing and number of cracks, concepts from continuum damage mechanics will be implemented. The connection between damage and plasticity on the macro scale will be described through hardening parameters. This material model will effectively introduce multi-scale modeling and save computational time.

Lars Dick-Nielsen
Technical University of Denmark (DTU).
Department of Civil Enginieering (BYG.DTU).
Brovej, Bygning 118
2800 Kgs. Lyngby,
Denmark
ldn@byg.dtu.dk

Henrik Stang
Technical University of Denmark (DTU).
Department of Civil Enginieering (BYG.DTU).
Brovej, Bygning 118
2800 Kgs. Lyngby,
Denmark
hs@byg.dtu.dk

Peter Noe Poulsen
Technical University of Denmark (DTU).
Department of Civil Enginieering (BYG.DTU).
Brovej, Bygning 118
2800 Kgs. Lyngby,
Denmark
pnp@byg.dtu.dk

DURABILITY OF CONCRETE – RELATIONSHIP BETWEEN SEVERAL STANDARD TESTING METHODS

Čaba Djember
Budapest University of Technology and Economics, Budapest, Hungary
Zsuzsanna Józsa, Supervisor

Durability of concrete generally depends on properties of concrete and environmental influences to concrete during its service life. Standards, by different testing methods give several requirements for concrete, but do not deal with relationship between the testing methods. This paper presents results of several standard tests, which were carried out on different concrete specimens with different grades. Concrete specimens were tested according to the following standards:

1. ASTM C 1202-97 Standard test method for electrical indication of concrete's ability to resist chloride ion penetration
2. EN 12390-8:2002 Depth of penetration of water under pressure
3. prEN 12390-9:2002 Freeze-thaw resistance with de-ice agent – Scaling
4. MSZ 4715/3-2:1989 (Hungarian National Standard) Frost resistance

With establishing of the relationship between test results it might be possible to reduce testing time and also to deduce on conformity of concrete to the specified requests. The two last mentioned tests take usually 1 to 2 months but the duration of the two first mentioned is just few days. If a big amount of specimens need to be tested in a short time, or if we want to estimate frost resistance of several different mixtures, these relationships between the properties could be very useful.

The results of tests are summarised in Table 1

Table 1 Test results

Strength class of concrete	Density [kg/m^3]	Passed Charges [Cb] (Chloride ion penetrability)		Maximum depth of water penetration [mm]	Scaled material [g/m^2]	Frost resistance	Corresponding exposure class
		CEM I	Other type				
High strength concrete (C50 and higher)	2400 or more	less than 800	less than 400	up to 10 mm	less then 250	f150	XF4 (H)
Normal strength concrete (between C50 and C20)	between 2400 and 2275	between 800 and 3500	between 400 and 2600	between 10 and 30 mm	between 250 and 3000	f50 but with air entrainment f150	XF2 (H) or not satisfied
Low strength concrete (C20 and lower)	less than 2275	more than 3500	more than 2600	more than 30 mm	more than 3000	up to f25	not satisfied

Hungarian National Application Document of EN 206-1:2000 defines XF4 (H) and XF2 (H) exposure classes and has special requirements. Tested according to prEN 12390-9:2002 average amount of scaled material should not exceed 250 g/m² and 500 g/m² and maximum individual amount should not exceed 500 g/m² and 700 g/m² respectively.

For high strength concrete it is possible to establish relationship between the test results. If the charge passed is less then 800 coulombs in case of concrete made from unblended Portland cement or 400 coulombs in case of concrete made from blended Portland cement and the depth of water penetration is less than 10 mm (but it is usually not more than 7 mm) then it meets the requirements for XF4 (H) exposure class according to MSZ 4798-1:2004 or for f150 frost resistance class according to MSZ 4715/3-2:1989.

Tests with normal strength concrete are still in progress in order to establish upper level of charge passed and depth of water penetration which correspond to XF2 (H) exposure class according to MSZ 4798-1:2004. It should be mentioned, that scale of depth of water penetration between 10 and 30 mm might be not enough to establish upper level of penetration for XF2 (H) exposure class correctly and water pressure of 700 kPa (according to ÖNORM B 3303) will be applied to make larger scale. For low strength concrete reduction of test time is not so important because they anyway do not adjust requests for XF2 (H) exposure class

Čaba Djember
Budapest University of
Technology and Economics
Department of Construction
Materials and Engineering
Geology
Műegyetem rkp. 3.
Budapest, Hungary
djember@freemail.hu

Zsuzsanna Józsa PhD
Budapest University of
Technology and Economics
Department of Construction
Materials and Engineering
Geology
Műegyetem rkp. 3.
Budapest, Hungary
zsjozsa@epito.bme.hu

UTILIZATION OF FBC-ASH IN PRODUCTION OF HYDRAULIC LIME

Karel Dvorak
Brno University of Technology, Brno, Czech Republic
Marcela Fridrichova

The topics investigated in the frameworks of the VVZ MSM Research Plan No. 0021630511 at the Institute of Technology of Building Materials and Components at the Brno University of Technology also include the utilization of fluidized ash in the production of hydraulic bonding agents. The main aim of investigation in this area is to develop a binder applicable in different areas where bonding agents with sufficient plasticity as well as rigidity and volume stability are required. This work has therefore attempted to find answers to the two major questions in this particular area of problems: Can fluidized ash be used to prepare a sufficiently reactive raw meal in order produce hydraulic minerals and Can the resulting raw meal be subjected to firing at sufficiently high temperature without a risk of reverse decomposition of anhydrite to calcium oxide and sulfur (VI) oxide.

The introduction to the work was the search of ashes from fluidized bed combustion sources on the territory of the Czech Republic. Fluidized bed combustion is modern method of desulphuration, priority was given to great energetic blocks because in this case a greater uniformity of produced FBC-ash can be expected. The FBC-ashes were analyzed chemically

The comparison of individual chemical samples analyses showed, that the filter FBC-ashes contain a lower portion of sulphates and of free lime than the fluids bed FBC-ashes. It is possible to conclude, that anhydrite II, as the direct product of combustion and the free lime are more absorbed in the fluid bed ash.

The pulverized raw mix for burning hydraulic lime was designed as two-component raw mix. The second basic component was besides the FBC-ash the high-percentage lime stone.

The calculation was performed for the two-components powdered raw mix always from the appropriate fluid bed fly ash and from the high percentage limestone Mokrá to the selected hydraulic modulus MH = 1.7 which corresponds with middle and strong hydraulic limes.

Raw mixes were burned in the laboratory to the temperature value of 1200 and 1250°C.

The mineralogical composition of the burnt clinkers was checked by the X-ray diffraction analysis and roughly also by the method of optical microscopy – see figures 1 to 4

We can conclude on the base of the X-ray analysis evaluation that during the burning firstly the decomposition of calcite took place and afterwards followed its reaction with anhydrite and the alumino-silicate phase from the FBC-ash. The main phase of all samples was belite, β-C_2S. Simultaneously the reaction between the lime, the amorphous aluminous phase and the anhydrite took place and also the formation of Klain salt, $C_4A_3SO_4$. All samples contained also free lime, CaO and the clinker mineral brownmillerit, C_4AF. The formation of Klain salt allows to deduce, that the anhydrite in the case of both burnings is combined with preference into this material and apparently it didn´t decompose even at these elevated temperatures.

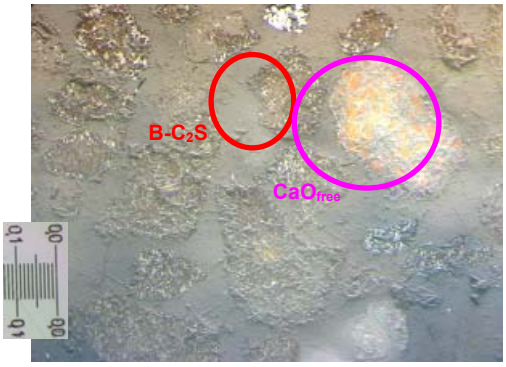

Figure 1 Filter FBC-Ash, burning temp. 1200°C

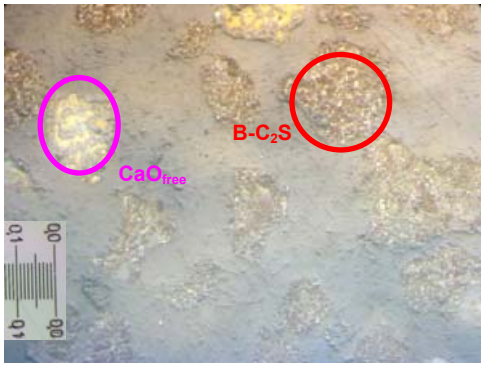

Figure 3 Fluid bed FBC-Ash, burning temperature 1200°C

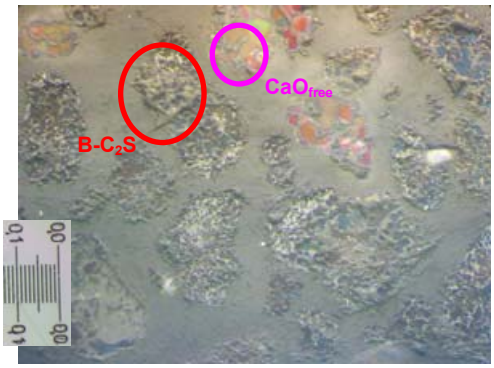

Figure 2 Filter FBC-Ash, burning temperature 1250°C

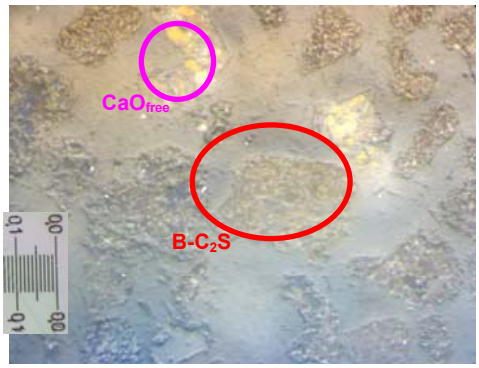

Figure 4 Fluid bed FBC-Ash, burning temperature 1250°C

We can conclude that concerning the utilization of FBC-ashes as one of input raw material component for the production of hydraulic lime, it is first of all necessary to research the problem of burning raw material mixes rich in calcium sulphate without permitting the decomposition of the sulphate and the liberation of SO_2 into the atmosphere. It was proved that practically the total content of anhydrite which is in the ash reacts even at the temperature of 1250°C together with CaO and alumino-silica phases under the formation of Klain salt, $C_4A_3SO_4$ and it does not escape into the atmosphere. Great contribution was the determination that by the reaction between the lime and silica components belite was formed which secures the hydraulicity of the given system.

Karel Dvorak
Brno University of technology
Faculty of Civil engineering
Institute of Technology of Building Materials and Components
Veveri 95
Brno, Czech Republic
Dvorak.k@fce.vutbr.cz

Ass. Prof. Marcela Fridrichova
Brno University of technology
Faculty of Civil engineering
Institute of Technology of Building Materials and Components
Veveri 95
Brno, Czech Republic
Fridrichova.m@fce.vutbr.cz

MULTIPLE SHEAR STEEL-TO-TIMBER CONNECTIONS IN FIRE

Carsten Erchinger
ETH Zurich, Zurich, Switzerland
Mario Fontana, Andrea Frangi, Supervisors

Multiple shear steel-to-timber connections with slotted-in steel plates and steel dowels show a high load-carrying capacity and a ductile failure mode due to the combination of timber and steel elements. A further advantage of this type of connection is the protection of the slotted-in steel plates against fire by the side timber members. Therefore, a high fire resistance may be achieved. As part of an intensive research programme called “Fire safety and timber construction” currently carried out in Switzerland, 18 fire tests on multiple shear steel-to-timber connections with slotted-in steel plates and steel dowels were performed under ISO-fire exposure. The connections were tested with different timber thickness, edge and end distances and diameter of the fasteners (6.3 and 12 mm). In addition to the unprotected connections some connections were tested protected by fire protective claddings, like 3-layer-timberboards, plywood, OSB or gypsum plasterboards for example.
Based on the main results, the paper shows the failure modes occurred in the fire tests compared to the failure modes at normal temperature, analyses the theoretical background and turns special attention to the efficiency of applied fire protective claddings. Comparisons to Eurocode 5, Part 1-2 (EN 1995-1-2) are given concerning the charring rate and the charring depth. The aim of the experimental work in conjunction with finite element temperature analysis is to provide a design model for the calculation of the fire resistance of multiple shear steel-to-timber connections with slotted-in steel plates and steel dowels.

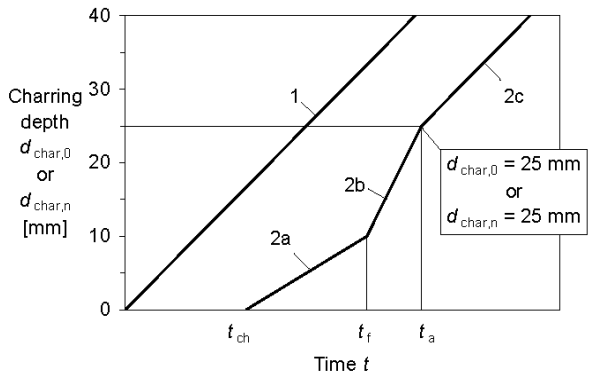

Figure 1 Multiple shear steel-to-timber connection after fire test (left) and charring model for unprotected (line 1) and protected (line 2) timber member (right) according to EN 1995-1-2

Figure 1, right shows the charring model for unprotected and protected timber member according to Eurocode 5, Part 1-2 (EN 1995-1-2). For surfaces protected by fire protective claddings the start of charring is delayed until time t_{ch}. After t_{ch} is reached charring commences at a lower rate than the charring rates for unprotected members until failure time t_f of the fire protection. After the fire protection has fallen off (failure time t_f) charring is increased because the temperature is already at a high level while no protective char-layer exists to reduce the effect of the temperature. For simplification, EN 1995-1-2 assumes that charring takes place at double the rate of initially unprotected surfaces. At the time t_a when the charring depth equals either the charring depth of the same member without fire protection or 25 mm whichever is the lesser, the charring rate reverts to the design charring

rate β_0. In all tests, the protections felt off from the bottom of the specimens first, i.e. only the bottom side is considered here. Figure 2 shows the comparison of measured and calculated charring depths (according to EN 1995-1-2). For 3-layer-timberboards and plywood an increase of the charring rate after the failure time t_f has been confirmed. However, a charring at double the rate of the design charring rate β_0 as assumed in EN 1995-1-2 was not observed. The ratio between the charring rate after the failure time t_f and the design charring rate varied between 1.2 and 1.5. For one connection with OSB, a ratio of more than 2.0 was determined, i.e. the calculation model underestimates the charring depth. For the connection with gypsum plasterboards, type F the ratio between charring rate after the failure time t_f and β_0 is about 2.0. The test result is situated under the safety line but the difference between measured and calculated charring depth is small (see solid box in Figure 2).

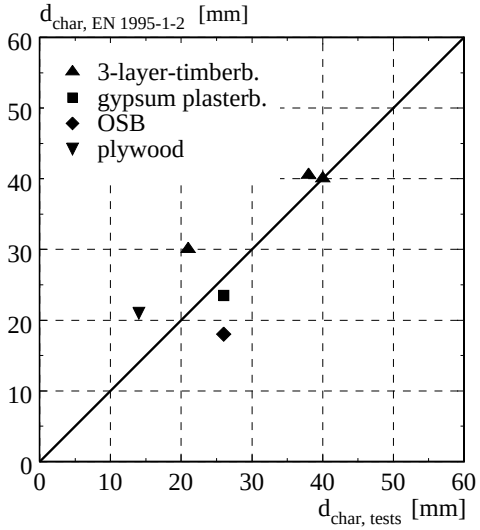

Figure 2 Charring of the timber specimens after failure time t_f

The residual cross-section of the charred timber members was surveyed by laser-scanning. With this method the charring can be determined wherever required with the data points received from the scanner and three-dimensional models can be created. For the surveying of the residual cross-section the laser-scanning method was applied for the first time and shaped up as a quick and more exact alternative to the mainly used manual method.

Carsten Erchinger
ETH Zurich
Department of Civil, Environmental
and Geomatic Engineering
Institute of Structural Engineering (IBK)
Wolfgang-Pauli-Str. 15
Zurich, Switzerland
erchinger@ibk.baug.ethz.ch

Prof. Dr. sc. techn. Mario Fontana
Dr. sc. techn. Andrea Frangi
ETH Zurich
Department of Civil, Environmental
and Geomatic Engineering
Institute of Structural Engineering (IBK)
Wolfgang-Pauli-Str. 15
Zurich, Switzerland
fontana@ibk.baug.ethz.ch, frangi@ibk.baug.ethz.ch

MECHANICAL PROPERTIES AND DURABILITY ASPECTS OF LOW CEMENT CONTENT CONCRETE

Sonja Fennis
Delft University of Technology, Delft, The Netherlands
J.C. Walraven, Supervisor
J.A. den Uijl, Supervisor

Recently environment-friendly building is one of the main focuses of attention in the concrete industry. To reduce the environmental impact of concrete, secondary materials can be used, for instance as cement replacing materials. Many by-products from other industries have characteristics which can positively influence concrete properties. However, regulations in the Netherlands do not permit the use of large amounts of cement replacing materials. Dutch regulations prescribe a minimum amount of cement in concrete (280 kg/m^3) to make sure that concrete properties such as strength and durability are guaranteed.
This research project is based on the idea that by making use of the particle packing optimization techniques, nowadays used in the production of high strength concrete, it is possible to optimize the particle packing in order to lower the cement content in concrete, without changing concrete properties in a negative way. To show the possibilities of this concept a preliminary investigation is conducted to determine the material properties of low cement content concrete (LCCC).

Three LCCC mixtures were designed with particle packing models. In the first mixture 175 kg/m^3 Portland cement and 75 kg/m^3 fly ash were used and in the second mixture 175 kg/m^3 blast furnace slag cement and 75 kg/m^3 fly ash. The last mixture contained 125 kg/m^3 Portland cement and 125 kg/m^3 fly ash. Compressive and tensile strength development in time were measured for one year, as well as drying shrinkage and creep. Stress-strain diagrams, moduli of elasticity and Poisson's ratios were determined after 28 and 364 days. An indication of the durability of LCCC is provided by electrical resistance measurements and water penetration measurements.

All the mixtures had sufficient workability for casting and vibration. The mixture with 125 kg/m^3 of Portland cement and 125 kg/m^3 fly ash, was less cohesive than the other mixtures and has higher air content. The hydration rate of LCCC is low, compared to normal concrete.

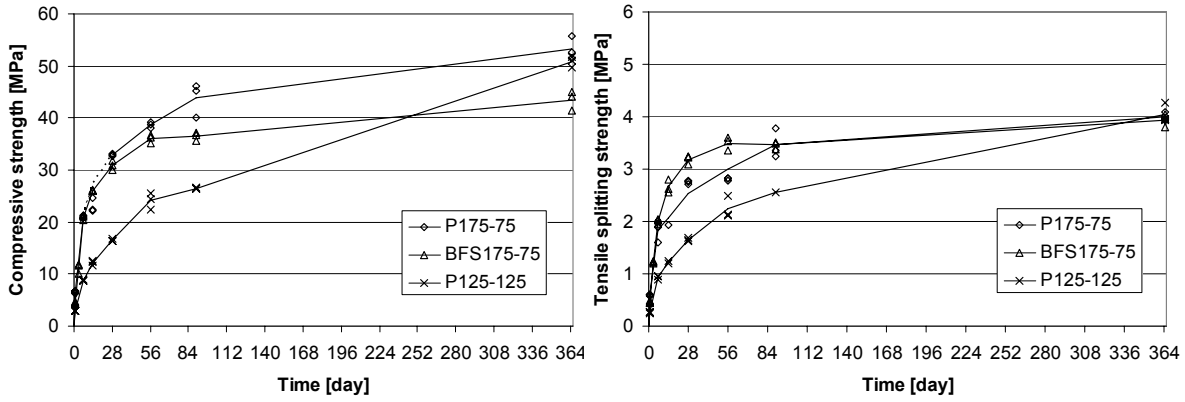

Figure 1 Cube compressive strength and splitting tensile strength

With an optimised packing density it is possible to produce concrete in strength class C20/25 with only 175 kg/m^3 Portland cement or blast furnace slag cement instead of 260-280 kg/m^3 cement as required by the Dutch standards. The mixtures 175 kg/m^3 cement are within strength class C20/25 after 28 days, whereas the mixture with 125 kg/m^3 reaches that order of magnitude after 90 days. When fly ash is combined with Portland cement, there is an additional strength gain from the fly ash in the long-term (Figure 1). The relationship between the average cube compressive strength and the splitting tensile strength of LCCC is the same as for normal concrete.

The measured Poisson's ratios of all three LCCC mixtures were around 0.2 and the measured moduli of elasticity complied with Dutch standards for normal concrete. The shrinkage and creep of LCCC are relatively low compared to normal concrete, although normally high shrinkage and creep values are predicted for concrete in the lower strength classes. This can be explained by the concrete composition, which is characterised by relatively low cement content, normal modulus of elasticity and a high packing density of the aggregate structure. Electrical resistance measurements and water penetration test show that LCCC with 125 kg/m^3 cement has a very high permeability.

The preliminary investigation presented in the paper shows that it is possible to optimize the concrete composition with packing density models in order to lower the cement content while retaining satisfactory mechanical properties. Future research aims at further optimizing the cement and filler content in ecological concrete by making use of particle packing models. The particle packing theory can be extended to the fine materials such as cement and fillers in order to improve the durability of LCCC.

Sonja Fennis
Delft University of Technology
Civil Engineering and Geosciences
Concrete structures
Stevinweg 1
2628 CN Delft, The Netherlands
S.A.A.M.Fennis@TUDelft.nl

Prof.dr.ir. J.C. Walraven
Delft University of Technology
Civil Engineering and Geosciences
Concrete structures
Stevinweg 1
2628 CN Delft, The Netherlands
J.C.Walraven@TUDelft.nl

Ir. J.A. den Uijl
Delft University of Technology
Civil Engineering and Geosciences
Concrete structures
Stevinweg 1
2628 CN Delft, The Netherlands
J.A.denUijl@TUDelft.nl

EARLY AGE SHRINKAGE CRACKING OF FIBRE REINFORCED LIGHTWEIGHT AGGREGATE CONCRETE

Oliver Fenyvesi
Budapest University of Technology and Economics, Budapest, Hungary
Zsuzsanna Józsa, Supervisor

Traditionally, reinforcing bars are used also to control cracks in concrete (caused by for example early age shrinkage or thermal expansion), which is a very expensive solution for these problems. Fibre reinforced concrete (FRC) is another optional solution. It has many advantages compared to normal steel reinforced concrete: it is more resistance against cracking, its toughness is higher. Its reinforcing materials: polymer, glass and carbon have higher corrosion resistance than steel has, higher tensile strength to weight ratio is available, it is easy to handle and apply them, have high magnetic permeability and they can even be cheaper. These are the reasons for performing laboratory tests in this field of concrete research.

Laboratory tests have been carried out according to Austrian Fibre-concrete directive with fibre reinforced lightweight aggregate concrete, in particular with regard to early age shrinkage and shrinkage cracks. During the laboratory tests compressive strength and flexural tensile strength were also examined. Two different relatively thin and short fibres fabricated from poly-acrylnitrile (PAN) and non alkali resistant E-glass were used.

Measurements were made according to the Austrian fibre-concrete directive 2002 (Faserbeton Richtlinie 2002). In *Figure 1* there is a special ring specimen made accordance to the Austrian directive to measure early age shrinking cracks length. There are steel laminas in the formwork which can be the starting point for cracks. The specimens were put in a special wind tunnel at the age of two hours and handled five hours long. After this experiment cracks developed on the surface of the specimen. With the same specimens further experiment was carried out in a traditional tumbler dryer. To compare concrete mixture's tends to crack, the length of cracks were measured and added to each other in case of every specimens after each curing. On *Figure 2* can be seen a crack on the specimen, its starting point is at the end of the lamina.

Figure 1 Ring specimen

Figure 2 Crack on ring specimen

During the laboratory tests fibres affect on early age shrinkage, on flexural tensile strength and on shrinkage cracks of course were examined. Compressive strength on standard cube specimens has been tested to verify the property of concrete.

The results were a little bit surprising: the early age shrinkage was the same in case of every (with or without fibres) mixture, but the summarized crack lengths were much longer in specimens made without fibres than in FRC (made with PAN or E-glass fibres) specimens. It means strain caused by early age shrinkage in case of FRC made with thin and short fibres is the same than of normal concrete. The conclusion is that with right mixtures and fibre reinforcement, except of applying extra steel reinforcing bars, cracks could be reduced, but strain caused by early age shrinking has to be calculated with during designing FRC structures.

Oliver Fenyvesi
Budapest University of
Technology and Economics
Department of Construction
Materials and Engineering
Geology
Műegyetem rkp. 3.
Budapest, Hungary
oliver@drotposta.hu

Zsuzsanna Józsa
Budapest University of
Technology and Economics
Department of Construction
Materials and Engineering
Geology
Műegyetem rkp. 3.
Budapest, Hungary
zsjozsa@epito.bme.hu

Proceedings-CD file name:
144_Feys.pdf

THE RHEOLOGY OF FRESH SCC: A COMPROMISE BETWEEN BINGHAM AND HERSCHEL-BULKLEY?

Dimitri Feys
Ghent University, Ghent, Belgium
Geert De Schutter and Ronny Verhoeven, Supervisors

Introduction

Self-Compacting Concrete (SCC) is a special type of concrete which does not need any form of external compaction. The addition of superplasticizers (SP) makes the concrete very fluid. In this way, SCC is able to fill a formwork of almost any shape completely. The reduction of the amount of coarse aggregates and the incorporation of mineral additives, so called fillers, prevent the concrete from blocking and segregation. This new type of concrete is suited for a new placing technique: The concrete will be pumped into the formwork from the bottom and will rise due to the applied pressure. In order to be able to understand the phenomena during pumping operations, the rheological properties of SCC must be investigated and controlled.

The rheology of fresh SCC

The rheological properties of fresh SCC have been investigated by using two different large scale rheometers: The Contec viscometer 5 and a Tattersall rheometer. In both rheometers, a similar test procedure has been applied in order to eliminate the influence of thixotropic effects.
Different rheological models have been applied to the obtained results. The application of a linear model (Bingham), characterized by a yield stress and a plastic viscosity, resulted in negative yield stresses, which is physically impossible.
When investigating the results more in detail, some shear thickening can be observed. In literature, this behaviour has been described by the Herschel-Bulkley equation, indicating shear thinning (n < 1), shear thickening (n > 1) or the Bingham model (n = 1).

$$\tau = \tau_0 + K \cdot \dot{\gamma}^n \quad (1)$$

The application of this equation resulted in a positive yield stress and an even better correlation of the data points ($R^2 > 0.99$). Although this model is not suitable for physical interpretation:

- The consistency factor 'K' has a dimension dependent on the value of 'n'. As a result, this dimension is variable and the parameter 'K' has no explicit physical meaning.
- Due to a mathematical restriction, this equation is forced to be horizontal for low values of the shear rate, resulting in an overestimation of the yield stress.

In order to overcome these problems, a third model has been applied: the modified Bingham model (fig. 1):

$$\tau = \tau_0 + \mu \cdot \dot{\gamma} + c \cdot \dot{\gamma}^2 \quad (2)$$

This model can be considered as an extension of the Bingham model with a second order term, but can also be interpreted as a second order Taylor development of the Herschel-Bulkley equation. As a result, it has been proved that the ratio of c/μ can also be regarded as a parameter able to describe shear thickening.

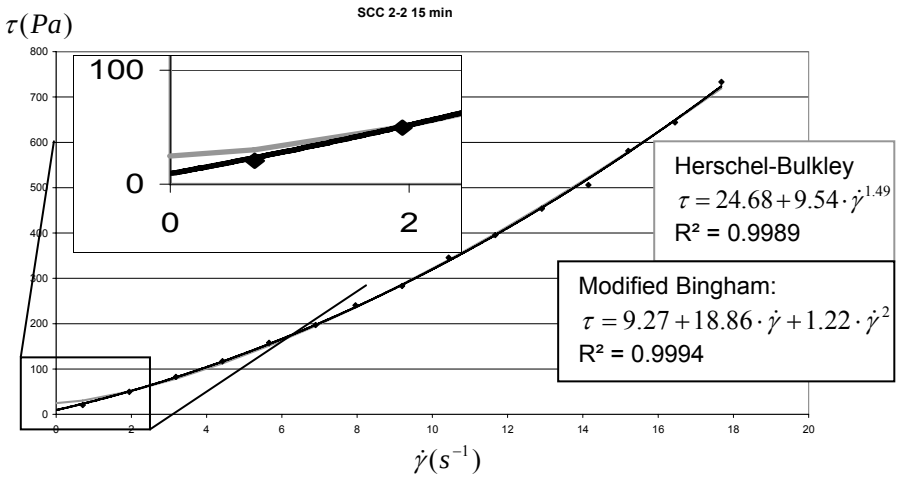

Figure 1: Application of the Herschel-Bulkley equation (grey curve) and the modified Bingham model (black curve) on the data of the reference mix. The enlarged area shows the estimation of the yield stress in the region of low shear rates

Dimitri Feys
Ghent University
Department of Structural Engineering
Magnel Laboratory for Concrete Research
Technologiepark 904
9052 Zwijnaarde, Belgium
Dimitri.Feys@UGent.be

Geert De Schutter
Ghent University
Department of Structural Engineering
Magnel Laboratory for Concrete Research
Technologiepark 904
9052 Zwijnaarde, Belgium
Geert.DeSchutter@UGent.be

Ronny Verhoeven
Ghent University
Department of Civil Engineering
Laboratory for Hydraulics
Sint-Pietersnieuwstraat 41
9000 Gent, Belgium
Ronny.Verhoeven@UGent.be

SHEAR TRANSFER OF CRACKED CONCRETE UNDER FATIGUE LOADING

Esayas Gebreyouhannes
University of Tokyo, Tokyo, Japan
Koichi Maekawa, Supervisor

The degradation of shear transfer due to aggregate interlocking mechanism under single sided fatigue loading was experimentally investigated in cracked normal strength concrete. Based on the experimental results, an analytical model was proposed in which damage is expressed in terms of the accumulated normalized shear slip with respect to the associated crack opening. The proposed model can be used to extend the range of applicability of previously developed models for the static response of cracked interfaces subjected to shear.

For the purpose of experimental investigation, a vertical single crack was introduced on plain concrete specimens, by splitting, and a finite lateral stiffness was provided to counteract the free dilation. Shear fatigue loading was then applied and the development of shear slip, crack opening and confining stress were recorded with cycling of load. A total of four specimens were tested. Of which one was subjected to static loading and the other three were subjected to fatigue loading, at a frequency of 1.5 Hz. Constant amplitude levels at low, moderate and high load levels were treated to investigate the sensitivity of damage to the loading amplitude.

In normal strength concrete crack occurs along the interfacial zone, which is the weakest link, leading to rough crack interface. Hence during loading, each incremental shear load is accompanied by shear slip associated with dilation. The dilation is attributed to the meandering nature of the crack interface. The overall behaviour under static loading is characterized by a gradually softening response and upon unloading the shear slip is almost irrecoverable. This indicates that the behaviour is governed by fracturing and plastic deformation.

It is observed that, the shear fatigue response of cracked interfaces at constant amplitude is characterized by continuous development of shear slip and dilation in a decreasing rate; the rate being dependent on the maximum load level, for the same initial crack width. Upon cycling of load the crack interface is subjected to continuous crack opening and closure. These cyclic movements with in the crack interface lead to gradual smoothening of the interface. Thus each subsequent loading is required to mobilize additional slip to develop an equal amount of shear load.

At low load level, τ_{max} = 1.07 MPa, (around 33% of the ultimate static capacity) the damaging effect is relatively small and with further cycling of load, a stable situation was attained, in which the incremental displacements are negligibly small. On the other hand, the damaging effect in case of moderate, τ_{max} = 2.26 MPa, and high, τ_{max} = 2.79 MPa, amplitude levels is relatively large with higher values for the later case. Besides, each subsequent loading cycle is accompanied by an associated incremental slip and dilation, although the dilation progress for high amplitude loading is not significant. Figure 1 shows the fatigue response at moderate maximum load level. The different rate of damage progress observed for different load levels is the reflection of the nature of contacting mechanisms under static loading. Generally the

damaging effect due to fatigue decreases with cycling of load, majority of the damage occurring during the early loading cycles. The accumulated shear slip at peak loading versus the number of cycles is observed to follow an almost linear trend on log scale.

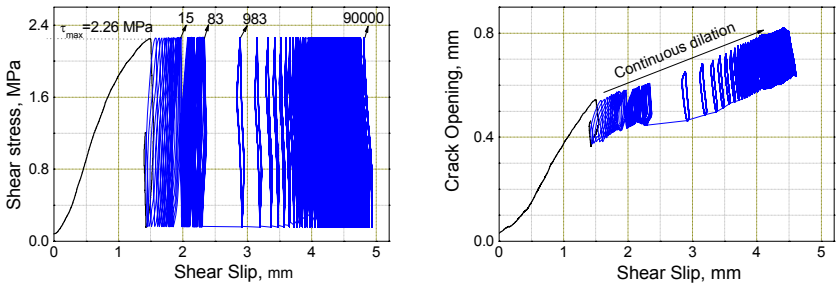

Figure 1 Response for Moderate Amplitude Shear Loading

The crack deformational path in case of fatigue loading is characterized by relatively smaller dilation as compared that of static loading for the same slip values. Hence the incremental slip in fatigue loading is less governed by overriding movements. This important difference indicates that, applying fatigue at low maximum load levels create increased probability of contact between the asperities, thus leading to longer life. Therefore the fatigue life of cracked interfaces is found to be highly dependent on the maximum shear load level.

Based on the physical understanding of the experimental results an analytical model is proposed for the shear fatigue of cracked concrete interfaces. The degeneration of shear response is expressed as a function of accumulated slip normalized by the crack opening. This fatigue modification factor was introduced in to the Contact Density Model [Maekawa et.al] in which the transferred shear stress along rough cracks is expressed as a function of intrinsic shear slip normalized by the crack opening. See Eq. [1].

$$\tau = X.\tau_o(\delta/\omega)$$

$$X = 1 - \frac{1}{10}\log_{10}\left(1 + \int\left|d\left(\frac{\delta}{\omega}\right)\right|\right) \quad ,\geq 0.1 \tag{1}$$

To put it in a nut shell, in this study it has been found that aggregate interlocking is a viable mechanism even under high cyclic loading and is characterized by gradual deterioration of the interface. The progress of damage is observed to follow a linear trend in the logarithmic scale. Accordingly a simplified model was proposed for the degeneration of shear response at high cyclic loading.

Esayas Gebreyouhannes
University of Tokyo
Department of Civil Engineering
Faculty of Engineering
7-3-1 Hongo, Bunkyo-ku,
Tokyo, 〒 113-8656, Japan
esayas
@concrete.t.u-tokyo.ac.jp

Prof. Koichi MAEKAWA
University of Tokyo
Department of Civil Engineering
Faculty of Engineering
7-3-1 Hongo, Bunkyo-ku, Tokyo,
〒 113-8656, Japan

NUMERICAL ANALYSIS FOR PREDICTING THE LOAD DISTRIBUTION IN WOOD STRESSED-SKIN PANELS

Christophe Gerber
The University of Technology, Sydney, Australia
Keith Crews & Christophe Sigrist, Supervisors

Between 2002 and 2006, a major research and development project has been undertaken at the University of Technology, Sydney, to investigate and quantify the structural performance of stressed-skin panel (SSP) floor systems. The project involved full-scale testing of 27 specimens, constructed in a variety of configurations and subjected to a series of non-destructive and destructive tests, which enabled identifying the serviceability and ultimate responses of SSP specimens.

Numerical procedures have also been developed within the frame of the subject research. A mathematical procedure derived from the grillage theory has been assembled using Matlab software package, and a finite element model (FEM) ─ discussed comprehensively in the paper ─ has been developed with the support of ANSYS software package. Both models are capable of accurately predicting serviceability responses of SSP structures. FEM also enabled identifying the load and/or stress distribution in SSP systems.

In order to account for the complexity of SSP decks, a hybrid FEM, which comprises solid, shell and contact elements, has been developed. FEM can simulate accurately the responses of SSP systems under uniformly distributed line loads and concentrated point loads, i.e. the quantitative and qualitative predictions of FEM accord well with the laboratory results. For example with a concentrated point load applied on an exterior joist, the plots (Figure 1) indicate that FEM predictions are very accurate for the joist under load and the adjacent joist. In Figure 2, the simulation of the deformed specimen under this eccentric point load is depicted.

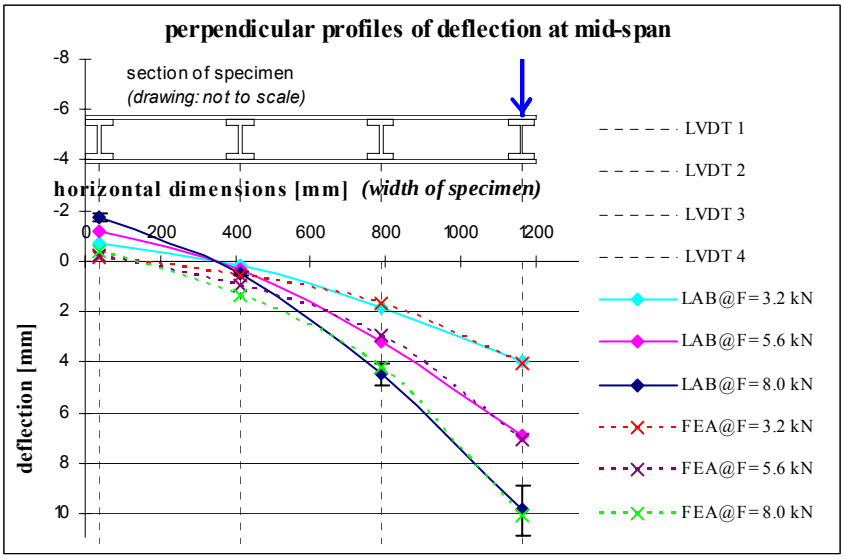

Figure 1: Point load on exterior joist – deflection profiles at mid-span

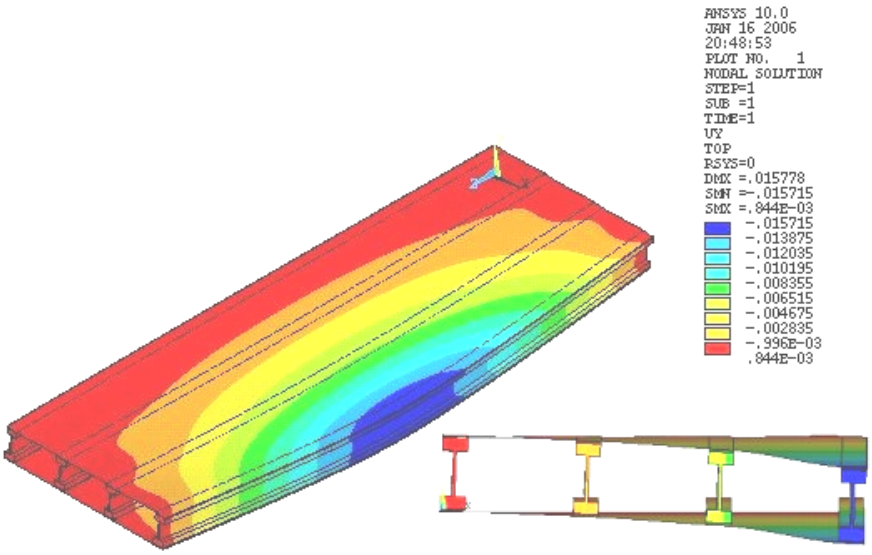

Figure 2: Point load on exterior joist –deformed deck and mid-span profile

The subject research has demonstrated that use of FEM has the ability to quantify the deflections and predict the deformed shape of SSP systems with different constructions and changing boundary conditions. On the basis of this work, it is concluded that the concept (model attributes) and parameterisation (material parameters) of the hybrid model proposed in this paper is appropriate for predicting the serviceability behaviour of SSP systems.

Christophe Gerber
The University of Technology, Sydney
Faculty of Engineering
City Campus, Rm 2/303
P.O. Box 123
Broadway, NSW 2007
Australia
cgerber@eng.uts.edu.au

Prof. Keith Crews
The University of Technology, Sydney
Faculty of Engineering
City Campus, Rm 2/510
P.O. Box 123
Broadway, NSW 2007
Australia
keith.crews@uts.edu.au

Prof. Christophe Sigrist
Berner Fachhochschule
School of Architecture, Civil and Wood Engineering
Route de Soleure 102
2504 Biel-Bienne
Switzerland
Christophe.Sigrist@bfh.ch

INVESTIGATION INTO THE EFFECT OF BITUMEN AGING

Eyassu Tesfamariam Hagos
Technical University of Delft (TU Delft), Delft, The Netherlands
A.A.A. Molenaar, M.F.C. van de Ven, Supervisors

Porous Asphalt (PA) surface layers, both single and two layer, reduce traffic induced noise effectively. The lower service life of a PA layer remains a major concern due to ravelling, i.e. the loss of aggregates from the surface layer. The two main factors contributing to the deterioration of the pavement surface are the actions of traffic and the environment. This paper deals with the environmental factors. Environmental factors include the effect of water damage and interaction with the atmosphere resulting in the aging (hardening) of the binder. The main theme of this paper is to look into the effect of aging of the bitumen/bituminous mortar in relation to PA durability. To understand the effect of aging on the bitumen performance and raveling failure of PA layer, rheological, mechanical, and chemical properties of bitumen were used to determine bitumen properties. Binders from accelerated laboratory aging and binders extracted from field specimens were compared to correlate lab and field aging conditions. Preliminary results of the investigation indicate that conventional aging methods do not seem to simulate field aging of PA in terms of the chemical changes in the process of bitumen aging. The results also strengthen the assertion that loss of stones from the PA surface (raveling) occurs as a result of age hardening and low temperature effects anticipated in the field. This implies that both high and low temperatures are important factors in view of the fact that the aging of the bituminous material occurs at a higher rate at high temperatures (summer periods) resulting in poor performance of the surface layer at low temperatures (winter periods) leading to raveling.

From the test results, it can be deduced that the aging of the binders has no significant effect on the fatigue performance of the binders according to the evaluation based on the fatigue parameter Np. The parameter Np is a fatigue resistance indicator that designates the fatigue life to crack propagation which is the transition from the damage initiation to damage propagation. An important assumption with regard to PA is that the higher the rate of damage development in the binder, the higher the acceleration of damage due to additional factors such as water damage or freeze and thaw actions leading to stripping of the stones. From a practical point of view, a plausible argument on the raveling of PA layers is that it occurs as a result of aging and low temperature effects (coupled with likely freeze and thaw cycles during the winter season) in addition to the actions of traffic. Besides, low temperatures are considered critical to the performance of PA since the self healing potential of bitumen at low temperatures is very low. This increases the damage accumulation in the binding material and is worsened by the effect of age hardening of the bitumen. Hence, age hardening of the binder, which is accelerated at higher pavement temperatures, contributes to damage development at low temperatures.

Investigation into chemical characterisation of unaged bitumen, laboratory aged bitumen and bitumen samples obtained from field specimen is shown in Figure 1. The Infra red (IR) spectrum in Figure 1 shows that the conventional laboratory aging method does not agree with field aging, the combination of UV exposure and temperature aging, however, seems to closely simulate the field aging process. Field aging results in two oxidation products known as ketones (C = O) and sulfoxides (S = O) identified by peaks at 1600 cm^{-1} and 1030 cm^{-1} respectively in Figure 1.

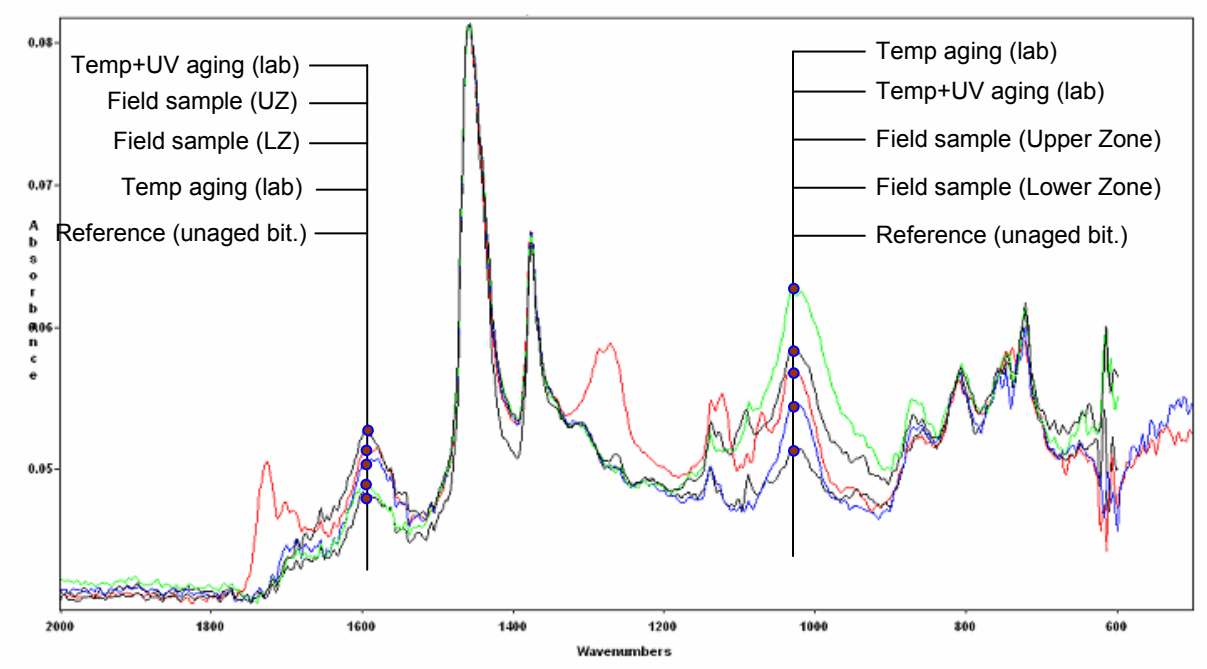

Figure 1: IR test results in the finger print region for reference bitumen, bitumen recovered from accelerated laboratory aging and field asphalt specimens

Based on the analysis of test results in relation to the effect of binder aging and durability of porous asphalt, the following conclusions are drawn:

1. At intermediate pavement temperature (20^{o}C), binder age hardening does not seem to have significant effect on the fatigue performance of the binder, according to the fatigue performance indication parameter Np.
2. Based on the chemical characterization (IR spectroscopy), the lower zone in PA layer is less aged than the upper zone.
3. According to the chemical results, the combined effect of temperature and UV light aging agrees with the upper zone field aging of a PA layer.
4. Aging occurs at high temperatures and raveling takes place mainly at low temperatures.

E.T. Hagos
Technical University of Delft
Civil Engineering and Geosciences
Road & Railway Engineering
P.O. Box 5048, 2600 GA
Delft, The Netherlands
E-e.t.hagos@citg.tudelft.nl

Prof. Dr. Ir.
A.A.A. Molenaar
Technical University of Delft
Civil Engineering and Geosciences
Road & Railway Engineering
P.O. Box 5048, 2600 GA
Delft, The Netherlands
E-aaa.molenaar@citg.tudelft.nl

Assoc. Prof. M.F.C. v.d. Ven
Technical University of Delft
Civil Engineering and Geosciences
Road & Railway Engineering
P.O. Box 5048, 2600 GA
Delft, The Netherlands
E-m.vandeven@citg.tudelft.nl

CONSIDERATION OF THE DYNAMIC EFFECT OF INCREASED TRAIN LOADS FOR THE FATIGUE EXAMINATION OF CONCRETE BRIDGES

Andrin Herwig
Ecole Polytechnique Fédérale de Lausanne, Switzerland
Eugen Brühwiler, Supervisor

Introduction

Currently, parameters such as the velocity, fundamental frequency and the influence length are taken into account defining dynamic amplification factors for bridge action effects in examination of bridges. In this paper, the influence of carriage weight on dynamic amplifications is mapped first for wheel forces than for bridge action effects by the use of simple models.

Wheel force amplifications due to track irregularities

Wheel force amplifications are the most important cause for the initiation of dynamic interaction between bridge main girders and fatigue effective freight trains. Resonance is unlikely to occur as the speeds generally are much lower than the critical speed for the fundamental mode of the bridge which is most relevant for bridge force amplifications.
The most important cause for wheel force amplifications are track irregularities which excite vibrations of car body and wheel set masses (Ludescher 2004). The transfer function of the model is erected for two different masses for the “car body”. The curve of the higher mass is situated clearly below the curve of the lower one which means that wheel force amplifications with higher car body mass are lower. Particularly demonstrative is a one-mass oscillator as carriage model, where a located track irregularity is simulated by introducing an impulse by the release of an imposed deflection. The amplification factors decrease with increased carriage weight which confirms the findings made with the two-mass oscillator.

Modelling of the system carriage + bridge

The carriage is modelled as one-mass oscillators whose mass represents the modal mass of the corresponding natural mode of the carriage. Only translatory movements in the vertical direction are of interest. A one-mass oscillator of the carriage is a sufficient model since vibrations of a natural mode leading to maximum amplifications consist in vibrations of mainly one of two masses (carriage mass or wheel set mass). Also for the bridge a one-mass oscillator is chosen, representing modal mass and stiffness of the fundamental mode which leads to maximum fatigue action effects when vibrations are excited. The two one-mass oscillators are assembled to a two-mass oscillator with an excitation at the base of the carriage (Figure 1). The main simplification is the circumstance that the vehicle doesn’t drive but is excited by forced sinusoidal displacements whose frequency corresponds exactly to the fundamental frequency of the system.

Bridge action effect amplifications

The response of the model shows lower amplification factors for higher carriage masses in the stationary state. Also an impulse like excitation by the release of an imposed displacement of the carriage shows the same tendency. On the real bridge, the carriage

changes its position which has an influence on the intensity of the excitation and also higher modes are excited. Furthermore, in particular heavy carriages influence the fundamental frequency of the system during their passage (Ludescher 2004). But the position of the carriage is a parameter which falls out when comparisons between mass ratios are made. Hence, a two-mass oscillator model can be used. The decrease of dynamic amplification factor with increased traffic load can be confirmed by the interpretation of measurements (Hirt 1976), (ORE 1990)

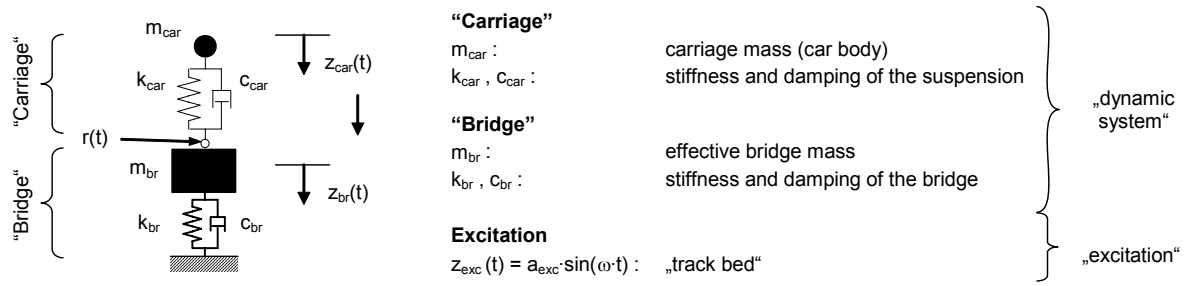

Figure 1: Model of the two-mass oscillator for the simulation of the carriage-bridge interaction

References

Hirt, M.A., 1976, Betriebsfestigkeit von Eisenbahnbrücken in Verbundbauweise am Beispiel der Morobbia-Brücke, EPFL, Switzerland.

Ludescher, H., 2004, Berücksichtigung von dynamischen Verkehrslasten beim Tragsicherheitsnachweis von Strassenbrücken, EPFL - DGC - MCS, Lausanne, Thèse N° 2894, Switzerland.

ORE, 1990, Messbericht SBB Nr. 1.1, Beanspruchung und Festigkeit der Fahrbahnplatte in Stahl- und Spannbeton bei Eisenbahnbrücken, Berne, Switzerland.

Andrin Herwig
Ecole Polytechnique
Fédérale de Lausanne
(EPFL)
Structural Institute-MCS
Station 18
Lausanne, Switzerland
andrin.herwig@epfl.ch

Eugen Brühwiler
Ecole Polytechnique
Fédérale de Lausanne
(EPFL)
Structural Institute-MCS
Station 18
Lausanne, Switzerland
eugen.bruehwiler@epfl.ch

INFLUENCE OF CURING ON THE PROPERTIES OF CONCRETE PAVEMENTS

Jürgen Huber
Technical University of Munich, Munich, Germany
Peter Schießl, Supervisor

The surface of concrete road pavements is extremely stressed by traffic and environmental impacts. In order to receive a high-quality concrete, selected raw materials in proper composition have to be processed accurately. The achievement of the designated properties in the surface-near concrete is only possible by means of good curing. Because of the missing formwork in comparison to structural engineering, concrete roads have to be cured intensively, in order to protect the fresh concrete from drying. On site normally liquid curing compounds are used because of the cheap and easy implementation in the whole construction process. These are to be applied directly after the drying of the concrete surface.

In extensive examinations several measuring methods und other parameters were tested and compared, in order to evaluate the effectiveness of different curing compounds and methods. Starting with basic tests concerning the time-dependent water-loss of concrete and the optimal application time for the application of curing compounds, a simple test using a litmus-paper was developed. Several test methods for the density (air-permeability, capillary adsorption, carbonation depth) and the strength (compressive strength, flexural tensile strength) were tested and evaluated. Subsequently these methods were used to evaluate the effectiveness of curing methods like different curing compounds, humid burlaps, water-curing and waterproof sealing under different external conditions (20°C / 65% RH and 30°C / 40% RH).

Examining the concrete properties, a dependency between the water-loss after a certain period of time (here: about 24 hours after mixing) and the measured density of the concrete was found. The effectiveness of a curing compound itself depends of the application time, see fig. 1.

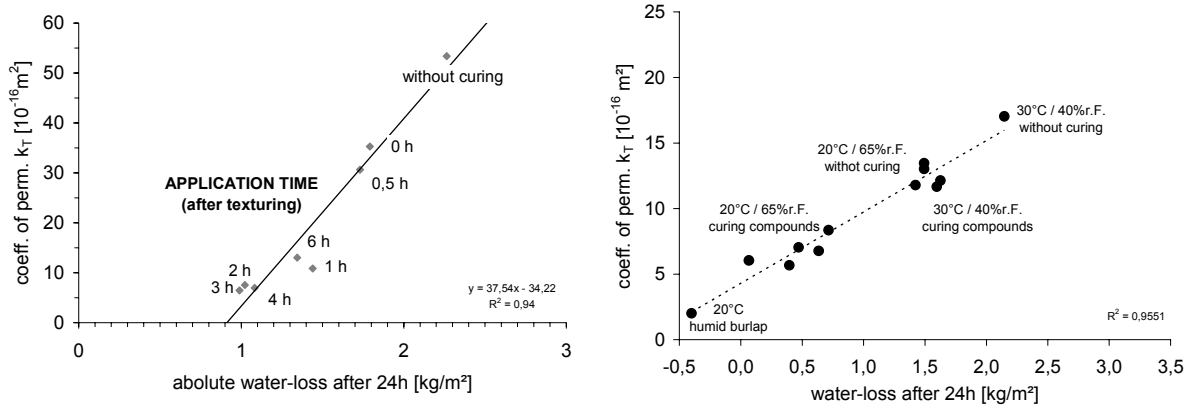

Figure 1: Permeability coefficient k_T and water-loss after 24 hours;
fig. left: Variation of the application time of one curing compound;
fig. right: Variation of curing compounds, curing and storing conditions

An analysis of the influence of curing on the secondary surface properties (grip) showed no significant correlation.

Subsequently to this practical approach the water distribution (free, physically and chemically bound water) of cured and uncured specimens is examined. In ongoing tests the depth- and time-depended water distribution is measured in order to develop a physical model for predetermining the concrete properties in relation to curing. This should be the basis for the optimization of the type and the duration of curing methods depending on the given concrete and environmental conditions.
Fig. 2 shows exemplarily the proportions and distributions of water of an uncured specimen with w/z = 0,45 at 24 hours after casting. The water-loss due to evaporation is measured by weighing, the free and physically bound water by drying at 105°C (W105) and the chemically bound water by drying at 1000°C (W1000).

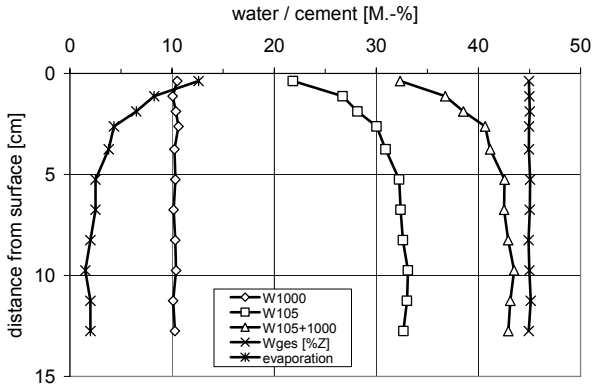

Figure 2: Water distribution in an uncured mortar 24 hours after casting; Climate: 23°C / 50% r.h.; CEM I 42,5R; w/z-ratio 0,45

24 hours after casting the water-loss due to evaporation (without curing) influences the free and physically bound water, but not yet the hydration progress. This takes place afterwards.

Jürgen Huber
TU Munich
Dep. For Civil Engineeriung
Cen. for Building Materials
Baumbachstrasse 7
81245 München, Germany
j.huber@tum.de

Univ.-Prof. Dr.-Ing. Dr.-Ing. E.h.
Peter Schießl
TU Munich
Dep. For Civil Engineeriung
Cen. for Building Materials
Baumbachstrasse 7
81245 München, Germany
schiessl@cbm.bv.tum.de

STRUCTURAL ASSESSMENT OF MULTI-CELL BOX GIRDER BRIDGES

Markus Just
Hamburg University of Technology, Hamburg, Germany
Viktor Sigrist, Supervisor

During the past decade structural assessment and strengthening of existing bridges have become a major challenge for structural engineers. Measures for repair of fully prestressed bridges, which are for example damaged by cracks in coupling joints, or strengthening tasks due to increased loads and stricter regulations, respectively, require detailed structural analyses of the existing structures. To get reasonable results from such investigations, suitable internal forces as input parameters are needed.
For box girder bridges under eccentric loading the load distribution and the flow of forces are of special interest. Therefore, the contribution focuses on the shear forces in such structures. Methods of analysing box girder bridges and their advantages and disadvantages are discussed.

In analysing box girder bridges single- and multi-cell cross sections have to be distinguished. For single-cell box girder bridges two classic analysis methods can be applied: The representation of the cross section as one single bar or the analytical solution with analogy to the theory of folded plates. For areas where the applied load is completely distributed both methods lead to similar results. However, for the distribution of the shear forces within the disturbed regions and for short-span bridges, only the theory of folded plates or Finite Element analysis give adequate results for the shear force in the webs of the bridge.
For analysing box girder bridges with multi-cell cross sections under eccentric loading the classic ways to determine the internal forces in structures fail. Modelling as single beams gives inadequate results and the theory of folded plates leads to very complex calculations. Hence, it is appropriate to use computer analysis methods to examine such structures. The two common ways of modelling box girder bridges, either as girder grids or with finite elements, are discussed in the contribution.

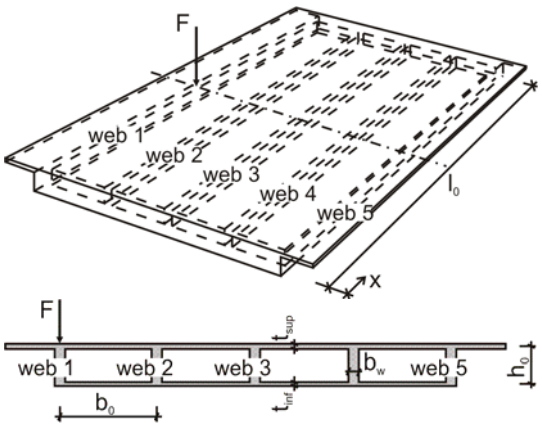

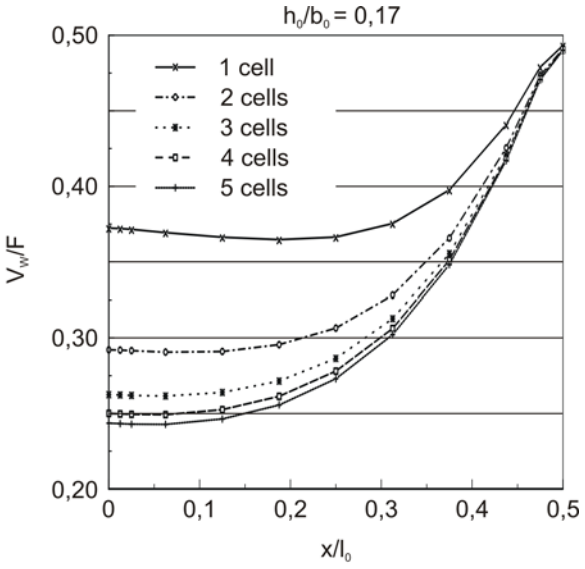

Above: Four-cell, single-span bridge
Right: Shear force in the loaded outer web for h_0/b_0 = 0.17

To understand the behaviour of multi-cell box girder bridges under eccentric loading first a parametric study with Finite Element models using shell elements was conducted. The results are presented in the second part of the paper.
It can be seen that the height-to-width ratio $\lambda = h_0/b_0$ of the cross section is the main parameter that influences the load distribution in eccentrically loaded box girder bridges. The maximum shear force in the loaded outer web decreases with decreasing λ and aligns for high values of λ. This statement is also true for the distribution of shear forces along the longitudinal axis, x.
The number of spans has only minor influence on the flow of forces in the loaded span. The distribution of shear forces in the webs is only affected by a second span, whereas additional spans lead to similar results.
Finally a load case according to DIN-FB 101 is introduced to demonstrate the practical relevance of an accurate modelling of eccentrically loaded box girder bridges. The results show that the dominating influence of the equally distributed loads evens out the shear forces in the web. However, it can be seen that the influence of eccentric loading is still significant enough to justify a detailed modelling.

The second possibility is to model box girder bridges as girder grids. Such models are easy to assemble and the computing time is reasonably shorter in comparison with Finite Element analyses. After describing the way of assembling girder grid models, the results of the calculations are discussed.
The analyses show, that a precise representation of the effects of eccentric loading is not possible on the basis of girder grid models. Especially the improper representation of the load transfer in lateral direction is a problem of girder grid models of multi-cell box girder bridges. But due to the mentioned advantages such models are still a suitable tool for first surveys of bridge structures.

The final part of the contribution gives an outlook on the necessary future steps in analysing multi-cell box girder bridges under eccentric loading. First material nonlinearities have to be introduced and then analyses of typically weak points in single- and multi-cell box girder bridges using stress fields have to be conducted.

Markus Just
Hamburg University of Technology
Institute of Concrete Structures
Denickestraße 17, R.3045
21071 Hamburg, Germany
markus.just@tu-harburg.de

Prof. Dr. Viktor Sigrist
Hamburg University of Technology
Institute of Concrete Structures
Denickestraße 17
21071 Hamburg, Germany
sigrist@tu-harburg.de

INFLUENCE OF DIFFERENT CFRP STRENGTHENING SYSTEMS ON THE BEHAVIOUR OF EXISTING CONCRETE ELEMENTS SUBJECTED TO BENDING

Marta Kaluza
Silesian University of Technology, Gliwice, Poland
Andrzej Ajdukiewicz, Supervisor

Abstract

The study was undertaken to compare active and passive strengthening systems for concrete members using externally glued CFRP-laminates. A series of four full-scale, reinforced concrete beams, 8.0 m long, was tested. Three were strengthened with CFRP and one was not strengthened, to act as a reference member. Variations between test beams were provided by different anchorage systems and whether the laminate was prestressed or not. The study was focused on the relationship between the different strengthening systems and the failure modes of the beams. Deflections of beams and cracks patterns for all strengthened elements are presented and discussed.

Introduction

Some buildings have to be replaced or strengthened by reason of necessity of load-bearing capacity increase. Strengthening system based on externally bonded Carbon Fibers Reinforced Polymer (CFRP) laminates can be regarded as being passive or active in behaviour. The passive method uses laminates bonded with no prestress or pre-tensioning. The active method uses some degree of pre-tensioning of the laminate before bonding.
This paper presents efficiency comparisons of three strengthening methods based on CFRP used for reinforced concrete beams: CFRP strip glued only, CFRP strip glued and additionally anchored at the ends, prestressed CFRP laminate with strip elongation 3‰. The limited current scope of this study means that results focus only on the most significant serviceability problems such as deflection, cracking and mode of failure for strengthened elements.

Experimental investigation and test results

Research was carried out on full-scale reinforced concrete elements with length of 8.0 m and rectangular cross-section of 0.25 m × 0.50 m. The elements were tested up to failure as simply supported beams in a typical four-point set-up. All strengthened beams were equipped with a set of strain gauges and a system of inductive sensors measuring beam deflection.
The introduction of CFRP laminate increased the equivalent moment of inertia and as a result caused an increase of flexural stiffness for the elements. This was directly responsible for the reduction in deformation of the strengthened beams.
The greatest reduction of deflection compared to the reference beam was observed for the prestressed element (see Figure 1). The prestress also caused a delay of debonding in comparison with the beam with glued and anchoraged laminate.
The second part of the study investigated crack development, regarding both pattern and width as well as load at onset.

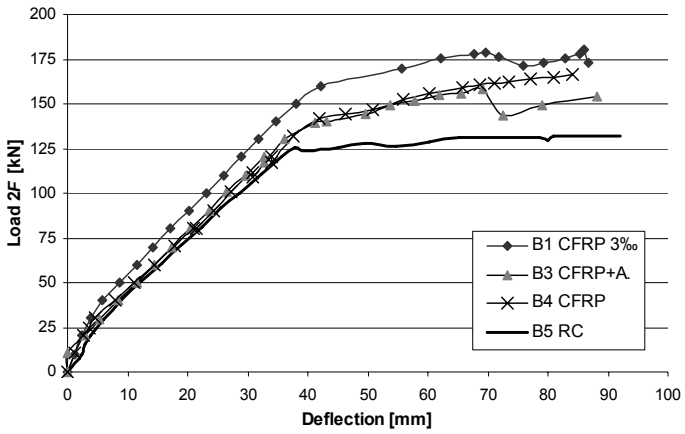

Figure 1 Load – deflection relation of all elements

Then the efficiency of the various strengthening systems at the ultimate load, obtained by considering the modes of failure and the failure loads of the beams, was discussed. In all tested elements several stages of failure were observed. The anchorages in beams B3 and B1 prevented premature debonding mechanisms and allowed for further element loading, even after complete delamination of CFRP laminate.

Conclusions

The following main tendencies in behaviour of strengthened elements were determined:

- In case of passive strengthening the insignificant reduction of deflection and lack of the influence on cracking were observed. At failure the increase in flexural capacity, up to 30%, in comparison with the non-strengthened beam was recorded.
- The prestressing of CFRP laminate has given the positive influence on deflection (significant reduction) and crack pattern of such strengthened beam. The strong reduction of the crack width was recorded. The load capacity was substantially increased – ca. 60% higher in comparison with the non-strengthened specimen.
- The usage of anchorages at the end of the laminate allowed to the further work of element after delamination.

The second part, currently in progress, will be concerned with the efficiency comparison of active strengthening applied for similar concrete beams, with different levels of prestress.

Acknowledgements

Special thanks to S&P Clever Reinforcement Company AG, Brunnen/Switzerland, for general help, know-how support and CFRP materials supply.

Marta Kaluza
Silesian University of Technology
Dept of Structural Engineering
Akademicka 5
Gliwice, Poland
Marta.Kaluza@polsl.pl

Andrzej Ajdukiewicz
Silesian University of Technology
Dept of Structural Engineering
Akademicka 5
Gliwice, Poland
Andrzej.Ajdukiewicz@polsl.pl

TIME DEPENDENT BEHAVIOUR OF ULTRA HIGH PERFORMANCE FIBRE REINFORCED CONCRETE

Aicha Kamen
Ecole Polytechnique Fédérale de Lausanne, Switzerland
Emmanuel Denarié, Eugen Brühwiler, Supervisors

Ultra High Performance Fibre Reinforced Concrete (UHPFRC) are produced by adding micro fibres and straight steel fibres (10 mm / 0.2 mm) to an ultra-compact cementitious matrix (cement CEM I 52.5, silica fume, fine sand with maximum size of 0.5 mm, water and superplasticizer). They contain a high volume of binder paste (0.88) with a very low water/binder ratio of 0.13.

UHPFRC are characterized by outstanding properties making them very suitable for rehabilitation. However, the influence of different curing conditions on the UHPFRC early age behaviour, particularly when these materials are used as overlays on new or existing structures, and their sensitivity to premature cracking are still not completely known. This paper reports on a series of investigations on a UHPFRC material to determine: (1) the relationship between the degree of hydration and the mechanical properties, (2) the autogenous shrinkage for various curing conditions, (3) the influence of fibres on the autogenous shrinkage.

The UHPFRC exhibits outstanding mechanical performance. From the test results and the fitted CEB-FIP models (see figure 1a), one can observe that the MOR and the elastic modulus tend to develop quicker at early age than the compressive strength. The MOR increased to 83% of its 90 day value after 3 days, the modulus of elasticity increased to 90% of its 90 day value after 7 days, and the compressive strength increased to 78% of its 90 day value after 7 days. Thus the relative rate of development of the modulus of elasticity is higher than the rates of the MOR and compressive strength. This quicker rise in elastic modulus results in a built-up of tensile stresses, which may increase the early age cracking sensitivity.

The loss on ignition test results shown that the development of the degree of hydration (α) is fast at early age due to the heat produced during the hydration reactions and this heat further accelerates the hydration process. The low UHPFRC degree of hydration (α = 26% at 90 days) was confirmed by the application of the Powers model adapted by Jensen *et Hansen.*

A strong correlation was found between the degree of hydration and the compressive strength. The development of the mechanical properties is accompanied by the change of material structure on the nano- and micro-scales and is related to the hydration process. A high strength is reached at low degree of hydration because this material is characterized by a low w/b ratio. This effect can be attributed to the initial dense packing of the cement particles which rapidly provides the small amount of gel required for bonding together the hydrating particles.

The autogenous shrinkage results confirm that this UHPFRC has a rapid kinetic of autogenous shrinkage. After 7 days, 39% of the 365 days value was reached. This quick autogenous shrinkage development at early age is attributed to the rapid hydration process, as shown before, the reduction of the internal relative humidity and the evolution of the

microstructure resulting in a modification of the pore structure. This modification is associated with a decrease of the mean pore radius size and an increased capillary tension, leading to a large shrinkage of the solid skeleton.

Elevated curing temperature initially increased the rate of autogenous shrinkage. In the long term, the predicted autogenous shrinkage was lower at temperatures higher than 20°C. The influence of temperature on the autogenous shrinkage evolution is attributed to the hydration process and the self-desiccation which accelerates at higher temperatures. The model proposed by Loukili was used to estimate the ultimate autogenous shrinkage for various curing conditions (20, 30, 40°C). The highest ultimate autogenous shrinkage is obtained at 20°C (see figure 1b). This result is in accordance with the evolution of the degree of hydration for different curing conditions obtained in our experiments.

The autogenous shrinkage results demonstrate that the presence of fibres (micro and macro fibres equal to 6%) decreases the autogenous shrinkage by 35% when compared to the matrix of UHPFRC without fibres. Indeed fibres can hinder the deformations in the micro-level. This result confirms trends documented in literature.

a) *b)*

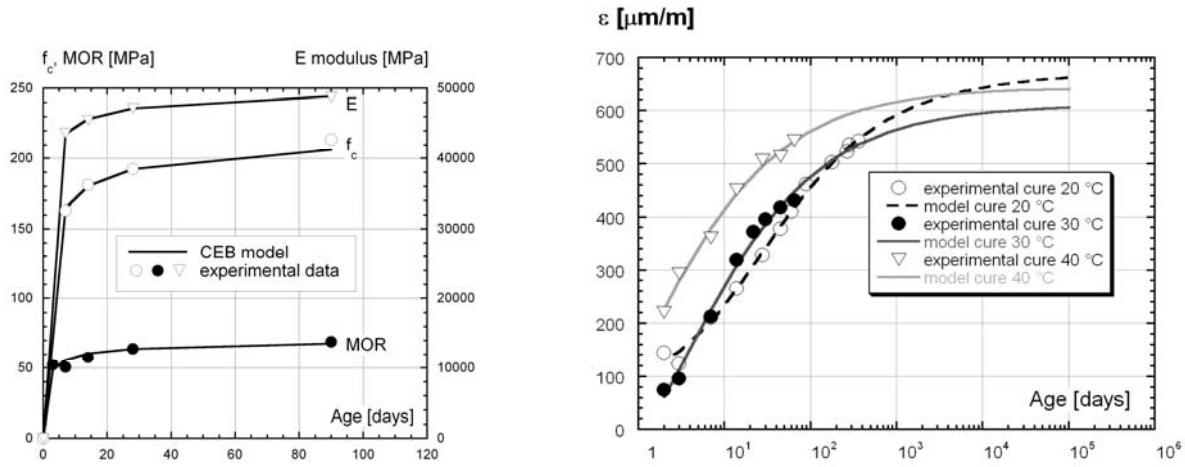

Figure 1 a) Mechanical properties as a function of time;
b) Predicted autogenous shrinkage for various curing temperatures

Aicha Kamen
Ecole polytechnique fédérale de Lausanne - EPFL
Environnement Naturel, Architectural et Construit -MCS
Institute of structures
Station 18
1015 Lausanne, Switzerland
aicha.kamen@epfl.ch

Eugen Brühwiler
Ecole polytechnique fédérale de Lausanne - EPFL
Environnement Naturel, Architectural et Construit -MCS
Institute of structures
Station 18
1015 Lausanne, Switzerland
eugen.bruehwiler@epfl.ch

Proceedings-CD file name:
222_Keunecke.pdf

MICROMECHANICAL PROPERTIES OF COMMON YEW AND NORWAY SPRUCE LOADED IN THE RADIAL-TANGENTIAL PLANE

Daniel Keunecke
ETH Zurich, Switzerland
Peter Niemz, Supervisor

Newly developed construction materials are more and more modelled on natural structures nowadays. Due to its relatively low density and at the same time high stability, wood is a typical prototype for lightweight construction. Thus, investigation on the relationships between structure and failure behaviour of wood by appropriate test procedures is an essential task for basic research in the field of wood.

A typical example for wood testing is described in this study by means of two gymnosperms, Common yew (*Taxus baccata* L.) and Norway spruce (*Picea abies* [L.] Karst.). They differ in their microscopic structure and the mechanical characteristics of their wood. Compared to spruce, the high dense yew wood is stronger and simultaneously more elastic when loaded parallel to the grain. However, no information about the transverse mechanical behaviour of yew is available from literature so far.

In this study, therefore, both wood species have been loaded in the radial-tangential plane (crack opening mode I). For this purpose a micro wedge splitting test was applied. The specimen geometry can be seen from figure 1.

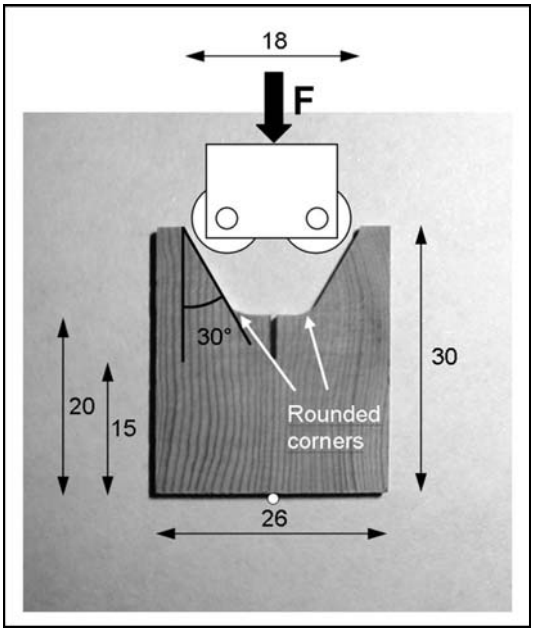

Figure 1 Yew specimen. All dimensions in mm. Specimen thickness: 4 mm

Characteristic fracture parameters (initial slope, critical load, work to ultimate load, specific fracture energy) were determined. The results show that yew wood was significantly stiffer than spruce wood. This means that yew is an outlier when compared to other gymnosperms since it is relatively elastic in the longitudinal direction (despite its high density) but at the same time very stiff in the transverse direction. The findings suggest the density respectively the cell geometry to be mostly responsible for the elastic behaviour in the transverse direction.

Daniel Keunecke
ETH Zurich
Department of Civil, Environmental and Geomatic Engineering
Institute for Building Materials
Schafmattstrasse 6
CH-8093 Zurich (Switzerland)
keuneckel@ifb.baug.ethz.ch

Prof. Dr. Peter Niemz
ETH Zurich
Department of Civil, Environmental and Geomatic Engineering
Institute for Building Materials
Schafmattstrasse 6
CH-8093 Zurich (Switzerland)
niemz@ifb.baug.ethz.ch

Proceedings-CD file name:
161_Khbeis.pdf

EXPERIMENTAL AND NUMERICAL INVESTIGATIONS OF POT BEARINGS

Halim Khbeis
Universitaet Karlsruhe (TH), Karlsruhe, Germany
Lothar Stempniewski, Supervisor

Keywords

Pot bearings, experimental research, FEM, thermoplastics.

Introduction

As becomes apparent with release of the new European standard EN 1337-5, the fundamental design rules for the load transmission of pot bearings, especially for lateral loads, did not enhance to the same degree as the choice of material or standard tests did. This pertains to the contact pressure distribution along the pot wall due to horizontal loads that are transferred via the piston rim, as well as to the negligence of three-dimensional effects for the load bearing behaviour. By taking an initial clearance between piston rim and pot wall it is becoming obvious that there will be a more concentrated load transfer than over the half circumference of the pot wall as assumed by the standard. The homogeneous connection of pot wall and pot bottom leads, as it results from the machining of the bearing pot out of a blank, necessitates the consideration of three-dimensional effects for a realistic prediction of the load bearing behaviour. Besides the stressing of the bearing pot a lateral load leads to an increase of the bearing clearance. As already noted (Roeder et al. 1999) this increase may lead to a failure of the internal seal and a leakage of elastomeric material. Although the internal seal is one of the most critical component of this structure, the standard design rules do not address the issue of the seal's sensitivity to the clearance.

Analyses of the Bearing Pot

Both numerical analyses and experimental research was conducted to investigate the load bearing behaviour of pot bearings. For the Finite-Element-Calculations the commercial solver ABAQUS v6.5 was used. The final Finite-Element-Model that was found by preliminary studies is built up by 3D 8-node continuum-elements with incompatible deformation modes (C3D8I). The elastomeric pad is considered by applying equally distributed surface loads in the original contacting joints of pad and pot. A simple J2-plasticity material law was used for the steel parts of the bearing. From such an analysis the locations for a later strain gauge application for biaxial load tests were identified. First horizontal load tests on a pot bearing with an internal diameter of 300mm showed a good agreement in the interesting, highest loaded parts of the bearing pot. With such a validated FE-model the investigation of the influence of further geometrical or loading parameters becomes possible, e.g. the dependence of the bearing clearance (gap width) on the ratio between horizontal and vertical loads or the horizontal load level. Such studies provide a basis for the investigation of the internal pot bearing seal.

Investigation of the Internal Pot Bearing Seal

Internal pot bearing seals perform the task of preventing elastomeric material form extruding from the pot. Due to their superb wear resistance that internal pot bearing seals are subjected to by the ongoing bridge movements, the use of thermoplastics is state-of-the-art for the material. For the purpose of investigating the behaviour such a seal was modelled for

plain-strain analyses with linear 4-node hybrid elements. The coupled deformation-pressure-formulation of these elements was necessary to manage the high Poisson ratio of plastics. Test results of fibre glass fibre-filled PTFE (Pohl 1999) have been used to calibrate the parameters for a two-network visco-plastic material law. Within these studies, the height of the seal and the compressive load has been varied for a constant seal width. The in-principle principle deformation is confirmed by several recent inspections on pot bearings (figure 1, right side) after tests as well as after several years in service (Khbeis et al. 2002). By plotting the increase of the resulting seal bulge against the gap width, a significant rising of the bulge becomes obvious, even for the load level of SLS according to EN 1337-5, which may result in damage and loss of serviceability of the seal with ongoing load cycles and reversed horizontal loads.

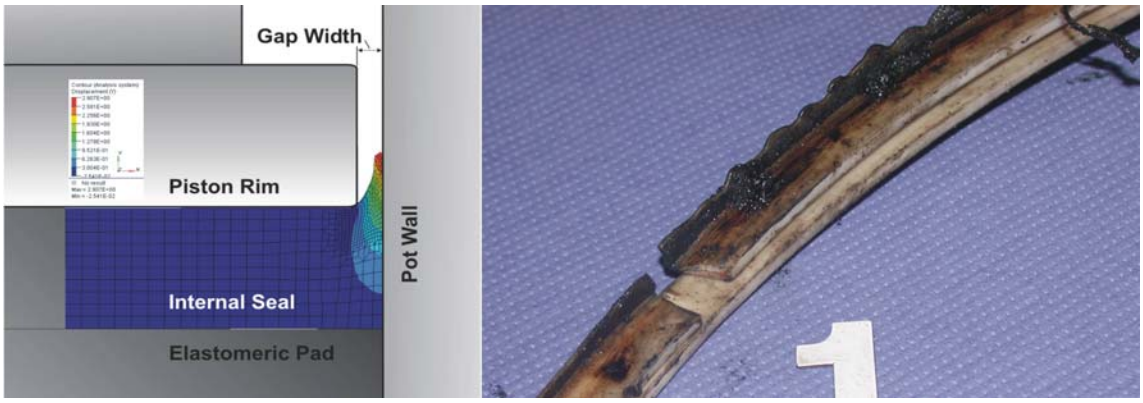

Figure 1 Principle deformation of the FE-mesh compared to a real bulge of an internal seal

Discussion and Future Prospects

With the present work it is shown that a prediction of the load bearing behaviour of pot bearings and internal seals under multiple load conditions is possible. Further tests and analyses have to be carried out for deducing more precise design rules for the load transfer in pot bearings that also address the sensitivity of the internal seals.

References

EN 1337-5, 2005, Structural bearings - Part 5: Pot *Bearings*, European Committee for Standardization, Brussels.

Khbeis, H., Zeller, W., Stempniewski, L., 2002, Testing of a Pot Bearing Ø 550 mm with a Newly Designed Seal, Report # 01 28 34 0973, MPA Karlsruhe, Germany.

Pohl, H., 1999, Computergestützte und experimentelle Untersuchungen von Manschetten-dichtungen aus glasfaserverstärktem PTFE-Compound, Ph.D. thesis, Universität der Bundeswehr Hamburg, Germany.

Roeder, C., Stanton, J., Campbell, I., 1999, High-Load Multi-Rotational Bridge Bearings, NCHRP Report 432, Washington, USA.

Dipl.-Ing. Halim Khbeis
Universitaet Karlsruhe (TH)
Department of Civil Eng.
Institute of Concrete
Structures and Construction
Material Technology
Gotthard-Franz-Straße 3
76131 Karlsruhe, Germany
halim.khbeis@ifmb.uka.de

Prof. Dr. L. Stempniewski
Universitaet Karlsruhe (TH)
Department of Civil Eng.
Institute of Concrete
Structures and Construction
Material Technology
Gotthard-Franz-Straße 3
76131 Karlsruhe, Germany
lothar.stempniewski
@ifmb.uka.de

DAMAGE DETECTION USING WAVELET TRANSFORM OF STATIC AND DYNAMIC STRUCTURAL RESPONSE

Anna Knitter-Piątkowska
Poznan University of Technology, Poznan, Poland
Andrzej Garstecki, Supervisor

The aim of the study is to discuss the efficiency of the discrete wavelet transform (DWT) in damage detection. Beam and plate structures are considered. Different signals of structural response in static and dynamic tests are analyzed. The experiments are simulated numerically using FEM. Measurement errors are accounted for by introduction of a white noise. The paper demonstrates by the way of examples, that the DWT analysis of the structural response signals can provide information on the existence and the location of a concentrated damage.

The detection, localization and estimation of damage in engineering structures has achieved much interest lately. New methods have been applied to structural identification lately, namely soft methods: artificial neural networks, genetic algorithms and fuzzy sets. In alternative approach, rooted in the theory of signal analysis, the wavelet transformation (WT) is used. The potential of WT in damage detection has been studied in (Gentile and Messina 2003, Wang and Deng 1999, Garstecki et al. 2004). It was demonstrated, that WT can very well extract the desired detailed information, caused by localized damage, from numerous data representing the global response of a damaged structure. Moreover, usually only experimental data referring to damaged structures are processed. In the majority of practical applications, WT is used in a discrete form, called the Discrete Wavelet Transform (DWT).

The aim of the present paper is to further recognize how the efficiency of DWT in damage detection depends on the type of excitation in experimental tests, the number of measurement points, the type of the structural response signal and the level of a white noise representing some measurement inaccuracy.

In this study the experiments are simulated numerically. Detection of damage in beam and plate specimens employing DWT is studied. Our task is to detect the damage and to specify its localization for various levels of a white noise in the structural response signals.

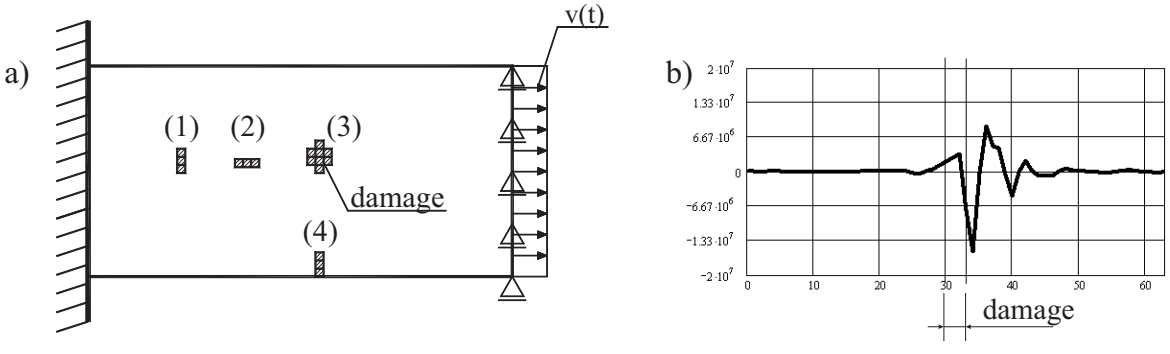

Figure 1 Plate structure; a) Various types of damage (FEM elements), b) Detail 1 of DWT of acceleration horizontal components, excitation by impulse velocity.

The damage is modeled as local stiffness reduction at small prescribed regions. We assume that the beams are subjected to static or harmonic concentrated loads. In the case of plates the experiments of the elastic wave propagation are used. Fig. 1a illustrates a plate with different forms of damaged zones, where the Young modulus has been reduced from

$E = 200\ GPa$ to $E_d = 10\ GPa$. Waves are induced by the displacements of the right edge of the plate with constant velocity $v = 10\ H(t)$ m/s, or impulse velocity $v = 10\ [H(t) - H(t - t_1)]$ m/s, where H is a Heaviside function and $t_1 = 1 \cdot 10^{-7}$ s. Various structural responses are analyzed. In the case of beams we use static vertical displacements and rotation angles or the amplitudes of dynamic displacement and acceleration. In plates, horizontal and vertical components of displacements (**u**), velocities (**v**) and accelerations (**a**) are subjected to DWT. Several different types of wavelets were used, however, most of them were Daubechies and the simplest Haar wavelets. Fig. 1b presents the DWT of the structural response signal in the form of the horizontal component of the acceleration in the set of 64 points distributed along the horizontal line in the plate. The wave was induced by the impulse boundary displacement. One can observe that damage was properly identified.
In this paper the one-dimensional DWT was used. The efficiency of the method was studied by the way of numerous examples, which proved that DWT provides good information on the existence and location of damage. The examples of damage detection in plates basing on wave propagation confirmed that the efficiency of damage localization strongly depends on the location of measurement points and on the point of time of measurements. Therefore detection of single or multiple damage zones requires the DWT processing of several structural response signals measured in various points in space and time domains. The damage was properly detected regardless of its location, in the middle or at the edge of the plate. The examples demonstrate that damage was properly localized also with some specified level of noise, representing measurement inaccuracy.
Great advantage of the wavelet transform is that the information on the response data of the undamaged structure is not required.

Acknowledgment

Support by Poznan University of Technology, grant BW 11-803/06, is kindly acknowledged.

References

Garstecki, A., et al., 2004, Damage detection using parameter dependent dynamic experiments and wavelet transformation, J. of Civil Eng. and Management, Vilnius Gediminas Technical University, Lithuania 10, No 3, 191-197.

Gentile, A., Messina, A., 2003, On the continuous wavelet transform applied to discrete vibrational data for detecting open cracks in damaged beams, Int. J. of Solids and Struct. 40, 295-315.

Wang, Q., Deng, X., 1999, Damage detection with spatial wavelets, Int. J. of Solids and Struct. 36, 3443-3468.

Anna Knitter-Piątkowska
Poznan University of Technology
Institute of Structural Engineering
Ul. Piotrowo 5
60-965 Poznań, Poland
anna.knitter@ikb.poznan.pl

Prof. Andrzej Garstecki
Poznan University of Technology
Institute of Structural Engineering
Ul. Piotrowo 5
60-965 Poznań, Poland
andrzej.garstecki@ikb.poznan.pl

A NOVEL FATIGUE TESTING FACILITY

Bernd Köberl
Vienna University of Technology, Vienna, Austria
Johann Kollegger, Supervisor

In case of a dynamic load structures can collapse even in case when the applied load is much lower than the ultimate limit static load. So the knowledge of the fatigue behaviour of different building materials is very important for the durability of structures.

For instance dynamic fatigue tests are carried out to evaluate the fatigue limit of stay cables as well as anchorages and couplings of post-tensioning tendons. For specimens with a maximum upper load of 2500 kN the axial stress range is applied by the means of servo-hydraulic controlled jacks. This approach enables testing frequencies up to 20 Hz. For specimens with a higher upper load the testing frequency decreases to less than one cycle per second. In Europe three accredited testing laboratories are able to do dynamic fatigue tests on big specimen like stay cables or tendons up to 55 strands. These laboratories (University of Technology in Munich, EMPA and LCPC (Laboratoire Central des Ponts et Chaussées)) apply the upper load and the cycling load by means of servo hydraulic controlled jacks. Due to the high test load for large specimens the testing frequency is lower than one cycle per second and so a fatigue test with two million load cycles takes 23 days. Furthermore a lot of energy is needed to cool down the oil of the hydraulic devices.

Development of a novel fatigue testing facility

The Institute for Structural Engineering at Vienna University of Technology has developed a novel fatigue testing facility for large specimens with testing frequencies from 25 to 50 Hz. The schematically setup can be seen in Figure 1. In the face of the high testing frequency the novel fatigue testing facility requires only a fractional amount of the energy which is needed by conventional facilities to carry out a test with two million load cycles. The dynamic load is applied via an unbalanced vibration generator and so no energy to cool down the hydraulic oil during the test is necessary. Due to the high testing frequency e.g. 25 Hz the time for two million load cycles decreases to 23 hours.

The specimen (e.g. a stay cable) and an auxiliary cable are tensioned with the aid of a static hydraulic jack. An unbalanced vibration generator which is placed at a coupling unit applies a harmonic load in axial direction to the specimen. On the one hand the coupling unit is used to connect the auxiliary cable and the specimen and on the other hand to carry the vibration generator. The stiffness of the testing frame has to be high, compared to the stiffness of the specimen and the auxiliary cable. If this condition is fulfilled the setup can simply be described as a single degree of freedom system. If the rational frequency of the unbalanced vibration generator, which can be adjusted by a frequency converter is equal to the eigenfrequency of the setup the applied load is increased because of resonance. Due to resonance the vibration generator has to apply only a fraction of the required load for the dynamic fatigue test, depending on damping of the setup. The eigenfrequency of the testing device depends on the stiffness of the specimen and the auxiliary cable as well as of the mass of the coupling unit.

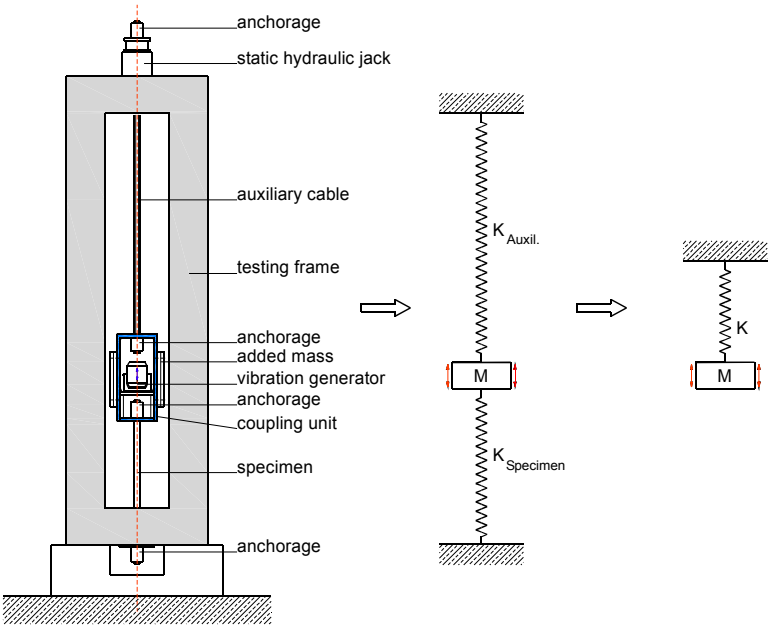

Figure 1 Fatigue testing facility and one degree of freedom model

A vertical and a horizontal testing facility for small specimens (rods made of steel ∅ 8 mm) were realized in the laboratory of the Institute for Structural Engineering to prove that the new testing method works. For both arrangements an extensive test program was carried out. The influence of variation of the added mass as well as variation of the stiffness of the auxiliary cable was researched. Tests were carried out with different upper loads and with different stress ranges. The acceleration of the coupling unit and the strains of the specimen were measured during the test. Analytical calculations of a single degree of freedom system as well as numerical finite element analyses were carried out to approve the measured values.

Due to the promising results of the preliminary tests and the support of Vienna University of Technology a novel testing facility for large specimens is currently built in the laboratory of the Institute for Structural Engineering. This testing unit should enable to carry out dynamic fatigue tests with a lower energy requirement as the known devices. The new testing method will decrease the duration for fatigue tests dramatically. The testing unit will be dimensioned for an upper load for fatigue tests up to 20.000 kN and a vibration range up to 2.500 kN.

Bernd Köberl
Vienna University of Technology
Institute for Structural Engineering
Karlsplatz 13/E212
1040 Vienna, Austria
bkoeberl@mail.tuwien.ac.at

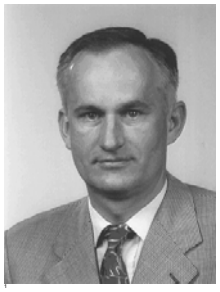

Johann Kollegger
Vienna University of Technology
Institute for Structural Engineering
Karlsplatz 13/E212
1040 Vienna, Austria
johann.kollegger+e212@tuwien.ac.at

CORROSION AND CATHODIC PROTECTION OF STEEL IN REINFORCED CONCRETE

Dessislava Koleva
Delft University of Technology, Delft, The Netherlands
K. van Breugel, J.H.W. de Wit, Supervisors

Corrosion of steel reinforcement in concrete can be successfully mitigated by electrochemical techniques, among which impressed current cathodic protection (ICCP) is a widely used method. In general ICCP efficiency is estimated according empirical criteria only. This contribution explores the efficiency of cathodic protection in a fundamental way by combining micro-level structural investigations and electrochemical approaches.

Materials: Reinforced concrete cylinders (OPC CEM I 32.5, w/c 0.6), dimensions H = 250 mm and D = 120 mm, containing 2 embedded construction steel bars (d = 12 mm), were used in the present study. After 28 days of curing, the specimens were conditioned in salt spray chamber (5% NaCl), aiming at acceleration of the corrosion process. All cells contained embedded reference electrode (Mn/MnO_2) and Mixed Metal Oxide (MMO) Ti mesh on the outer surface (serving as counter electrode or anode). Cathodic protection was applied to the specimens from group P, starting at 60 days and 150 days of age, using steady and pulse DC in different regimes (from 5 to 30 mA/m^2 applied on different cells for the whole test period and from 12 to 50% duty cycle at 500 Hz to 1 kHz for the pulse regime).

Experimental techniques: Half-cell potential mapping and Polarization Development/Decay (according ASTMC876 NACE RP0290-2000); Electrochemical methods: Linear Polarization Resistance (LPR), Potentiodynamic Polarization (PDP) and Electrochemical Impedance Spectroscopy (EIS); Wet chemical analysis (according ASTMC 1218); Scanning electronic microscopy (SEM), using environmental SEM (ESEM Philips XL30) in backscattered electrons mode (BSE) and energy dispersive X-ray analysis (EDAX). All electrochemical methods aimed at investigation of electrochemical parameters for the steel surface, mainly determination of the Polarization resistance (R_p) in every technical condition. Electrochemical measurements were performed at open circuit potential (OCP) for all cells (after 24 h depolarization of the reinforcement for the protected specimens). LPR was performed by external polarization in the range of ±20 mV vs OCP, scan rate 0.16 mV/s, PDP was performed in the range of -0.15 V to +1.2 V vs OCP. The EIS measurements were carried out in the frequency range 1 MHz (or 50 kHz) to 10 mHz by superimposing an AC voltage of 10 mV. Relevant to properties of the bulk matrix, section images of the specimens were used in the ESEM investigation. In addition, morphological aspects and chemical compositions of products, associated with corrosion and cathodic protection, were investigated using EDAX.

With ICCP, polarization of the steel reinforcement is achieved by supplying direct current (DC) to the steel embedded in concrete structures, making corrosion thermodynamically impossible to occur. The repulsion of aggressive anions (e.g. chloride) which takes place along with the protection itself is beneficial as far as corrosion risk for the steel is concerned. Alkali ions accumulation in the vicinity of the steel surface can occur as well, as consequence of the CP current flow. Along with ion migration and diffusion due to the CP current, the heterogeneities and instabilities inherent to the concrete material may lead to non-uniform distribution of the current and thus result in localized unprotected or overprotected areas. In addition, the previous research by the authors reveals CP current to

induce structural alterations in the bulk concrete and in the pore space, to cause micro-cracking, which along with softening of the C-S-H leads to reduced concrete durability.
Aiming at minimization of side effects on one hand and sufficiently protecting the steel reinforcement on the other, in this study an improved cathodic protection (CP), based on pulse regime was investigated in reinforced concrete, compared to conventional CP.
Using electrochemical techniques, the steel reinforcement parameters are determined and the empirical criteria of CP efficiency was proved with experimental evidences. With this respect and as a result of cathodic current, the fundamental approach of sustained negative open circuit potential of the steel surface is accompanied by rendered less aggressive environment at the steel/cement paste interface and consequently induced re-passivating conditions. The latter is more obvious in pulse CP conditions, hence underlines the viability and better efficiency of pulse compared to conventional CP. Furthermore, the effects of pulse and steady current on the material structure, electrical properties and ion transport in the bulk matrix were investigated. In addition to that a mechanical approach in terms of steel/cement paste bond-strength properties was evaluated. The research reveals that the pulse current is less detrimental to concrete microstructure and beneficial for electrical properties and ion transport mechanisms. A steady current (as normally used in conventional CP applications) tends to bring about unfavourable modifications of the material structure both in the bulk (reducing porosity) and in the interfacial transition zone (enlarging the gap at aggregate surface and the steel/cement paste interface) to a significant extent, leading to a high level of structural heterogeneity of the materials. Microstructure observations and chemical analysis reveal the underlying mechanisms to be a more homogenous material microstructure (including slightly refined pore structure), a dense ITZ (small gap) structure, and promoted ion and water transport. The latter is additionally supported by the amount and morphology of product layers, formed on the steel surface in pulse CP conditions. Moreover, the structure of the steel/cement paste interface is maintained more or less intact in pulse CP conditions, the latter suggesting for reduced possibilities for bond strength degradation, compared to conventional CP applications.

D.A. Koleva
Delft University of Technology
Faculty of Civil Engineering and Geosciences,
Materials Science Group
Stevinweg 1, 2628 CD Delft, NL
d.a.koleva@tudelft.nl

Prof. K. van Breugel
Delft University of Technology
Faculty of Civil Engineering and Geosciences,
Materials Science Group
Stevinweg 1, 2628 CD Delft, NL
k.vanbreugel@tudelft.nl

Prof. J.H.W. de Wit
Delft University of Technology
Faculty of Materials Science and Engineering
Corrosion technology & Electrochemistry Department
Mekelweg 2, 2628 CD Delft, NL
j.h.w.deWit@tnw.tudelft.nl

COMPUTER-BASED DEVELOPMENT OF STRESS FIELDS

Neven Kostic
Ecole Polytechnique Fédérale de Lausanne, Switzerland
Aurelio Muttoni, Supervisor

Computer-aided approaches for the efficient development of suitable stress fields are useful tools for the structural design of concrete structures. The paper describes a new procedure that is used within a previously proposed approach for the automatic generation of strut-and-tie models. Once the geometry of the strut-and-tie model is known, the stress fields can be created. A new method is also proposed to generate stress fields characterized by rectangular compression fields and nodes in a pseudo-hydrostatic stress state.

Stiffness-based procedure

Some elements of the initial strut-and-tie model are not as efficient in transmitting the forces as others and they can thus be removed. The full paper presents an automatic stiffness-based procedure for the generation of strut-and-tie models. Starting from an initial strut-and-tie model with a large number of members (fig. 1a), the least effective members are successively removed by means of an iterative process. The proposed procedure automatically leads to reasonable and well known strut-and-tie models (fig. 1b).

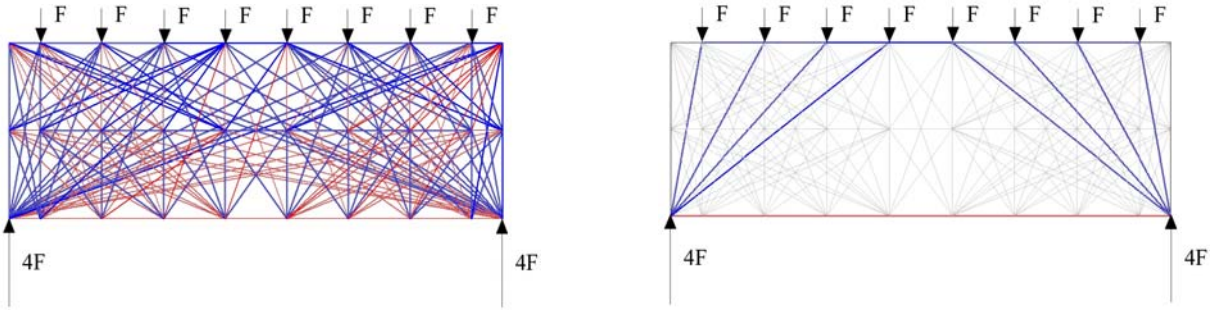

a) *Initial strut-and-tie model*

b) *Final model obtained with the proposed procedure*

Figure 1: Strut-and-tie models for a deep beam

Geometry based procedure

Once a suitable strut-and-tie model has been developed, it should be transformed into a stress field. Based on a known strut-and-tie model a geometry based procedure is used here to obtain a stress field where all the nodes are in a state of pseudo-hydrostatic stresses (fig. 2). This can be achieved by formulating an objective function based on as the difference between each strut angle and a right angle (to the square) for all compression fields.

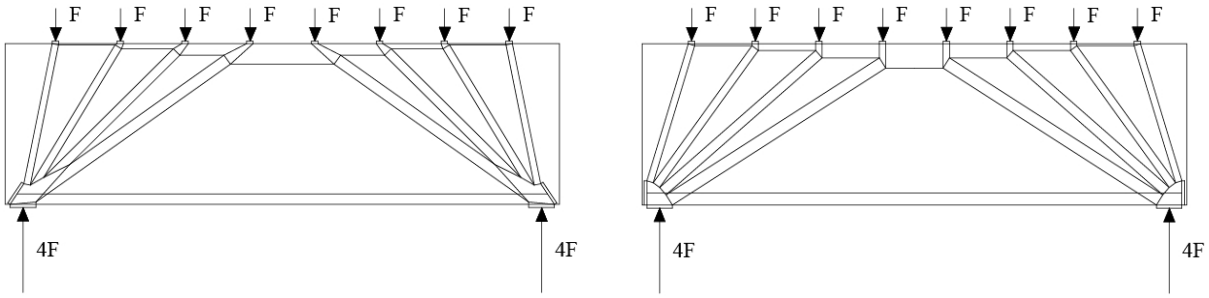

a) Initial stress field *b) Stress field with pseudo-hydrostatic nodes*

Figure 2: Stress field for deep beam, as obtained by means of the proposed procedure

In such a way, the nodes are in a pseudo-hydrostatic state of stress that makes the check of the stresses in the concrete very simple. It is also shown that this procedure leading to the automatic generation of stress fields with all the nodes in a pseudo-hydrostatic state of stress can be applied to any strut-and-tie model.

Neven Kostic
EPFL – ENAC –IS-BETON
Bât. GC
Station 18
CH-1015
Lausanne
Switzerland
neven.kostic@epfl.ch

Prof. Dr. Aurelio Muttoni
EPFL – ENAC –IS-BETON
Bât. GC
Station 18
CH-1015
Lausanne
Switzerland
aurelio.muttoni@epfl.ch

FATIGUE FAILURE PROPERTIES OF HIGH AND ULTRA HIGH STRENGTH FIBRE REINFORCED CONCRETE

Eleni Lappa
Delft University of Technology, Delft, The Netherlands
Cor van der Veen, Supervisor
Joost Walraven, Supervisor

Recent developments in concrete technology have enabled high and ultra high strength concretes, and with these materials thin, slender structures can be constructed. However, when used in applications that are expected to experience repeated loads in their service life, such as bridges, then fatigue can be a possible failure mode and a sufficient knowledge of the fatigue material properties is essential for structural design. Since these materials are relatively new, there is still lack of knowledge regarding the fatigue material properties, which created the need for the present study.

Three different mixtures, one ultra high strength mixture and two high strength mixtures, were used in the present study. The ultra high strength mixture is named BSI/CERACEM and is available as a patented premix from the industry; it is a relatively coarse concrete with a maximum aggregate size of 7 mm and has a steel fibre reinforcement of 2.5% by volume of 20 mm long, 0.3 mm thick fibres. One of the two high strength mixtures is named HSFRC; technically speaking it is a mortar and not a concrete with a maximum aggregate size of 2 mm. The steel fibres are 13 mm long, 0.16 mm thick and are added at a volume percentage of 1.6%. The other high strength mixture is named hybrid HSFRC, and is also a mortar with 0.5 mm maximum aggregate size. The term 'hybrid' refers to the combination of two different fibre lengths: 0.5% of 13 mm long, 0.2 mm thick steel fibres and 1% of 60 mm long, 0.75 mm thick hooked-end steel fibres.

The main experimental test method used in the study was a four point bending test on un-notched beams of dimensions 125/125/1000 mm. The beams were loaded in their third points at a span of 750 mm. This test setup was used for both static and fatigue tests.

The results of the static tests are shown in Figure 1: as can be seen, all three mixtures have a deflection hardening phase, an important characteristic for the static load bearing behaviour. This is further highlighted by comparison with a different ultra high strength mixture, denoted as UHPC in the figure, which fibre content does not provide this characteristic and shows a less ductile behaviour.

The results of the fatigue tests are shown in Figure 2. Of the three mixtures, the HSFRC had the best fatigue performance: at upper load levels of 70% of the average static peak load only one of the seven tested specimens failed, the others were tested up to ten million load repetitions without failure. The load had to be decreased to 60-65% for the hybrid HSFRC and BSI/CERACEM to observe such a phenomenon. Moreover, the BSI/CERACEM had the highest scatter in the fatigue results. Therefore, no regression line is given in the graph for that particular mixture. The main reason for the scatter is the workability: the HSFRC and the hybrid HSFRC were comparable in terms of workability and better flowable in the fresh state compared to the BSI/CERACEM; this improved workability resulted in a lower scatter in both the static and the fatigue test results. The scatter in the fatigue test results could be reduced by correcting the applied load level in accordance with the number of fibres present in the

critical cross section, determined by image analysis. More information on that as well as more detailed results of the fatigue tests are provided in the full version of this paper.

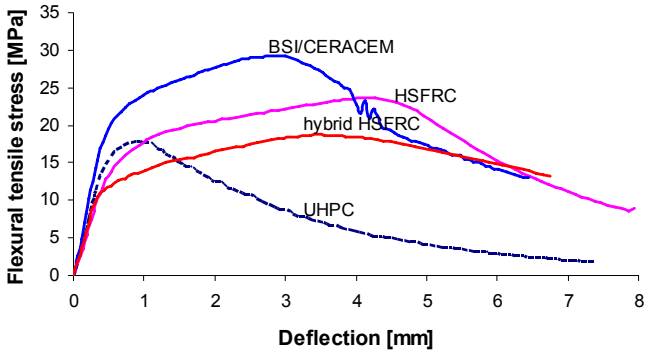

Figure 1 Results of the static four point bending tests

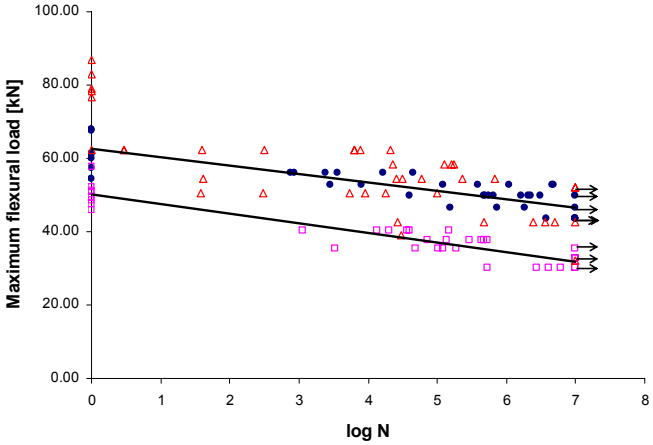

Figure 2 Fatigue test results: BSI/CERACEM is marked by triangles, HSFRC with circles and the hybrid HSFRC with squares. Static tests are included, and arrows indicate run-outs.

Eleni Lappa
Delft University of Technology
Civil Engineering and Geosciences
Concrete structures
Stevinweg 1
2628 CN Delft, The Netherlands
E.S.Lappa@TUDelft.nl

Prof.dr.ir. J.C. Walraven
Delft University of Technology
Civil Engineering and Geosciences
Concrete structures
Stevinweg 1
2628 CN Delft, The Netherlands
J.C.Walraven@TUDelft.nl

THE DESIGN OF MEASURING SHRINKAGE CREEP OF EARLY AGE CONCRETE BY THE RING TEST

Xiaochun Li
HoHai University, Nan Jing, People's Republic of China
Shengxing Wu, Supervisor

Concrete, one of most widely used building material, has been used more than 100 years. Difference from original concrete, modern concrete material has made a great progress made from sand, coarse aggregate, fine aggregate, water, cement and additive. On the same time, there is a growing interest in studying early age cracking of concrete in recent years. The driving force which is a major source of deleterious cracking in the construction stage is the occurrence of stresses in the hardening concrete due to restrained volume change related to thermal deformation and shrinkage. If the structure is restricted or the deformation is inconsistent within the structure, stress is produced, and will cause cracking when it overcomes the tensile strength. Due to viscoelastic behaviour of early age concrete, creep contributes to 40-50% reduction of the elastically induced stress in the restrained specimen. An overview of the ring test developed in recent years and mechanism of uniaxial tensile creep test will be described in the first part of this paper. Then, an innovative test equipment based on the ring test is outlined.

The ring test is one of the simplest and most versatile means, which has been commonly used for nearly half a century. It was introduced in 1942 by R. W. Carlson in MIT and was originally used to study the cement paste and the cement mortar. With the modern development, the ring test is one of the standard test methods for cracking research suggested by RILEM TC-119. As the stresses are sensitive to the ring radius ratio, a standard for the ring test was recently developed by AASHTO (American Association of State Highway and Transportation Officials) (AASHTO 2000). Four strain gauges cling to the inner surface of the steel ring to record the stresses every 30 min. When one or more strain records descend abruptly by 20-30 microstrain, the time is defined as the initial crack time. When the concrete ring begins to shrink, the steel ring core provides the restraint, so tensile tangential stresses are developed in the concrete ring. When the tensile stress developed exceeds the tensile strength of the concrete, cracks will be initiated. The cracks are observed ocularly. The characteristics of the cracks, quantified by terms of maximum width, average width, number and time of occurrence, evaluate the performance of the concrete.

Based on the test mechanism of shrinkage creep, a new equipment is designed with two concrete rings to measure creep of early age concrete. Two concrete rings are cast with the inner diameter of 300 mm (12 *in.*), the outer diameter of 450 mm (18 *in.*), and the height of 75 mm (3 *in.*). After demolding, the circumference of each specimen is sealed. In such a way, drying can develop only from the top and bottom of the concrete ring. A linear variable differential transformer (LVDT) is used to measure the change in diameter of each unrestrained ring. The LVDT is mounted on a steel frame that is glued to the specimen surface as shown in Figure 5. One specimen is prepared to measure the free shrinkage deformation with the inner ring left free. The other specimen is subjected to hydraulic pressure at the inner surface to keep the diameter stable. Once the value of LVDT overcomes the displacement threshold (5 μm), the hydraulic mechanism is activated to increase to recover the original diameter. A computer is used to control load increase. The cycle is repeated. The incremental load in each cycle causes elastic strain. The nature of the cycle follows Eq. 3.1.

$$\Delta\varepsilon(t)=\Delta\varepsilon_{el}(t)+\Delta\varepsilon_{sh}(t)+\Delta\varepsilon_{cr}(t)=0 \tag{3.1}$$

The sum of the shrinkage and creep strain up to a given time t_k can be calculated as follows.

$$\varepsilon_{sh}(t_k)+\varepsilon_{cr}(t_k)=-\frac{1}{2}\sum\left|\varepsilon(t_i)-\varepsilon(t_{i-1})\right| \tag{3.2}$$

where ε_{sh}, ε_{cr} and ε_{el} are shrinkage strain, creep strain and elastic strain of the restrained specimen, respectively; $\varepsilon(t_i)$ is the strain measured at time t_i, intermediate between 0 and t_k, with the previous measurement being at time t_{i-1}; $|\varepsilon(t_i)-\varepsilon(t_{i-1})|$ is the value of the preceding increments of deformation between time t_{i-1} and t_i.

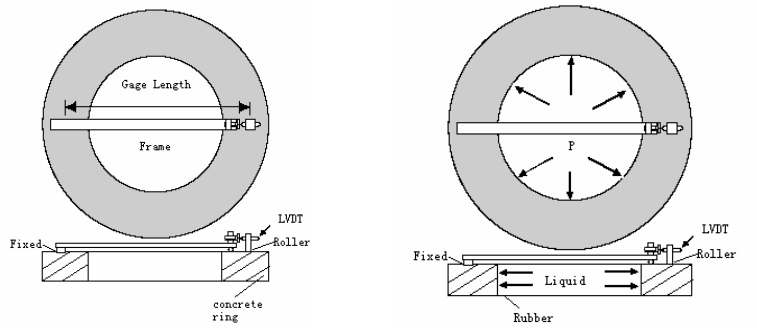

Figure 5 Free Shrinkage (left) and Restrained Shrinkage Concrete Ring (right)

The new equipment for measure creep has the following advantages:
(1) For the dog-bone specimens restricted in the end, stress concentration can not be avoided. But, for the concrete ring specimen used in the innovative equipment, as the nature of central symmetry, pressure on each point is the same.
(2) The swallow-tailed ends of the specimen are difficult to cast in custom-made mould. However, the concrete ring is easy to cast around a hollow steel cylinder.

Xiaochun Li
Hohai University
Structure Department
Civil Engineering Institute
Xi Kan Road 1
Nan Jing, China
lxchhu@hotmail.com

Shengxing Wu
HoHai University
Structure Department
Civil Engineering Institute
Xi Kan Road 1
Nan Jing, China
sxwu@hhu.edu.cn

FATIGUE BEHAVIOUR OF CFRP-REPAIRED CORRODED RC BEAMS

Mindy Loo
University of New South Wales, Sydney, Australia
Stephen Foster, Supervisor

Introduction

Corrosion is a major deterioration problem in marine structures and bridges. These structures are often subjected to oscillating loads which cause fatigue, significantly reducing the expected life of the structure. In the last decade, the problems related to corrosion and fatigue have become more important due to the advent of new materials with high strength used to rehabilitate and extend the service life of existing structures. One such application is the externally bonded carbon fibre reinforced polymer (CFRP) which has shown significant advantages compared to traditional methods of strengthening because of its outstanding mechanical properties, light weight and the simple application to structural members.
The fatigue behaviour of structural members, such as reinforced concrete (RC) beams, rehabilitated with CFRPs has been experimentally studied and documented by a number of researchers. Similarly, studies of CFRP-repaired corroded RC beams have been well documented by researchers. However, only two studies investigated the fatigue behaviour of corroded RC beam repaired with CFRP. To date, no model has been developed to predict the combined behaviour of corrosion and fatigue of CFRP-repaired RC structures.
In this study, the fatigue performance of CFRP-repaired corroded RC beams is studied both experimentally and numerically. A literature review and detailed experimental procedures are presented in this paper.

Literature Review

Only two experimental groups have investigated the fatigue behaviour of RC beams damaged by corrosion and repaired with CFRP (Masoud et al., 2001 and Masoud, 2002). Both studies provided limited data and test variables as there were only nine small-scaled test specimens included in the studies. There is a need for more data, especially from large-scaled test specimens to corroborate future analytical and numerical models.
Two documented studies have modelled CFRP strengthened RC members under cyclic loading (El-Tawil et al., 2001, Khomwan and Foster, 2004). El-Tawil et al. (2001) used a fibre section model to analyse cyclically loaded repaired beams tested in Barnes and Mays (1999) and Shahawy and Beitelman (1999). The model results generally compare favourably in the earlier stages but drift significantly from the test data as the number of cycles increased. Khomwan and Foster 2004 presented a finite element model for soffit repaired beams which was undertaken by attaching a layer of repair elements to the beam via a layer of interface elements or bond. The softening effect of the concrete due to fatigue was not considered in the model which significantly affected the model results. In addition, the analysis was time consuming. The total time to model the beam was 90 hours using a 3.0 GHz Pentium IV computer.

Experimental Program

The main objective of the experimental program is to investigate the potential of CFRP flexural repair technique in restoring/improving the fatigue life of corroded RC beams.
Three series of RC beams (A, B and C) are used in this study and have size ratios of 1:2:4. All of the beams have the same tensile and compressive reinforcement ratio of 0.8 and 0.4 respectively. For each series, there are three beams of which two are undergoing accelerated corrosion to achieve a target of 10% mass loss at the tensile steel reinforcement (Figure 1). Once target mass loss is achieved, deteriorated concrete is to be removed from the beam soffit and repaired with mortar followed by CFRP repair process. The beams will finally be tested under a constant amplitude fatigue loading until failure.

(a) (b)

Figure 1 Test specimens of (a) Series A and Series B in a water tight tank during dry cycle and (b) Series C during wet cycle.

Conclusions

The results from this study will contribute to the limited pool of studies on fatigue behaviour or corroded RC beams repaired with CFRP. Test data from this study will allow the development of a numerical model capable of simulating such structures. It is envisaged that the potential of CFRP in restoring damaged RC beams can be fully maximised for use in the RC rehabilitation industry.

Mindy K.Y. Loo
School of Civil &
Environmental Engineering
University of New South
Wales
Sydney
Australia 2052
z3142594
@student.unsw.edu.au

Dr. Stephen Foster
School of Civil &
Environmental Engineering
University of New South
Wales
Sydney
Australia 2052
s.foster@unsw.edu.au

EVALUATION OF THE CONCRETE TENSILE STRENGTH BY MEANS OF SPLITTING TENSION TESTS

Viktória Malárics
University of Karlsruhe (TH), Karlsruhe, Germany
Harald S. Müller, Supervisor

For the determination of the tensile strength of concrete, the splitting tension test on cores is widely accepted in practice. In order to conclude from the determined splitting tensile strength $f_{ct,sp}$ on the uniaxial tensile strength f_{ct}, conversion factors are used. In accordance with e.g. CEB-FIP Model Code 90 the uniaxial tensile strength f_{ct}, amounts 0.9 times the splitting tensile strength $f_{ct,sp}$. Besides the fact that the values calculated in such a manner are much too small for modern concretes, the conversion provides values being not consistent themselves. Therefore the actual tensile strength of the concrete is underestimated, especially for increasing concrete strength. In accordance with the working hypothesis, this means that the tensile strength increases more than the splitting tensile strength at increasing concrete strength. This behaviour can be traced back to the complex tensile state, which is created within the test specimen during the splitting tension test. The specimen is primarily subjected to compressive stresses in the direction of the linearly distributed load. Perpendicular to this direction tensile stresses dominate. With increasing strength, the concrete reacts more sensitive to such biaxial stress conditions, resulting finally in a premature failure.

In this research project a consistent conversion formula between the splitting tensile strength $f_{ct,sp}$ and the uniaxial tensile strength f_{ct} will be derived applying methods of fracture mechanics. The derived conversion formula is to encompass the entire spectrum of concretes used in practice. Therefore an extensive experimental programme was carried out. Based on the obtained experimental investigations, the splitting tension tests and the uniaxial tension tests are analysed numerically. Related fracture mechanical considerations are under development.

To investigate the interdependency of the compressive strength and the splitting and uniaxial tensile strength, concretes with different classified strength categories (C20/25, C40/50, C70/75, C100/115) as well as two self-compacting concretes (C45/55) using different aggregates (gravel and crushed aggregate) were tested.

Figure 1 Centering device for splitting tension tests (left). Setup of the uniaxial tension tests on unnotched and notched prisms (centre) and on cores (right)

The compressive strength f_c was determined for each normal-strength and high-strength concrete using cubes with an edge length of 150 mm, cylinders with a diameter D of 150 mm and a height H of 300 mm as well as cores with a diameter of 150 mm and a height of 300 mm. The splitting tensile strength tests were performed on test specimens with D/H = 150/300 mm as well as on cores with D/H = 150/300 mm. For the uniaxial tension tests, specimens with different prism and core geometries were chosen. The concrete tensile strength f_{ct}, the tangent modulus of elasticity E_0 as well as the ultimate strain ε_{tu} were determined on dog-bone shaped prisms. In order to record the complete stress-deformation relation, notched prisms were used. The uniaxial tensile strength f_{ct} was additionally determined on cores (see Figure 1).

The numerical simulations were carried out using the finite element program ATENA which, amongst others, realistically approaches for concrete failure at biaxial stress condition. The material parameters were determined on the basis of experimental investigations and are incorporated into the FE computation. The parameter combinations for the splitting tension test simulations resulted from the three different load bearing strip widths b = 5, 10 and 20 mm and four models with different material parameters. The splitting tension test was simulated for cylinders with D/H = 150/300 mm and D/H = 75/150 mm. For both cylinder geometries, the proportion of grid refinement and sample dimensions was held constant. For the simulation of the uniaxial tension tests both notched and unnotched prisms were used.

The splitting tension tests revealed, that with increasing concrete compressive strength the ratio between the splitting tensile strength $f_{ct,sp}$ and the uniaxial tensile strength f_{ct} increases. This observation contradicts the original working hypothesis.

Both experimental and analytic test results show, that the uniaxial tensile strength f_{ct} can not be computed from the splitting tensile strength $f_{ct,sp}$ on the basis of a single constant conversion factor. Furthermore, the attempts to derive a single formula, showing generally the ratio of uniaxial tensile strength to splitting tensile strength, did not yield satisfying results. Possible explanations are manifold. One main reason lies in the failure mechanism of the splitting tension test. It is affected by the concrete strength, sample dimensions and the ratio of load bearing strip width to cylinder diameter. Not only these individual effects but rather their combination plays a substantial role and affects the material behaviour during the splitting tension test. A detailed scientific understanding of the related processes is subject of the author's thesis.

Viktória Malárics
University of Karlsruhe
Institute of Concrete Structures and
Building Materials
Kaiserstr. 12,
76128 Karlsruhe, Germany
malarics@ifmb.uka.de

Prof. Dr.-Ing. Harald S. Müller
University of Karlsruhe
Institute of Concrete Structures and
Building Materials
Kaiserstr. 12,
76128 Karlsruhe, Germany

INVESTIGATION OF WOOD PROPERTIES BY MEANS OF NEUTRON IMAGING TECHNIQUES

David Mannes
ETH Zurich, Switzerland
P. Niemz, E. Lehmann, Supervisors

Neutron radiography represents an innovative new non-destructive testing method in the field of wood research. It is complementary to existing X-ray techniques both methods working along the principle of transmission measurements. Neutrons are led from a source via a collimator on a specimen and the hereby attenuated beam is subsequently registered by a detector. To which extent the beam is attenuated depends on the inner constitution of the sample.
Unlike X-ray radiography, where the interaction occurs between the X-Ray photon and the electron shell of the participating atoms within the specimen the interaction of the incoming neutrons occurs with the nuclei of the specimen's atoms. This results in a different interaction probability of neutrons and X-ray with different elements and thus a varying sensitivity for these elements. From this results the neutron's high sensitivity for some "light" elements like hydrogen, making neutron radiography particularly suitable for investigations on hydrogenous materials like wood and wood based materials.

The utilisation of modern digital detector systems and the high sensitivity permit the detection and quantification of hydrogenous materials even in low concentrations. This makes neutron radiography an ideal instrument for investigations on the penetration behaviour of water, adhesives or preservatives into the wood structure (Figure 1).

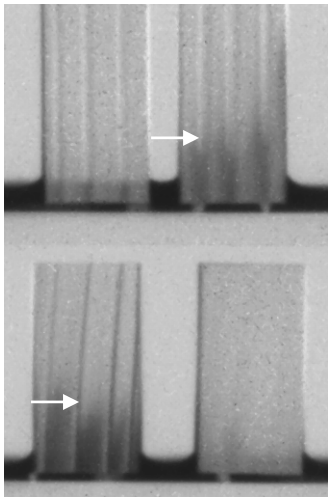

*Figure 1 Water uptake (arrows) in wood samples (Oak (*Quercus spec.*) above, Spruce (*Picea abies*) below left, beech (*Fagus sylvatica*) below right) after 8h of wetting ascertained by means of neutron imaging methods*

On the other hand the high sensitivity limits the investigation to relatively small sample dimensions. It is therefore important to define clearly the aims of planned investigations and thus choosing the testing method appropriate under the given restrictions. In the presented project different wood species were tested in order to obtain their respective macroscopic cross-section or attenuation coefficient for thermal neutrons and X-ray. The attenuation

coefficient indicates the interaction probability of a material with the incident radiation. It is a benchmark which is necessary for a proper design of the specimens (Figure 2).

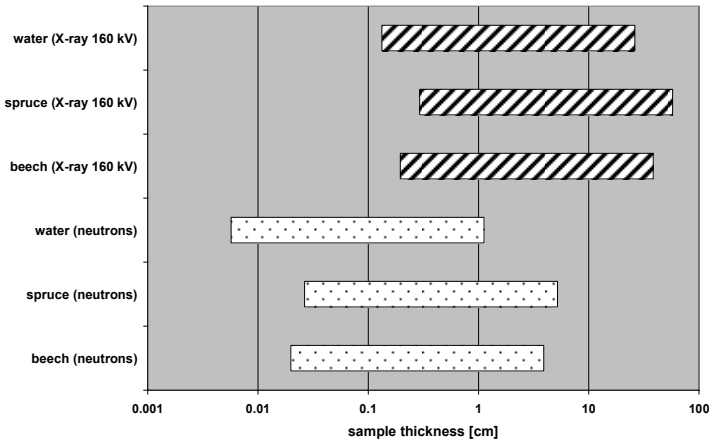

Figure 2 Minimum and maximum sample thickness for X-ray (160 kV) and thermal Neutrons for water and different wood species (logarithmic scale.)

David Mannes
ETH Zurich
D-BAUG
Institute for Building
Materials
Schafmattstr. 6
Zurich, Switzerland
mannes@ifb.baug.ethz.ch

Prof. Dr. Peter Niemz
ETH Zurich
D-BAUG
Institute for Building
Materials
Schafmattstr. 6
Zurich, Switzerland
niemz@ifb.baug.ethz.ch

Dr. Eberhard Lehmann
Paul Scherrer Institut (PSI)
Neutron Imaging and
Activation Group
Villigen, Switzerland
Eberhard.lehmann@psi.ch

Proceedings-CD file name:
157_Meyer.pdf

THE INFLUENCE OF THE FOAM BEHAVIOUR ON THE PROPERTIES OF FOAMED CEMENT PASTE

Dominik Meyer
ETH Zürich, Zürich, Switzerland
Jan G.M. van Mier, Supervisor

Foamed concrete has favourable properties, as low weight and superior thermal insulation, which are based on the large porosity. Due to this fact the strength is rather low and the material is not common as a building material. Little is known about the relation between the foam properties and the properties of the hardened foamed concrete. The problem of foamed concrete is the reproducibility of the foam and the hardened material. Caused by the low stability of the foams the lost volume during mixing of the preformed foam with the concrete, setting and hardening are strongly varying. It is important to reduce the variability of the fresh foam parameters as density and stability, the parameter that causes this variation. Foam stability is hard to evaluate, caused by the different influences on the foam. The parameter we use to describe foam stability is drainage.
To investigate the relationship between the properties of foam and hardened foam concrete a new type of foaming device was constructed, using the technique of membrane foaming from food processing, producing more different foams and to control the bubble size and the bubble size distribution. Foam with lower drainage is more stable during the mixing and hardening process, it is easier for scaling and mixing, and ultimately the reproducibility of the foamed concrete is higher. By comparing industrial produced protein foam for foamed concrete production and foam of equal mixture produced with the new membrane foaming device, the influence of different foam structures on the properties of hardened cement paste is shown. The tests which were completed can be separated into tests on fresh foam, rheology tests on cement paste and foamed cement paste and tests on hardened material. Therefore different mixtures were produced with different parameters as w/c-ratio, amount of foam in the mixture and different foam properties.
On the aspect of rheology more stable foams do not affect the rheology properties of foamed cementitious materials negatively. With the foam a respectable volume of water is introduced to the cement paste and so the w/c ratio is thereby influenced. This change has an effect on the rheological parameters, but the effect is not that bigger compared to changing the w/c ratio of plain cement pastes.
Regarding the mechanical properties the main parameter influencing the strength of foamed cement pastes is density. For equal density, w/c ratio and pore structure have an effect on the strength parameters. By comparing the properties of plain and foamed cement paste it can be seen that the foam has larger effect on strength than on density. The effect on the compressive strength is even bigger than on the bending strength; however for bending strength the scatter is much bigger (see Figure 1).
Foam properties such as foam stability and foam bubble structure have a big influence on the properties and the quality of foamed cementitious materials, the most influenced parameter being the pore structure. The bubble structure of the foam and the amount of foam in the mixture influence the pore structure of the hardened material. The stability of the foam also influences the pore structure and is an important parameter for mixing, reproducibility and variation of quality of foamed cementitious materials. Effects like bubble coalescence are influencing foam stability and thus the pore structure. More stable foams lead to a lesser amount of foam volume that is destroyed during mixing, setting and hardening.

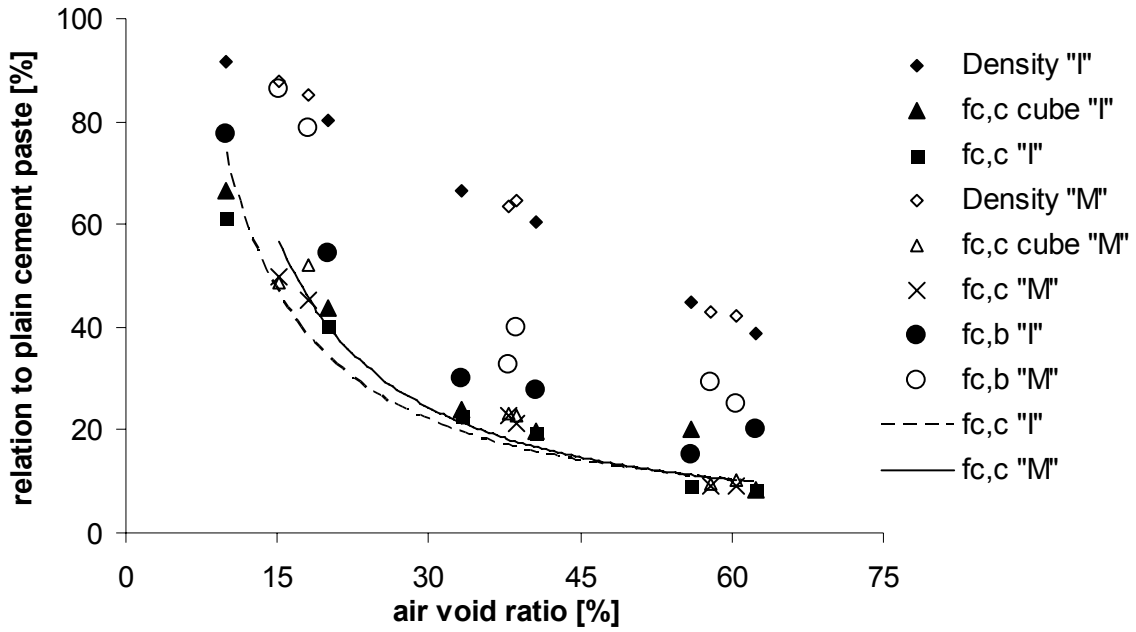

Figure 1 Relationship between plain cement paste and foamed cement paste in percent
"M" … Sample produced with foam out of the membrane foaming device
"I" … Sample produced with foam out of the industrial foaming device

The effect of different foam types on the strength properties at equal density and w/c ratio is low and due to the large effect of density, difficult to distinguish.
In Figure 1 the relationship between the plain cement paste without foam and the foamed cement paste is shown as function of the air void ratio, which is directly related to the amount of foam that is added and so to the density of the foamed material.

Dominik Meyer
ETH Zurich
Department of Civil, Environmental and
Geomatic Engineering
Institute of Building Materials
Schafmattstrasse 6
8093 Zurich, Switzerland
meyerd@ethz.ch

Prof. Dr. Jan G. M. van Mier
ETH Zurich
Department of Civil, Environmental and
Geomatic Engineering
Institute of Building Materials
Schafmattstrasse 6
8093 Zurich, Switzerland
jvanmier@ethz.ch

THE POSSIBILITY TO USE OF INDUSTRIAL WASTE MATERIALS AS FILLERS IN POLYMERIC REPAIR MATERIALS

Gabriela Michalcová
Brno University of Technology, Brno, Czech Republic
Rostislav Drochytka, Supervisor

Introduction

Continuous expansion of industrial production in the recent past has resulted in a huge growth in production of waste materials. Large volumes of industrial waste lead to creation of various waste dumps and to their ecological unwholesomeness. In addition to the problems of storage and disposal of waste materials, diminishing reserves of natural resources represent another reason for their exploitation.
The Institute of Technology of Building Materials and Components, Faculty of Civil Engineering, Brno UT, has been involved in research and development of new building materials filled with waste materials for a number of years. Currently, manufacture of some of them has already been implemented and one may expect that the rate of saturation of the market by these building materials is going to grow in the near future.
This article describes a possibility of utilization of industrial waste materials as fillers in polymeric repair materials in the field of rehabilitation of concrete structures. These repair materials are not going to be used in the field of rehabilitation of concrete structures only; they may also be used as secondary protection for new concrete surfaces.

Characteristics of materials used

Binders – epoxy resin (ER): The ERs with trade names of Lena P 102 and Lena P 130. Lena P 102 – a stiff and penetrating substance for wet or new concrete, existing epoxy floors and other problematic surfaces. Range of use: concrete and other mineral base materials, moist and wet concrete, new and non-cured concrete, metals and originally epoxy surfaces, as a bonding layer between old and new concrete and for other problematic surfaces. Lena P 130 – a substance intended for making of polymeric concrete. Range of use: preparation of mixtures for polymeric concrete floor layers in industrial rooms, repair shops, warehouses etc. subject to high stress.
Fillers – waste industrial materials : Blast furnace slag from the company Třinecké železárny Czech Republic, waste foundry sand from cast alloy foundry UXA Ltd. Brno Czech Republic, fly ash from power plant Chvaletice Czech Republic. Raw material – silica sand.

Work sequence

First the mixes of repair materials with industrial waste materials have been proposed and reference (waste free) mixes has been selected. Reference mixes and newly proposed mixes have been subjected to basic quality testing: pull-off strength, bending strength and compressive strength. Mixes suitable for further testing have been selected on the basis of those initial tests. Further supplementary testing has been carried out: water tightness, absorbability, wearability, freeze-thaw resistance, modulus of elasticity under conditions of bending, resistance to UV radiation, specific gravity, pull-off strength to wet base material and permeability for water vapour and carbon dioxide. Not all type of tests and

requirements on quality of material for rehabilitation of concrete structures are mentioned in standards. The Concrete Structures Repair Association has published Technical Conditions for Rehabilitation of Concrete Structures (Drochytka et al. 2003); it describes types of tests, testing procedures and minimal required values for materials to be used in the field of rehabilitation of concrete structures. The publication replaces standards and all repair materials containing waste products must comply with the requirements stated there.

Conclusions

Comparison of test results obtained from test specimens of individual mixtures and of the values as given in the publication Technical Conditions for Rehabilitation of Concrete Structures (Drochytka et al. 2003) provides the finding that mixtures with industrial waste materials satisfy, and sometimes even significantly exceed, the thus required values.
Properties of newly manufactured epoxy repair materials, especially those with blast furnace slag, surpass the properties of mixtures filled with silica sand.
The possibility to use of industrial waste materials as fillers for epoxy based repair materials in the field of rehabilitation of concrete structures has been proven. Their usage is advantageous from the point of view of decrease in manufacturing costs of epoxy based repair materials. Ecological perspective is also important – one protects non-renewable natural sources of high-quality silica sands used e.g. in manufacture of the typical Czech cut-glass. The reserves of high-quality glass sands in the Czech Republic are estimated to last for not more than 15 years. Another not insignificant positive element may be seen in the utilization of constantly growing volumes of industrial waste.
Development of above mentioned mixtures containing waste materials as fillers is still in progress. Materials meet requirements of main document in the Czech Republic, Technical Conditions for Rehabilitation of Concrete Structures (Drochytka et al. 2003) and search for other test and its implementation required by EU standards is also in progress.

Acknowledgments

The given problems are solved in the framework of the Grant Project no. 103/05/H044 called: ”Stimulation of Doctorands Scientific Development in the Branch of Building-Materials Engineering” and in the framework of the research project MSM 0021630511 called: “Progressive Building Materials with Utilization of Secondary Raw Materials and their Effect on Service Life of Structures”.

Gabriela Michalcová
Brno University of Technology
Faculty of Civil Engineering
Institute of Technology of Building
Materials and Components
Veveří 331/95
Brno, Czech Republic
michalcova.g@fce.vutbr.cz

Prof. Ing. Rostislav Drochytka, CSc.
Brno University of Technology
Faculty of Civil Engineering
Institute of Technology of Building
Materials and Components
Veveří 331/95
Brno, Czech Republic
drochytka.r@fce.vutbr.cz

ARTIFICIAL NEURAL NETWORK (ANN) FOR POROUS ASPHALT MAINTENANCE

Maryam Miradi
Delft University of Technology, Delft, Zuid Holland
A. A. A. Molenaar, Supervisor

In this study we analyzed Porous Asphalt (PA) with Artificial Neural Network (ANN). The reason we chose PA was mainly the fact that more than 65% of Dutch highways are covered with PA, but the maintenance of PA in the current system is questionable. In the Dutch maintenance system, road experts decide about PA lifespan and maintenance moments based on a rough estimation during their annual visual inspection. This traditional way of maintenance has many disadvantages because it does not take into account all the factors that affect the PA lifespan such as, mixture properties, climate, and traffic load. The inspectors decide just based on the existing damage (ravelling) of PA. Ravelling is the main damage of PA which is the release of stone/minerals from the surface of PA.
PA is a rather expensive asphalt top layer with many advantages such as water drainage and noise reduction. Because PA has about 20% of air voids in its structure, it can drain the rain water through the voids to lower asphalt layers and in the same way reduce the mechanical noise produced by rolling of vehicles tires on the surface of the road. However, its lifespan is short (4 years). The recent researches have shown that the increasing of PA lifespan from 4 years to 8 years results in a reduction of 20% in the maintenance costs and a reduction of 10% in the traffic delay hours due to maintenance works. This will be only possible with analysis of all important factors of PA lifespan with modelling techniques.
Last decades has observed an increasing interest for intelligent or biologically-inspired modelling techniques to analyze the complex road materials and to forecast the right moment of road maintenance. Especially, ANN has drawn many attentions because of its strong abilities in solving very complex problems with no prior knowledge necessary.
During the project ITC/ANN instructed by Dutch ministry of transport, we developed two ANN models, FMeq5 and FMeq8, using the steps shown in Figure 1.

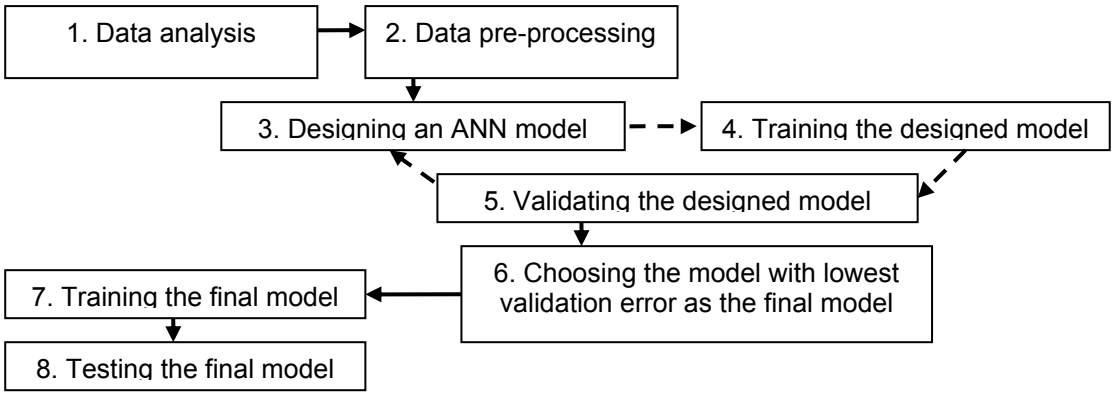

Figure 1 Steps for development of ANN

Proper data is the most essential requirement for developing ANN models. This study used the database provided by Strategic Highway Research Program Netherlands (SHRP-NL) research program which was performed between 1990 and 2000 and had initiatives from SHRP U.S., containing 102 PA sections with a length of 100 m. We developed ANN model, FMeq5, which can forecast the total amount of ravelling 5 years after construction, in other

words the output of FMeq5 is ravelling 5 years after construction. FMeq5 allows us to determine the mixture composition needed to prevent ravelling over the first five years of its lifespan. FMeq5 receives density, bitumen, void content, coefficient of variation of void content, type of stone, %fine, %coarse, warm days, cold days, and cumulative volume of traffic 5 years after construction as input parameters. Table 2 shows a part of the forecasting of FMeq5 reporting the actual output, the predicted output, and the absolute error (AE).

Table 1 Forecasting of FMeq5

Actual value	Predicted value	Absolute Error (AE)
2.5	2.629079	0.129079
8.75	9.249869	0.499869
0.25	0.204455	0.045545
0.25	0.621248	0.371248
13.5	13.504501	0.004501

In a similar way, we developed the model FMeq8 to forecast the total amount of ravelling 8 years after construction. We selected density, bitumen, void content, coefficient of variation of void content, type of stone, warm days, cold days, and total amount of ravelling 5 years after construction as input parameters of FMeq8. Table 2 compares the relative importance of input parameters of FMeq5 and FMeq8. It shows that for ravelling of PA, mixture properties always contributes between 50% and 60%. Gradation properties contribute if PA courses are not older than 5 years. Climate cause ravelling up to 23% in the first 5 years of PA lifespan but after 5 years this contribution starts to disappear. The traffic stays les important than climate. When the PA courses are 8 years old, the existing ravelling of the first 5 years, is 38% important in further development of ravelling.

Table 2 Comparison of importance percentage of FMeq5 and FMeq8

Input name	Model FMeq5	Model FMeq8
Density, Bitumen, Void Content, CV of Void Content, Stone type	53	57
Gradation	14	0
Climate	23	5
Traffic	10	0
Meq 5 years after Construction	N/A	38

Maryam Miradi
Delft University of Technology
Department of Civil Engineering
Road and Railway Engineering
Stevinweg 1
2628 CN Delft, The Netherlands
m.miradi@citg.tudelft.nl

Prof. dr. ir. A. A. A. Molenaar
Delft University of Technology
Department of Civil Engineering
Road and Railway Engineering
Stevinweg 1
2628 CN Delft, The Netherlands
a.a.a.molenaar@citg.tudelft.nl

SYNCHRONIZATION OF PEDESTRIAN LOADS IN LIGHTWEIGHT STRUCTURES

Tommaso Morbiato
IUAV University, Venezia, Italy
Anna Saetta, Supervisor

Pedestrian-structure interaction defining the dynamic self-excited forces experienced in lightweight structures such as footbridge decks is investigated. Self-excitation depends on a double threshold: critical density mutually entrains pedestrian phases reducing random cancellation of forces until structure oscillation is activated; again, if critical, oscillation induces more and more individuals to synchronize with self-excited base motion. Related research fields can be catalogued by the working domain (frequency or time), and by the focal distance from the phenomenon (single pedestrian to crowd action).
By frequency domain, approach is stochastic and thus more general. At single pedestrian level inter-subject and intra-subject random variables are considered (Kerr and Bishop 2001), and continuous force power spectra are defined (Eriksson 1994). At crowd level wind engineering analogies are deployed leading to structural lateral stability criteria such as Pedestrian Scruton Number (Newland 2003), while another formulation considers pedestrians as vertical distributed random loads on a line-like structure, introducing a not yet quantified walking coherence function (Brownjohn et al. 2004).
By time domain, approach is deterministic thus allowing a more direct insight to lateral synchronization mechanism and the possibility to account in integration for geometry non-linearities typical of light-weight structures. A physical synchronization model having not yet been provided, the paper derives a synchronization transition model for the latter threshold from non-linear sciences (Pikovsky et al. 2001) and applies it numerically integrating human-structure interaction equations: SDoF base motion and phase dynamics. Single pedestrian load models can be conventional sinusoid series weighted by dynamic factors from discrete spectral analysis (Bachmann 1987) but can also account for phase-lag parameter between pedestrian and pavement (Barker 2002) as in the case of lateral horizontal force model at the foot to deck interface used for integration in this paper.
At crowd level Dallard et al. 2001b propose to distribute total lateral modal force measured in Millennium Bridge tests uniformly among pedestrians, thus defining linear correlation between modal force and deck velocity. Such approach has three main drawbacks: response unrealistically goes to infinity above N_{cr} (critical number of pedestrians) regardless to saturation bounds on walking compatible deck velocity (Nakamura and Fujino 2002) and to the non-stationary nature of the phenomenon (Charles and Bui 2005); furthermore, deck velocity term being frequency linearly dependant gives the same N_{cr} for stiff or flexible deck in transverse direction; finally, response is generated regardless to motion amplitude, influence of which in entrainment being yet clear in literature (Nakamura 2003, Ricciardelli 2005), and linearly linking both probability of lock-in and effective force incredibly even in Dallard et al. 2001b introductory report. After Solférino experiences (Charles and Bui 2005) N walkers are given a time dependant synchronization rate N_{eq}/N by energy balance between field tests time histories and an equivalent crowd N_{eq} walking at the bridge resonant frequency on an equivalent simply supported beam.
Thus generally speaking, crowd level models in literature account for synchronization in a non-phenomenological manner. From a more phenomenological point of view then, let us consider phase as the variable effectively controlling synchronization: each pedestrian is given a phase-lag with base motion, and with any other walker. The paper demonstrates how individual force can even double by simply playing with different values of phase: maximum response is obtained for pedestrian being ahead in phase quadrature (-1.57 rad), which also maximizes cyclic work expression.
While large crowd field tests report excessive lateral response but usually lack in phase-lag analysis, there is experimental evidence (Fujino et al. 1993, Nakamura 2003, Gamage and

Lasenby 2002) of small groups of pedestrians walking on a lively light-weight footbridge and changing their phase up to a quasi stationary value of -1.57 to -2.00 rad with lateral deck motion, that is in the active range to increase resonance. The paper presents the mathematical tools to treat this interaction with force expressed by its phase and structural DoF dependencies, and including phase dynamics (Kuramoto 1984): self-excitation is modelled and the phenomenon parametrically studied. In other words we can determine the condition for a pedestrian to fall entrained by deck motion modifying his phase to a constant value, and the dynamic load produced. The solution system obtained is integrated in time adopting a non-linear Newmark scheme. On a further perspective, using this phenomenological synchronization-to-1 approach, crowd effects can be evaluated as the result of simulation on N similar phase-histories.

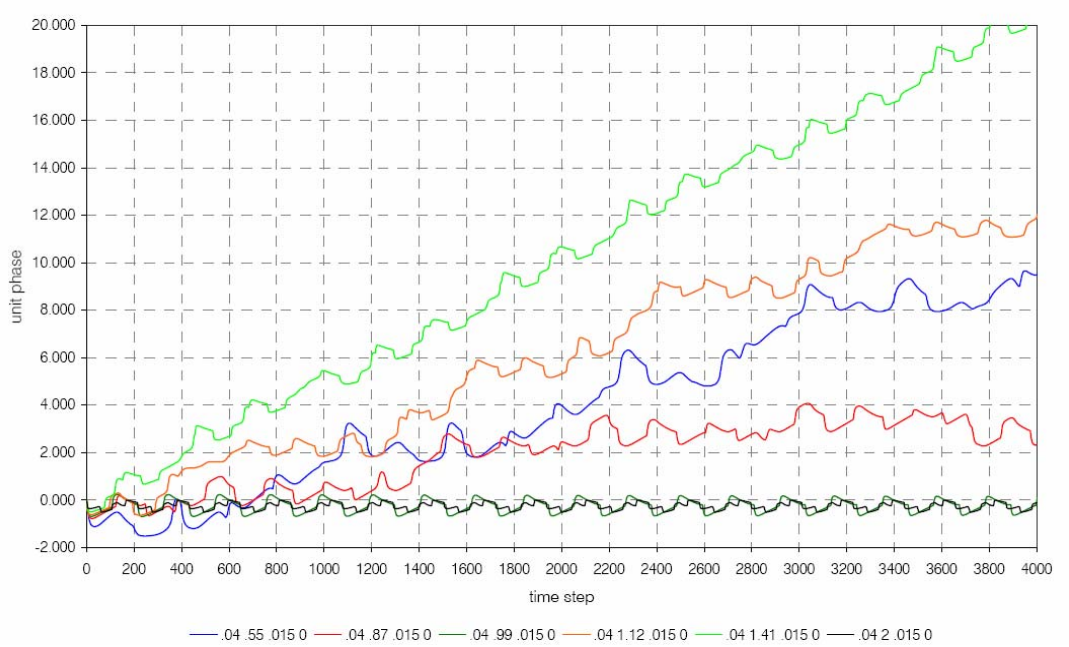

Results show that pedestrians walking with a period T of 99% the T' base oscillation (0.93 Hz test cable-stayed bridge's first lateral frequency) and a random set of time-zero phase-lags, are all phase attracted to values of around -1.57 rad. The figure presented in this summary then shows influence of detuning in the synchronization setup: a constant phase entrainment value is reached for T'/T = 1, is partially or not at all reached for]0,1[< T'/T <]1,2[, and is reached again for T'/T = 2 (T'/T values in figure are the second legenda parameter). The latter is a synchronization of the higher order type 2:1, experimental evidence of which in the pedestrian-structure interaction has been reported e.g. while observing 0.5 Hz Millennium bridge's first lateral mode being excited by 1 Hz walkers (Dallard et al. 2001b).

Tommaso Morbiato
IUAV University
Dipartimento di Costruzione dell'Architettura
Campus Terese
Dorsoduro 2206
30123 Venezia Italy
morbiato@ing.unitn.it

Anna Saetta
IUAV University
Dipartimento di Costruzione dell'Architettura
Campus Terese
Dorsoduro 2206
30123 Venezia Italy
saetta@iuav.it

EXPERIMENTAL AND NUMERICAL INVESTIGATION OF THE DIE SWELL PHENOMENON OF RUBBER BLENDS

Herbert W. Müllner
Vienna University of Technology, Vienna, Austria
Josef Eberhardsteiner, Supervisor

Rubber profiles fabricated by means of extrusion are widely used in civil engineering, e.g., in pipeline constructions and for window sealings. The dimensioning of injection heads for the extrusion of rubber profiles is exclusively based on empiric knowledge of the non-linear flow behaviour of elastomers, basically of the so-called die swell. The swelling of the extrudate when emerging from a capillary is typical for viscoelastic fluids. Therefore, the experimental investigation and numerical treatment of the die swell is of high interest. This was one of the motivations for starting a research project in the field of rubber blend technologies. The knowledge of die swell phenomenon is important for manufacturing rubber profiles. Thus, the final goal of this project is the numerical prognosis concerning tools for the extrusion of rubber. The research work was performed in a co-operation with Semperit Technische Produkte Ges.m.b.H. & Co KG which provides the rubber blends as well as the experimental devices.

For the material characterisation of polymers and rubber blends, respectively, experiments with both, a capillary-viscometer and a torsion-viscometer are commonly carried out. Capillary viscometry simulates polymer extrusion in a simplified way. It allows the characterisation of polymers by means of determination of the viscosity function. In this context, the viscosity function describes the dependence of the stationary dynamic viscosity and the shear strain rate. Such materials have a so-called non-Newtonian melt behaviour which is modelled by means of a generalised Newtonian fluid description. Additional, for many polymers and rubber blends, the viscosity decreases with increasing shear strain rate. This material behaviour is called pseudo-plastic or shear-thinning. Because the corresponding function for rubber blends is linear in a double-logarithmic scale, the constitutive modelling is done in terms of the power law relationship by Ostwald and de Waele in (Michaeli 2003).

The elastic properties of rubber blends can be investigated by means of an adaptation of the capillary-viscometer. With a laser scanning device the diameter of the swelled strand is measured after the exit of the circular capillary. Using different ratios of length and diameters of the capillary the die swell phenomenon can be characterised with such experiments. In order to back calculate the strand diameter after the exit of a capillary additional experiments are required. With the measured pressure and the corresponding stamp velocities only, it would be necessary to introduce several unknown material parameters in order to describe the die swell phenomenon of different materials.

The secondly most often used experimental device for the material characterisation of rubber blends is a rubber process analyzer which belongs to the group of torsion-viscometers. This device is used for the determination of the viscoelastic properties, i.e. the compliance of springs and dashpots of viscoelastic models, such as Maxwell and Huet model, respectively. Most publications in this scientific field are related to polymers. Although rubber blends have similar rheological behaviour the methods for the material characterisation of polymers are not always applicable for rubber blends. The challenging of the material characterisation is to use common polymer methods for the characterisation of rubber blends without introducing new empiric material parameters.

In the present contribution the die swell after the exit of the capillary of a capillary-viscometer is numerically investigated under application of measurements with a rubber process analyzer. The used approach is shown in the figure below.

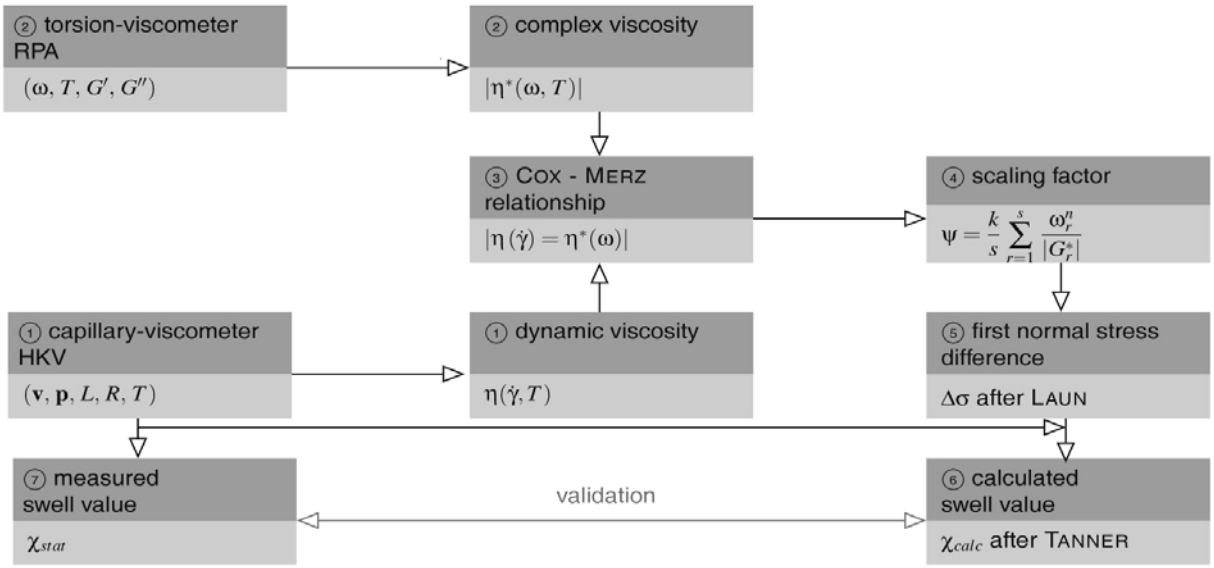

With a capillary-viscometer the determination of the viscosity function $\boldsymbol{\eta}(\dot{\boldsymbol{\gamma}})$ is done (1). Alternatively, with a RPA it is possible to back calculate a complex viscosity $|\boldsymbol{\eta}^*(\boldsymbol{\omega})|$ which depends on a chosen angular frequency (2). Under application of the rule by (Cox and Merz 1958) the comparison of both viscosity functions is possible (3). For many polymers the validity of this relationship has been proven. For the investigated rubber blends this rule is only applicable under usage of a scaling factor (4). Numerical simulations of the die swell phenomenon require information concerning the normal stress state in the capillary. Therefore, the empirical equation by (Laun 1986) can be used (5). This rule is applicable for rubber blends when using the already identified scaling factor. Thus, the required data for the back calculation of the strand diameter for an arbitrary capillary experiment is available. With the relationship by (Tanner 1970) the die swell for circular capillaries can be obtained (6). A successful validation can be done by comparison with the experimental determined strand diameter (7).
Details of the used references of this summary can be found in the full paper.

Herbert W. Müllner
Vienna University of Technology
Institute for Mechanics of Materials and Structures
Karlsplatz 13 / 202
1040 Vienna, Austria
Herbert.Muellner@tuwien.ac.at

Josef Eberhardsteiner
Vienna University of Technology
Institute for Mechanics of Materials and Structures
Karlsplatz 13 / 202
1040 Vienna, Austria
Josef.Eberhardsteiner@tuwien.ac.at

VISCOUS FLOW SURFACE FOR ASPHALT MIXTURES AND AGGREGATE SKELETON COMPONENT

Patrick Muraya
Delft University of Technology, Delft, The Netherlands
A.A.A. Molenaar & M.F.C. van de Ven, Supervisors

This paper presents a study on failure behaviour in asphalt mixtures that was performed as part of a research that is currently being conducted at the Delft University of Technology on permanent deformation of asphalt mixtures. Central to this research is the characterization and analysis of the contribution of both the aggregate skeleton and the mortar to the permanent deformation characteristics of the total asphalt mixture for selected mixtures. The selected mixtures for this research included continuously graded and gap-graded mixtures.

The study involved separate characterization of the of the failure behaviour of the total asphalt mixture and the aggregate skeleton in relation to a flow surface. The separate characterization allowed the evaluation of the contribution of the skeleton towards the failure behaviour in the total asphalt mixture.

The aim of this study was to evaluate the contribution of the aggregate skeleton towards the failure in the total mixtures for three asphalt mixtures namely porous asphalt concrete (PAC), stone mastic asphalt concrete (SMA) and dense asphalt concrete (DAC). The aggregate skeleton and the total mixture were characterised separately. The characterization of the total asphalt mixture was performed through the use of uniaxial monotonic strain controlled failure tests while the aggregate skeleton was characterised using confined monotonic strain controlled failure tests.

The approach applied in order to minimise the number of compressive and tensile failure tests required for the total asphalt mixtures with regard to the number of mixtures, test conditions and test repetitions consisted of two steps. In the first step, the indirect tensile test (ITT) which is relatively easy to conduct, was used to determine the temperature susceptibility of the three asphalt mixtures with regard to stiffness. In the second step, an experimental design technique on the monotonic strain controlled compressive and tensile failure test was implemented for the asphalt mixtures.

The test conditions in the experimental design consisted of 9 test conditions as shown in Figure 1. These test conditions included 8 equidistant test conditions located at the circumference of the circle at which one test was performed for each test condition and one central test condition located at the centre of the circle and at which five test repetitions were performed to estimate the scatter in the data. The advantage of such an experimental design is the fact that the properties and the scatter of the data in an entire domain of temperature and loading time can be described by only 13 tests. Such a dramatic reduction in the number of tests cannot be envisaged under traditional test practices which would require at least 3 temperatures, 3 loading times with 3 tests repetitions being conducted at each test condition making a total of at least 27 tests.

Figure 1 Centra 1 posite design

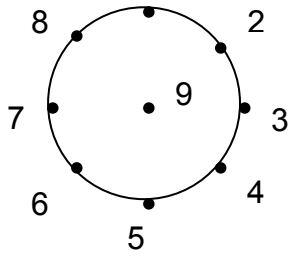

The results from the strain controlled monotonic failure tests for the asphalt mixtures and the aggregate skeleton were characterised using a response surface that was developed by Desai. The main advantage of the Desai surface model in comparison to other yield surface models is that it offers a closed surface that can describe the ultimate failure surface as well as the surface at initiation of dilation or plasticity.

The following conclusions were reached:

1. Response surfaces showed that at high temperatures and low strain rate the asphalt mixtures rely on the aggregate skeleton alone to provide resistance against failure.
2. Although the role of the aggregate skeleton is still significant at high temperatures and high strain rates, the role of the mortar appears to be more prevalent. The significance of the role played by the mortar towards resistance against failure becomes important at low temperatures.
3. Although the resistance to dilation at high strain rates may be offered by the mortar in combination with confinement, the resistance at low strains is entirely dependent on the effect of confining stress on the aggregate skeleton.

Patrick Muraya
Delft University of Technology
Road and Railroad Research Laboratory
Stevinweg 1
Delft, The Netherlands
p.muraya@citg.tudelft.nl

Ir. M.F.C. van de Ven
Delft University of Technology
Road and Railroad Research Laboratory
Stevinweg 1
Delft, The Netherlands
m.vandeven@citg.tudelft.nl

Prof. dr. ir. A.A.A. Molenaar
Delft University of Technology
Road and Railroad Research Laboratory
Stevinweg 1
Delft, The Netherlands
a.a.a.molenaar@citg.tudelft.nl

INVESTIGATION OF THE INTERACTION BETWEEN RADIONUCLIDES AND CONCRETES

Andreas Neumann
University of Karlsruhe (TH), Karlsruhe, Germany
Harald S. Müller, Supervisor

Introduction

After completion of operational periods of nuclear power plants (npps), enormous amounts of construction debris accrued during dismantling have to be disposed of safely, considering environmental as well economical aspects. The interaction of radionuclides with the concrete matrix is of major concern regarding the dismantling of npps and the subsequent reuse and/or the safe disposal of the construction debris, mainly consisting of concrete. Therefore, within a research project funded by the BMBF, experiments with Co-60, I-131, Sr-85, Cs-137 as well as with their inactive isotopes were carried out in order to determine the transportation characteristics of radionuclides in concrete.

Experimental programme

Construction debris originating from a German npp and bench-scale concretes of the strength class C30/37 (w/c = 0.5) according to the European standard EN 206 were applied in order to determine the migration properties of radionuclides regarding the distribution of radionuclides, their releasing behaviour as well as their diffusion through the concrete matrix and capillary suction of isotopic solutions.

Results and Discussion

Activity distribution of Cs-137 in concrete debris of an npp

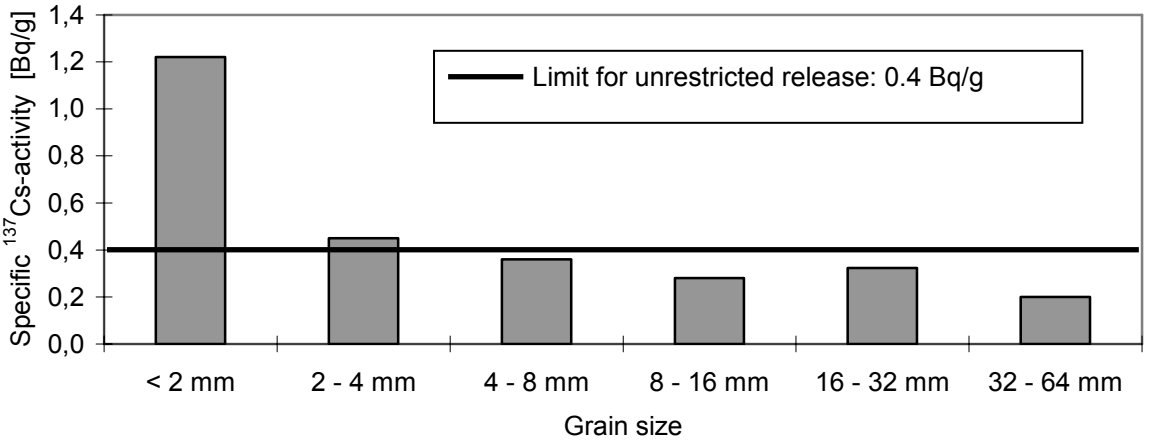

Figure 1 Activity distribution depending on grain size

In Figure 1 the Cs-137 activity distribution of concrete of an npp is plotted versus the grain size and compared with the limiting value for unrestricted release (0.4 Bq/g, see horizontal black line). Thus, grains exhibiting a diameter greater than 4 mm, could be released from the regulatory control of the AtG and set free for conventional disposal and reuse respectively.

Diffusion and capillary suction

The experiments were carried out with relevant isotopes of npps (Co-60, Cs-137, I-131, Sr-85) and for comparable purposes with their inactive natural isotopes. In Table 1 the determined diffusion coefficients are given.

Table 1 Diffusion coefficients of radioactive and inactive isotopes

Diffusion coefficients of concrete C30/37 [m^2/s]				
Natural isotopes	Cs-nat	I-nat	Co-nat	Sr-nat
D_a	$6.65 \cdot 10^{-13}$	$5.56 \cdot 10^{-12}$	-	-
Active isotopes	Cs-137	I-131	Co-60	Sr-85
D_a	$3.22 \cdot 10^{-14}$	$8.53 \cdot 10^{-13}$	$1.20 \cdot 10^{-14}$	$5.98 \cdot 10^{-15}$

These results reveal a decrease of the apparent diffusion coefficients D_a by the following order: I-131 > Cs-137 > Co-60 > Sr-85. It can be seen that iodine and cesium migrate faster through the concrete than cobalt and strontium. In the experiments carried out with inactive isotopes Sr-nat and Co-nat are retarded due to precipitation and carbonation. Thus D_a could not be determined.

The results of the capillary suction experiments of the isotopes being applied for diffusion experiments exhibit a similar behaviour. The penetration profiles of strontium and cobalt, i.e. their measured inventory depending on the penetration depth, differ from those of cesium and iodine such, that the decline of their penetration profiles into the concrete matrix is more distinct due to the strong sorption of strontium and cobalt onto the concrete matrix.

Conclusions

The release and the reuse of radioactive waste in order to save disposal costs and to reduce the impact on the environment may not be accomplished by dilution, as such a procedure is ruled out by § 79 of the Radiation Protection Ordinance. However, the utilization as a recycled aggregate for conventional purposes could be achieved by classifying the debris depending on the grain size, as the experiments showed that the Cs-137 inventory is accumulated in the small fractions.

The results of capillary suction as well as the diffusion experiments indicate that cesium and iodine constitute very mobile species in the high alkaline pore solution of the concrete matrix. Thus, for in-depth decontamination procedures, i.e. for the precise determination of the layer thickness which has to be removed from the concrete walls, the penetration depth of the cesium and the iodine isotope is relevant.

Dipl.-Min. Andreas Neumann
University of Karlsruhe (TH)
Department of Civil Engineering, Geo- and Environmental Sciences
Institute of Concrete Structures and Building Materials
Gotthard-Franz-Strasse 3
76131 Karlsruhe, Baden-Württemberg, Germany
neumann@ifmb.uka.de

Prof. Dr.-Ing. Harald S. Müller
University of Karlsruhe (TH)
Department of Civil Engineering, Geo- and Environmental Sciences
Institute of Concrete Structures and Building Materials
Gotthard-Franz-Strasse 3
76131 Karlsruhe, Baden-Württemberg, Germany

Proceedings-CD file name:
168_Niederegger.pdf

LOCAL BUCKLING OF STIFFENED ELEMENTS WITH NONLINEAR STRESS-STRAIN RELATIONSHIP

Philipp Niederegger
ETH Zurich, Zurich, Switzerland
Mario Fontana, Supervisor

Stainless Steel and aluminium are appreciated because of their high corrosion resistance, easy maintenance and aesthetic appearance. Unlike carbon steel, stainless steel and aluminium exhibit low proportionally limit and extensive strain-hardening capacity. In the absence of a yield plateau it is common practice to define the 0.2% proof stress as an equivalent yield stress for stainless steel and aluminium.
Because aluminium and stainless steel are frequently used for thin walled sections, they are often prone to local buckling. In standards it is the common approach to use the effective width method considering the decrease of the resistance due to local buckling. However this design method does not consider the nonlinear material behaviour.
This paper presents experimental and numerical results of four-side supported steel, stainless steel and aluminium plates subjected to in-plane compression. Additionally the ultimate loads are compared to the designs strengths using the European Standards. The experimental part contained 18 tests on thin plates with measurements of 300 mm x 100 mm and thicknesses of 1.0, 1.5 and 2.0 mm. The tests were conducted using a fairly simple test setup (Fig. 1). For this test setup the unloaded long edges of the plates were supported by linear guides which were connected by spring supported threaded rods. The short edges of the plates were tied to a swivel and the test conducted displacement controlled. For every thickness and material two tests were conducted.
Additionally a parametric study using the finite element programme ABAQUS was made. Fully integrated S4 shell elements with a mesh size of 5 mm x 5 mm were used to model the plates. To be able to implement material properties into the finite element model tensile coupon tests were performed. Local geometric imperfections were modelled using the first buckling mode of the plate (amplitudes of 0.10 mm and 0.25 mm).
The results of the two test series showed good agreement regarding the ultimate loads. Comparison of the test results with the finite element results showed a softer behaviour for little deformations concerning the load-displacement curve and that the ultimate load was reached at a higher strain. Main reason for these differences was the fact that the two extensometers which measured the movement in the axial direction contained also a part of the deformation of the end bearings. The influence of these additional deformations was determined conducting further tests and the test curves were corrected by these bearing deformations. Now the experimental and numerical curves (load-displacement and load-deflection curves) suited well bearing in mind that residual stresses were not considered for the finite element calculations (Table 1). Comparison of the experimental ultimate loads and the design strengths according to Eurocode showed that the test results were 1% to 20% higher.
The occurring failure mechanisms of the tests were compared to the mechanisms using the calculation method by Mahendran (1997). The mechanism was either a flip-disc or a roof-shaped mechanism. The type of mechanism depends on the width to thickness ratio b/t, the magnitude of imperfection, yield stress f_y and Young's modulus E. Flip-disc mechanisms are observed on plates with large slenderness b/t, roof-shaped mechanisms on those having a smaller b/t ratio. Although Mahendran's model was originally derived from mild steel plate tests the application to stainless steel and aluminium tests showed good agreement. Only the failure modes of two aluminium specimens diverged from the model.

The experimental and numerical studies presented in this paper as well as the results of additional stub column tests on welded square hollow sections will constitute the basis for the development of a new design approach for stiffened elements subjected to buckling. These stub column tests will hopefully confirm the observations made and enable the development of a uniform design approach for elements with nonlinear stress-strain relationships.

Figure 1 Test setup

Label	$N_{um,exp} / N_{u,FE}$		$N_{um,exp} / N_{u,EC}$
	u_1 = 0.10mm	u_1 = 0.25mm	
S-10	1.01	1.03	1.14
S-15	0.97	0.98	1.19
S-20	0.99	1.02	1.01
A-10	1.04	1.05	1.07
A-15	1.11	1.12	1.19
A-20	0.93	0.96	1.06
CrNi-10	0.95	0.96	1.16
CrNi-15	0.96	0.99	1.09
CrNi-20	1.01	1.09	1.20
Mean	1.00	1.02	1.12
COV	0.055	0.055	0.061

Table 1 Comparison of test strengths with finite element strengths and design strengths according to Eurocode

Philipp Niederegger
ETH Zurich
Department of Civil, Environmental and Geomatic Engineering
Institute of Structural Engineering
HIL D 41.1
Wolfgang-Pauli-Str. 15
Zurich, Switzerland
philipp.niederegger@ibk.baug.ethz.ch

Mario Fontana
ETH Zurich
Department of Civil, Environmental and Geomatic Engineering
Institute of Structural Engineering
HIL D 36.1
Wolfgang-Pauli-Str. 15
Zurich, Switzerland
fontana@ibk.baug.ethz.ch

MODELING OF RESIDUAL STRESSES IN TOUGHENED GLASS

Jens H. Nielsen
DTU, Kgs. Lyngby, Denmark
Henrik Stang, John Forbes Olesen and Peter Noe Poulsen, Supervisors

Glass has been used in buildings for centuries but, until recently, not widely used as load carrying structural elements. Glass has many excellent properties such as high compressive strength, high stiffness and superior environmental resistance. However, glass is extremely brittle and the tensile strength, which is governed by flaws and fracture processes, is typically in the range from 10 MPa to 90 MPa which is much less than the compression strength. Furthermore, the tensile strength is unreliable due to the random distribution of surface flaws and impurities which induce cracks.

By quenching glass from high temperatures the strength properties can be improved. This process is referred to as the thermal toughening process. The thermal toughening process of glass relies on hot glass quenching using air cooling. The temperature gradient and the sudden transition between liquid and solid state in the glass generate stresses. During quenching, the surface layers will become stiff and able to carry stresses while the core remains liquid and unable to carry any stresses. When layers towards the center are cooled, the outer layers are already stiff, and the contraction of those layers will generate compressive stresses near the surface while tensile stresses are generated in the layers closer to the core in order to maintain equilibrium. A schematic view of the principle is given in the figure below.

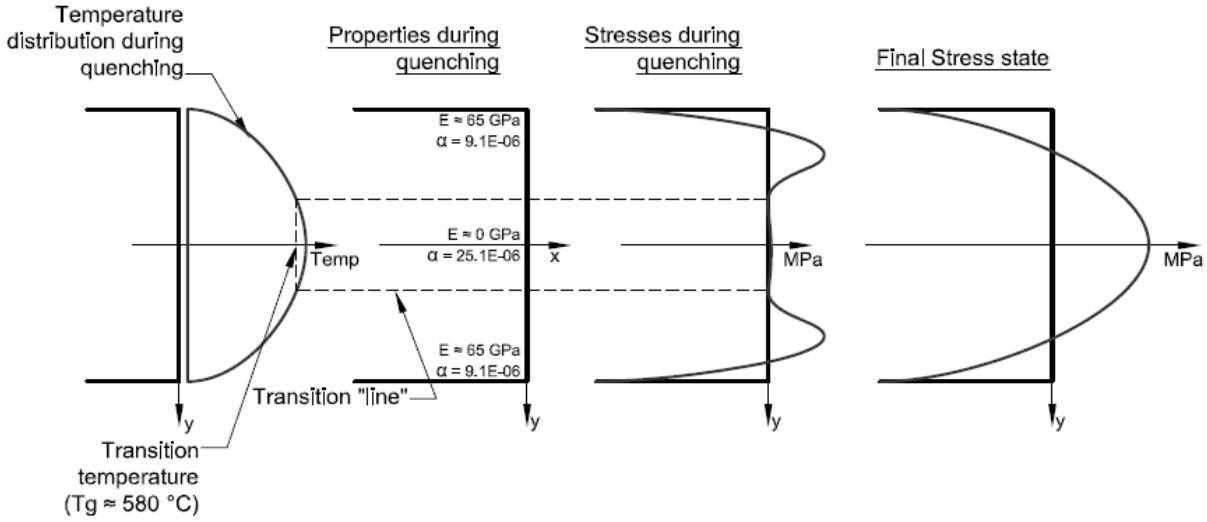

At the present time there is a lack of guidelines for structural design in glass. Often it is necessary to prove the load carrying capacity of key structural elements using full scale tests. The present work focuses on modeling of bolted connections in toughened glass. Such models have to include both the residual stress state from the toughening process and the contact forces between bolt and bearing.
This paper describes the toughening process and a simple model for estimating the residual stresses in a plate far from the edges and the assumptions made for this model are

explained. The coupled non-linear heat transfer and mechanical equations for this problem are presented below.

$$\frac{\partial T}{\partial t} + \nabla \cdot (-c\nabla T) = 0 \qquad \text{, Fouriers heat equation}$$

$$\dot{\sigma} = \frac{E(T)}{\int_0^a E(T)dy} \int_0^a \frac{E(T)}{1-\nu}\alpha\dot{T}dy - \frac{E(T)}{1-\nu}\alpha\dot{T} \qquad \text{, Incremental mechanical equation}$$

It shall be noticed that the equilibrium condition is given on incremental form, thus care should be taken calculating the total stresses using proper tolerances and step sizes.

The mechanical equation above is derived and explained, the coupled equations are solved in the Finite Element program Comsol Multiphysics 3.2, using second order temperature and stress elements. This approach is able to predict final stresses as well as transient stresses. A brief parameter investigation on the quenching time and convergence is carried out. Furthermore, an example of the transient stresses in the early stage of quenching is presented and the Partial Differential Equations for a simple 2D and 3D approach are presented.

The model still needs improvement in order to include viscoelastic properties of the glass close to the transition temperature. Later the model will be extended to the three dimensional space.

Jens Henrik Nielsen
Technical University of Denmark
Department of Civil Engineering
BYG-DTU
Brovej 1, build. 118
DK-2800 Kgs. Lyngby
jhn@byg.dtu.dk

Professor
Henrik Stang
Technical University of Denmark
Department of Civil Engineering
BYG-DTU
Brovej 1, build. 118
DK-2800 Kgs. Lyngby
hs@byg.dtu.dk

Associate Professor
John Forbes Olesen
Technical University of Denmark
Department of Civil Engineering
BYG-DTU
Brovej 1, build. 118
DK-2800 Kgs. Lyngby
jfo@byg.dtu.dk

Associate Professor
Peter Noe Poulsen
Technical University of Denmark
Department of Civil Engineering
BYG-DTU
Brovej 1, build. 118
DK-2800 Kgs. Lyngby
pnp@byg.dtu.dk

ASSESSMENT OF MASONRY ARCH RAILWAY BRIDGES ASSISTED BY NON-DESTRUCTIVE TESTING

Zoltan Orban
University of Pécs – Pollack Mihály Faculty of Engineering, Hungary
György L. Balázs, Supervisor

The paper presents methods of assessment and inspection of masonry arch railway bridges. Some results of a test programme are demonstrated where the efficiency of various non-destructive testing methods for the inspection of arches was studied. A multi-level assessment procedure is recommended with the adaptation of advanced tools for structural analysis and testing. It is shown that non-destructive investigation can provide valuable information regarding the condition of the bridge and help establishing basic input parameters for structural analysis. Streamline of further research is presented.

Introduction

Masonry arch bridges form an integral part of the railway infrastructure in Hungary and worldwide. They are the oldest structure types in the railway bridge population with thousands still in service. In order to promote interoperability between European railway networks and provide that the railways can accommodate increased axle loads, train speeds and a greater volume of freight traffic, it is necessary to assess the load carrying capacity of existing masonry arch bridges. Assessment of masonry arch bridges is difficult as the structural behaviour of arches are very complex, there is little knowledge or experience of design of these structures, and a large part of the structures is hidden from view. To provide confidence in the assessment result, reliable input parameters are required for the calculations. Accordingly effective inspection and measuring methods to establish the parameters are necessary. As well as the predominant use of visual inspections, and destructive investigation there is a tendency in recent years towards using non-destructive testing techniques.

Assessment of the load-carrying capacity

Several methods are available for the assessment of the load-carrying capacity of masonry arch bridges. These include simple conservative methods (such as the semi-empirical MEXE method) and recently developed computerized methods (such as adaptations of the mechanism method and FEM systems). Besides their particular limitations, conservative methods often underestimate the load carrying capacity, which may result in uneconomical or unnecessary mitigation measures being taken to maintain or replace bridges. Conversely the use of sophisticated new methods is generally hindered by the difficulty in provision of input parameters or prolonged data processing.

Review on testing methods

Several inspection methods are used to investigate the condition or to determine the structure of masonry arch bridges. The most common method is still the pure visual inspection. Destructive testing is also used although there is a tendency in recent years towards using non-destructive testing techniques. Most assessment procedures require the masonry strength and some other mechanical properties as the major input parameters for assessment. Destructive Testing (DT) of masonry bridges is therefore necessary in many

instances, although it should be noted that the results of most destructive tests are affected by significant uncertainties and they may provide only local information on some part of the structure, and cannot be directly extended to the whole bridge. While conventional DT methods focus mainly on the mechanical characteristics of the materials, Non-Destructive Testing (NDT) and Slightly-Destructive Testing (SDT) methods can provide an overall qualitative view on the arch condition.

The testing programme

The number of references and projects that have utilized NDT methods on masonry arches is very low and only a few calibration tests have been carried out until now. A testing programme has been therefore initiated by the Hungarian Railways that is aimed at working out an Inspection system for masonry structures with the utilisation of the potential in non-destructive testing. This testing programme was part of a multi-phase research project that is partially supported by the International Union of Railways and the Hungarian Research Fund (OTKA, Grant Nr. T046691). The following testing methods are involved in the programme: georadar, infrared thermography and seismic methods together with calibratory core drillings and boroscopy survey. Besides testing the efficiency of the above mentioned methods on masonry arches it was also important to find forms of representing measured data that are meaningful for engineers.

Conclusions

The results of the performed testing programme have confirmed that NDT is a promising tool in confirming unknown geometrical data and finding hidden characteristics of masonry structures such as the presence of internal voids, flaws, layering condition, mapping of non-homogeneity, moisture content, etc. which may otherwise be detected only by destructive or other complicated tests. However a great deal of further research is needed to increase the reliability of the interpretation of NDT results. The paper discusses some of the results of the performed survey and demonstrates possibilities in applying them in practice.

Zoltán Orbán
University of Pécs – Pollack Mihály Faculty of Engineering
Department of Structural Engineering
Boszorkány u. 2.
H-7624 Pécs
HUNGARY
orbanz@witch.pmmf.hu

Prof. György L. Balazs
Budapest University of Technology and Economics,
Department of Enginering Geology and Building Materials
Műegyetem rkp. 3.
H-1111 Budapest
HUNGARY
balazs@vasbeton.vbt.bme.hu

STRUCTURAL BEHAVIOUR OF REINFORCED CONCRETE BEAMS WITH CORRODED REINFORCEMENT

João Pina
Instituto Superior Técnico, Lisboa, Portugal
António Costa, Supervisor

The degree to which performance of reinforced concrete is impaired as a result of reinforcement corrosion is a matter of great concern to those responsible for assessment and maintenance of affected structures. In the last decade, increasing attention has been devoted to the problem of assessing the residual strength of corroded structures. Several tests have been conducted on damaged RC elements such as beams, columns or slabs. Other studies aimed at characterizing the bond deterioration as a function of corrosion penetration, the evolution of corrosion induced cover cracking or the changes in steel mechanical properties.

Figure 1 Two point flexural test on a corroded beam

Structural response of corroded elements was also investigated numerically. The first developments considered the reduction of steel cross sectional area and the weakening of concrete cover due to cracking, but none was suitable for modelling the structural effects of slip between corroded bars and the surrounding concrete. More recently, two-dimensional finite element models of corroded concrete beams were presented. These models used an interface element between concrete and steel elements which incorporates a bond-slip constitutive relation. By changing some of this constitutive relation's parameters, different degrees of bond deterioration can be modelled. These 2D models are very computationally demanding, and therefore, are inappropriate for modelling the whole structure.

In the present paper, a one-dimensional finite element procedure is proposed. Assuming plane sections remain plane after deformation (Bernoulli hypothesis), all points on the same section are obliged to stay on the same plane. On the other hand, the slip between concrete and reinforcing bars violate such presumption. This slip phenomenon has increased significance in corroded structures where reinforcement corrosion leads to severe bond deterioration. The option pursued here is to keep the Bernoulli hypothesis for the concrete body plus sound reinforcement while corroded rebars are treated separately. In this way, a fiber beam element is used to model the RC element and the sound rebars, and the

contribution of each corroded rebar fiber to the beam element stiffness and forces is obtained separately by running an embedded bar finite element model.

The fiber beam element used in the numerical implementation is based on the Euler-Bernoulli beam theory for geometrical linear behaviour. The term “fiber” comes from the fact that the constitutive relation between beam forces and deformations, at a section level, is obtained by the integral along the section of $\sigma - \varepsilon$ relations. Each integration point is considered as a fiber subject to axial solicitation.

The key issue in this numerical procedure is the coupling of the embedded bar element with the fiber beam element. In a fiber beam element model, values for σ and $k = \partial\sigma/\partial\varepsilon$ are computed at each fiber, so it is necessary to find a way of computing those values for the section fibers corresponding to those separately modelled corroded bars. The pursued option, is to run the beam model using past estimates for the missing quantities, and then using the resulting ε_c values from the referred fibers as the load action for the embedded bar model.

In parallel with the numerical development, an experimental campaign consisting on 17 RC beams subjected to reinforcement corrosion is being carried out. These beams will be submitted to a two point flexural load test similar to the one conducted on the last numerical example. The load shall be applied by displacement control, monotonically, up to the failure of the specimens. This experimental campaign will be finished by April of 2007 and its results will be used to validate the proposed numerical procedure.

Despite many research efforts have been focused on studying the effects of corrosion on reinforced concrete elements, the goal of accurately predicting the structural response of a corroded structure is far from being accomplished. The proposed numerical procedure is computationally cost efficient when compared to some recently developed 2D models, as it takes advantage of the Bernoulli hypothesis to reduce the number of degrees of freedom. This efficiency gain may be determinant on the success of a future application where the whole concrete structure is included in the model. Moreover, the preliminary results indicate that the proposed procedure can represent the main features of the overall structural response of corroded structures.

João Pina
Instituto Superior Técnico
Departmento de
Engenharia Civil e
Arquitectura
Av. Rovisco Pais, 1049-
001 Lisboa, Portugal
jpina@civil.ist.utl.pt

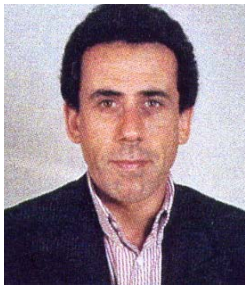

António Costa
Instituto Superior Técnico
Departmento de
Engenharia Civil e
Arquitectura
Av. Rovisco Pais, 1049-
001 Lisboa, Portugal
acosta@civil.ist.utl.pt

FATIGUE BEHAVIOUR AND APPLICATION OF HORIZONTALLY LYING SHEAR STUDS

Jochen Raichle
University of Stuttgart, Stuttgart, Germany
Ulrike Kuhlmann, Supervisor

So-called horizontally lying shear studs are headed studs which are positioned close to the surface, see Fig. 1. They allow the development of new and innovative composite structures, see Fig. 2.

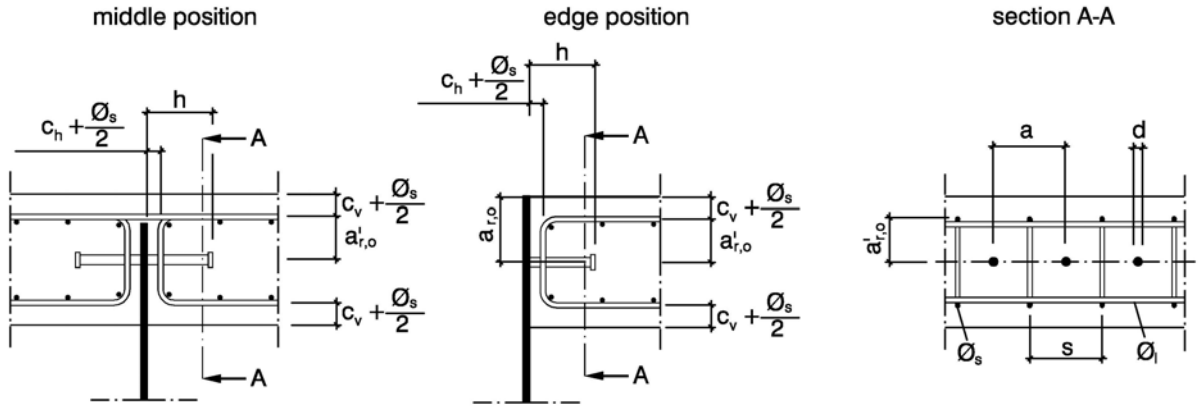

Figure 1 Edge distance a`$_{r,o}$ and other parameters for headed studs

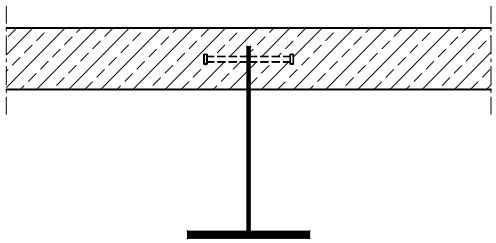

Figure 2 Composite girder with horizontally lying headed studs

Research at the University of Stuttgart on this topic already resulted in design rules for static resistance under longitudinal and vertical shear and for fatigue resistance under longitudinal shear in prEN 1994-2 and DIN 18800-5.

This paper presents additional ongoing studies to this topic.

At the time three different test series with altogether 25 specimens are performed to investigate the fatigue resistance of horizontally lying headed studs under vertical loading. Two of the series were accomplished with different effective edge distances a´$_r$ as essential parameter. Shearing of the studs and concrete outbreak were observed as failure modes, see Fig. 3. A third test series will be performed to investigate the reduced static strength after a high cycle preloading.

Figure 3 Failure modes concrete outbreak and shearing of the studs

A first approach to investigate the performance of horizontally lying shear studs in beams has been done on five slim-floor beams. There was no failure of a horizontally lying headed stud and the slip measurements between steel and concrete only showed small values up to the calculated serviceability load. Further systematic analysis of the girder tests have to be done.

Promising developments in bridge building are composite girders with corrugated steel webs. Due to the corrugation the web has no stiffness in longitudinal direction, so that the longitudinal prestressing of the concrete slabs is most effective. In addition in contrast to plane webs corrugated webs are stiff for transverse bending moments. This enables to omit the laborious and expensive frames in transverse direction and reduces the critical details for fatigue.

In a common project chaired by Prof. Novák of the Institute for Lightweight Structures and Conceptual Design (ILEK) of the University of Stuttgart a test series with 25 specimens to determine shear resistance in longitudinal direction is going to be tested in the near future. Four specimens will be tested without any mechanical shear connection in order to quantify the shear force transferred by the corrugated web. Eleven other specimens will be tested with various arrangements of horizontally lying shear studs and seven specimens with concrete dowels. Subsequent to this series another series will be tested to investigate the resistance for bending in transverse direction.

Jochen Raichle
University of Stuttgart
Institute of Structural Design
Pfaffenwaldring 7
70569 Stuttgart, Germany
jochen.raichle@ke.uni-stuttgart.de

Prof. Dr.-Ing. Ulrike Kuhlmann
University of Stuttgart
Institute of Structural Design
Pfaffenwaldring 7
70569 Stuttgart, Germany
ulrike.kuhlmann@ke.uni-stuttgart.de

FIRE RESISTANCE OF STRUCTURAL MEMBER PROTECTED BY INTUMESCENT SURFACE SYSTEM

Elio Raveglia
ETH Zurich, Zurich, Switzerland
Mario Fontana, Supervisor

Intumescent coatings on steel with a thickness between 300 to 3500 µm are used for fire protection. Intumescent coatings have a number of advantages compared with other type of fire protection. They have an attractive architectural appearance and are lightweight. Their main feature is that at high temperatures the chemical components of the coating react and expand to form a compact insulating layer. The final thickness of the expanded coating increases by between 30 and 60 times the original dry film thickness. The created insulating layer delays the temperature rise in the protected steel, preventing it to catch up the critical steel temperature Θ_{cr} which causes collapse of the steel member.

Figure 1 Expanded coating on a steel plate

Figure 1 shows the expanded coating on a steel plate. The assessment of intumescent systems needs consistent test data. However the official approvals from different European countries show a large variety of required system thickness. The differences between the required dry film thicknesses are not only due to the differences of the experimental setups but in parts are also due to different assessment methods. Fire tests supply temperature-time relationships for different specimens coated with different thicknesses of intumescent material. The results are assessed by a consistent harmonised method to calculate nominal thermal conductivities λ_p to be used for fire resistance calculations. The method is based on the differential equation for the heat flux given in the following equation:

$$\Delta\Theta_a = \frac{d_p \cdot U}{c_a \cdot \rho_a \cdot A \cdot \lambda_p} \cdot (\Theta_{f,t} - \Theta_a) \cdot \Delta t \qquad \text{where:} \qquad (1)$$

d_p : thickness of the fire protection material [m]
U/A : section factor [m^{-1}]
λ_p : thermal conductivity of the fire protection material [W/m·°C]
ρ_a : steel density [kg/m^3]
c_a : specific heat of steel [J/kg·°C]
$\Theta_{f,t}$: furnace temperature at the time t [°C]
Θ_a : steel temperature [°C]
Δt : time increment [s]

The thermal conductivity λ_p is calculated using equation (1) putting in as variables the results from fire tests.
At present, structural fire resistance design is based on the “standard fire condition”, under which the temperature-time relationship $\Theta_{f,t}$ in the furnace follows the prescribed standard given in (ISO 834,1975). Fire tests on intumescent coatings are mostly performed under this standard fire condition. The thickness d_p of the insulating layer used to calculate the thermal

conductivity is the dry film thickness. This is due to the fact that a prediction of the end thickness of the up-foamed layer is difficult to be made. Because the nominal thermal conductivity is related to the dry film thickness it is very small and amounts between 0.005 and 0.03 W/m·K. The effective thermal conductivity related to the up-foamed layer lies between 0.30 and 0.90 W/m·K and can be determined by multiplying the thermal conductivity related to the dry film thickness with the expansion rate of the foamed layer. The value of the thermal conductivity is then comparable with that of lightweight concrete.
We found it to be impossible to give a constant nominal value for the thermal conductivity λ_p because it depends on many factors. The main parameters are the critical steel temperature, the coating thickness and the section factor.
After calculating the thermal conductivities for different tests and critical temperatures, the data is processed using the linear regression method with the three main influence parameters d_p, U/A and Θ_{cr}.

$$\lambda p = C0 + C1 \cdot \Theta cr + C2 \cdot d\,p + C3 \cdot U / A \qquad (2)$$

The values of the constants C_o, C_1, C_2 and C_3 is calculated using linear regression order to obtain the best fit for the whole data set. The values of the constants are calculated with the algebraic method of the least squares.
Using equation (1) and (2) the fire resistance can be calculated and after this confronted with acceptability criteria. In an iterative procedure based on equation (1) and the thermal conductivities λ_p calculated with equation (2), the dry film thickness is varied until the limiting steel temperature is reached at the required fire resistance time. The results are presented in tables with the limiting steel temperatures going from 400°C to 700°C, in steps of 50°C and fire resistance times of 30 and 60 minutes.

A comparison with test data shows that the proposed method shows good agreement. The calculated fire resistance times are very similar to the results of the fire tests.
The first goal of the PHD project was to create a harmonizing assessment method for the thermal conductivity of intumescent coatings. In a second phase the study will be extended to use intumescent coatings on other structural members like heavy cross sections or tension rods. This phase aims to develop design methods for different type of steel members. In a third phase the influence of locally missing protection on the fire resistance is studied.

Elio Raveglia
ETH Zurich
Department of Civil, Environmental
and Geomatic Engineering
Institute of Structural Engineering (IBK)
Wolfgang-Pauli-Str. 15
Zurich, Switzerland
raveglia@ibk.baug.ethz.ch

Prof. Dr. sc. techn. Mario Fontana
ETH Zurich
Department of Civil, Environmental
and Geomatic Engineering
Institute of Structural Engineering (IBK)
Wolfgang-Pauli-Str. 15
Zurich, Switzerland
fontana@ibk.baug.ethz.ch

Proceedings-CD file name:
192_Redaelli.pdf

TESTING OF REINFORCED HIGH PERFORMANCE FIBRE CONCRETE MEMBERS IN TENSION

Dario Redaelli
Ecole Polytechnique Fédérale de Lausanne, Switzerland
Aurelio Muttoni, Supervisor

In recent years, an important research effort has been made to study Ultra High Performance Fibre Concretes (UHPFC) as construction materials. So far, the knowledge about their behaviour in real-scale structural elements remains fragmentary, and only few structures have been realized that really exploit UHPFC properties.
A research program is under way at the Ecole Polytechnique Fédérale de Lausanne (Switzerland) to asses the effectiveness of UHPFC as a construction material and to define best suited structural applications.
The study of full scale tension members with ordinary steel reinforcement is believed to be an important step in the understanding of the structural response of UHPFC. A first test series has been carried out to investigate the serviceability and ultimate behavior of reinforced UHPFC ties with different types of steel, namely hot-rolled and cold-worked steel. The reinforcement ratio was also varied.

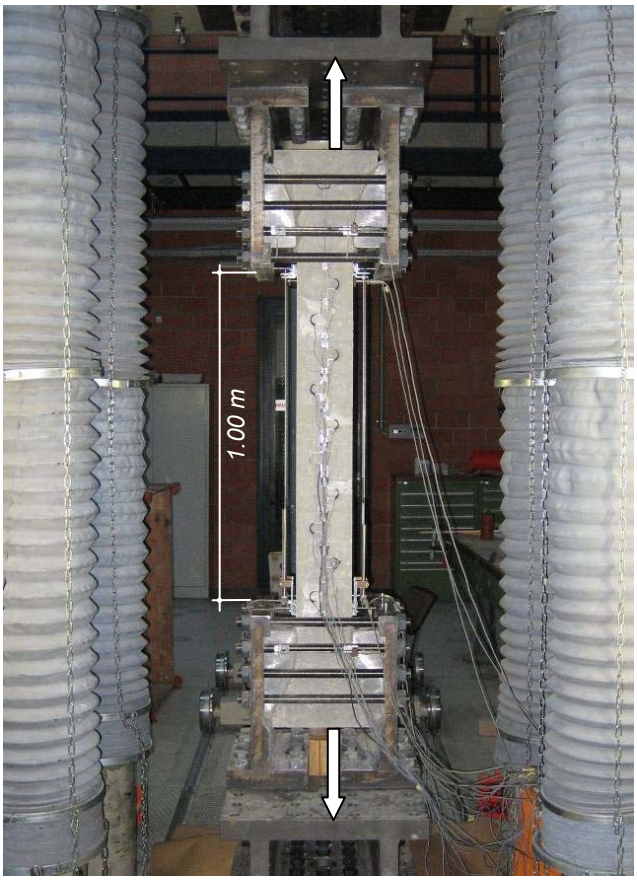

Figure 1 Test setup for full scale UHPFC tensile members with ordinary reinforcement and a measurement length of 1.00 meter.

The evolution of the crack pattern was observed and followed through different loading phases up to failure. Force – elongation curves allowed to clearly detect the influence of the type and amount of reinforcing steel on the structural response at ultimate.

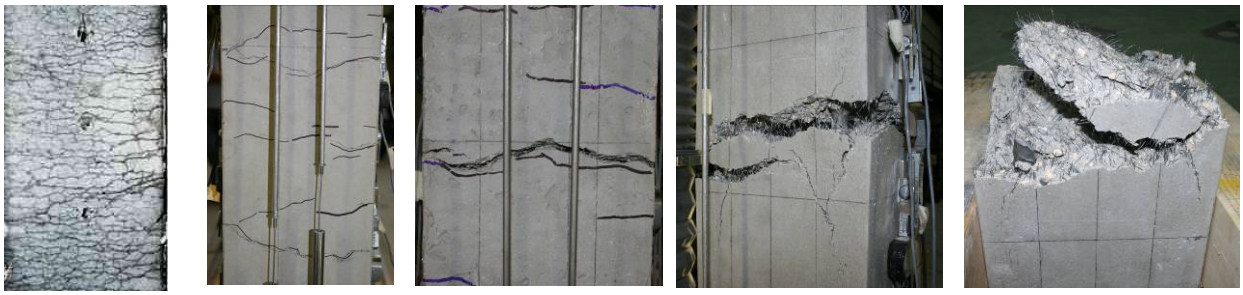

Figure 2 Crack pattern at different stages.

The following conclusions can be made:

- At the serviceability limit state, the behaviour of tensile members is very positively affected by the interaction between UHPFC and steel.
- At the ultimate limit state, the interaction between UHPFC and reinforcement leads to severe strain localization in tension.
- UHPFC tensile members cannot be made fully ductile by adding ordinary reinforcement. Alternative solutions are needed.
- An alternative definition of the amount of minimum reinforcement to avoid brittle failure in UHPFC members under tension has been proposed.

Dario Redaelli
EPFL – ENAC – IS-BETON
Bât. GC
Station 18
CH-1015
Lausanne
Switzerland
dario.redaelli@epfl.ch

Prof. Dr. Aurelio Muttoni
EPFL – ENAC – IS-BETON
Bât. GC
Station 18
CH-1015
Lausanne
Switzerland
aurelio.muttoni@epfl.ch

PUNCHING IN RC FOOTINGS CONSIDERING THE SOIL-STRUCTURE-INTERACTION

Marcus Ricker
RWTH Aachen University, Aachen, Germany
Josef Hegger, Supervisor

The punching shear capacity of footings determined by different codes varies significantly. The amount of the soil reaction to be deducted from the punching load differs from one code to another. The aim of the present investigation is to derive an advanced design model for footings taking into account the soil-structure-interaction. Since the middle of the last century several investigations into the punching behaviour of reinforced concrete footings have been performed. Mainly two test setups were used: either the test specimens were bedded on springs and a concentrated load was applied, or the footings were supported on the column stub and a uniform surface load was applied. Thus, the footings were tested under unrealistic boundary conditions. The main disadvantage of these experimental investigations is that the redistribution of the soil pressure underneath the footing is not accounted for. Therefore, at RWTH Aachen University punching tests on five reinforced concrete column footings supported on sand were performed by the Institute of Structural Concrete and the Institute of Geotechnical Engineering (Figure 1 (left)). The test parameters included the sand consistency, the shear span ratio, and the shear reinforcement. The concrete mixes were designed to reach a compression strength of 20 MPa. Each specimen was carefully instrumented with dial gauges. The experimental results indicate that the shear slenderness seems to affect the punching shear capacity significantly. Furthermore, the inclination of the shear failure plane is steeper than observed in punching tests on flat slabs (Figure 1 (right)).

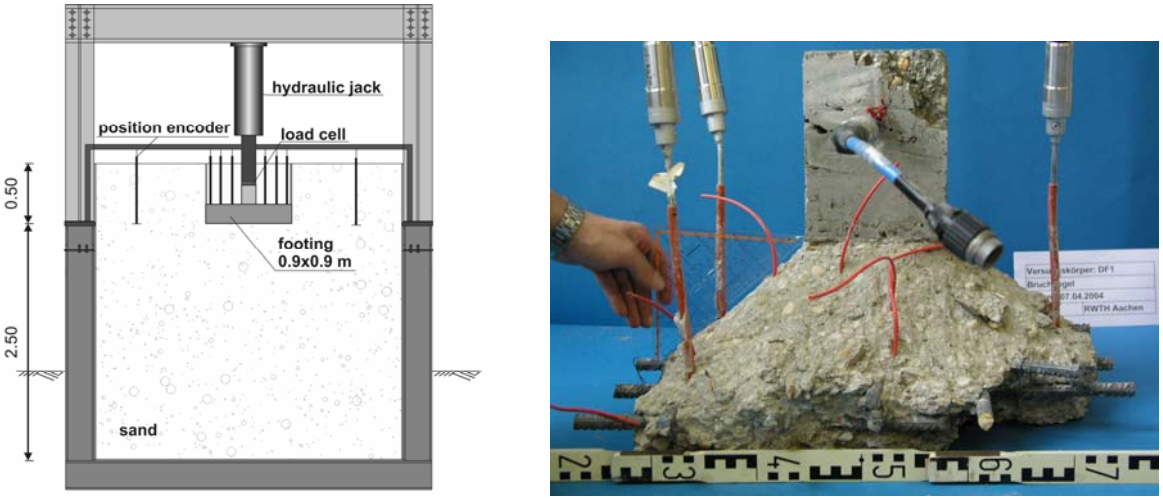

Figure 1 Test setup (left)
Punching Cone (right)

In addition to the experimental investigations a test databank containing about 200 punching tests on footings was established. The punching shear capacities predicted by different codes, and mechanical models respectively were compared with the tests from the databank. The comparison based on the ratio of the observed failure load V_{test} and the calculated punching resistance V_{calc} at ultimate limit state. In order to allow an evaluation of the different models the ratios V_{test}/V_{calc} were plotted versus the main punching parameters (d, ρ_l, f_c, λ).

To gain a further insight into the load carrying behaviour nonlinear finite element simulations were performed. Generally, the numerical simulations reproduce the measured failure loads, soil distribution, and strains satisfactorily. Furthermore, the analysis confirmed the assumption that the load carrying behaviour of the more compact footings is comparable to a strutted frame.

Finally, based on the investigations mentioned above an advanced design model was derived. The punching tests on footings taken from the literature as well as the own experimental investigations revealed a strong influence of the shear slenderness. With decreasing shear slenderness the punching capacity declines. For this reason the empirical design rule of Eurocode 2 was modified with a term taking into account the shear slenderness.

Based on the results of the investigations the following conclusions can be drawn:
(1) The shear slenderness significantly affects the punching shear resistance of footings.
(2) The observed angle of the failure cone was about 45° in all test specimens.
(3) Close to the failure load a concentration of the soil pressure underneath the column stub was measured in the present tests.
(4) The building codes tend to overestimate the punching resistance for compact footings with small shear slenderness.
(5) The mechanical models are not able to calculate the correct inclination of the punching cone for footings. Therefore, the models often overestimate the amount of the soil pressure reducing the shear force.
(6) A new equation was derived which ensures the required safety level of Eurocode.

This research program (AiF-No. 13620, DBV-No. 245) was supported by the Deutsche Beton- und Bautechnik Verein E.V. (DBV) by the funds of the Federal Ministry of Economy of Germany with a contribution of the Arbeitsgemeinschaft industrieller Forschung (AiF). The authors express thanks to the AiF and participating companies for their financial support. The tests were conducted in cooperation with the Institute of Geotechnical Engineering at RWTH Aachen University.

Dipl.-Ing. Marcus Ricker
RWTH Aachen University
Faculty of Civil Engineering
Institute of Structural Concrete
Mies-van-der-Rohe-Str. 1
D-52074 Aachen, Germany
mricker@imb.rwth-aachen.de

Univ.-Prof. Dr.-Ing. Josef Hegger
RWTH Aachen University
Faculty of Civil Engineering
Institute of Structural Concrete
Mies-van-der-Rohe-Str. 1
D-52074 Aachen, Germany
heg@imb.rwth-aachen.de

Proceedings-CD file name:
133_Rybinski.pdf

STRUCTURAL BEHAVIOUR OF STEEL TO CONCRETE JOINTS ON BASIS OF THE COMPONENT METHOD

Markus Rybinski
University of Stuttgart, Germany
Prof. Dr.-Ing. Ulrike Kuhlmann, Supervisor

Introduction

Anchor plates are used to transfer loads between steel and concrete structures, see Figure 1. Based on two test series of reinforced concrete specimens with anchor plates under shear and tension forces carried out by the Institute of Structural Design at the University of Stuttgart a first mechanical model has been developed describing the load-carrying capacity of anchor plates with welded studs in reinforced concrete elements.

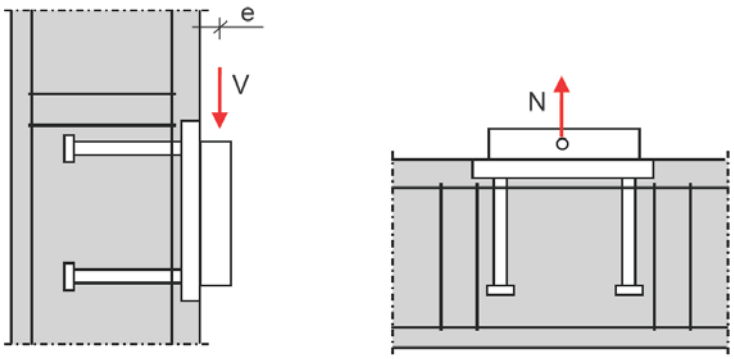

Figure 1 Anchor plates with welded studs submitted to shear or tension

Mechanical model

Based on the component model, a first design model has been developed and has been verified by more than 20 accomplished tests. This design model for anchor plates loaded with shear, tension or combined tension and shear forces is independent of the kind of fastener e.g. headed studs, dowels or welded reinforcement for load transmission of tension forces and headed studs, block shear connectors for load transmission of shear forces

By identifying the effective components of steel-to-concrete joints, characterising their structural behaviour and assembling them into the whole joint with the component method, the load-carrying capacity of the whole joint can be calculated. Within the scope of this first mechanical model only the maximum strength was considered. The stiffness and the ductility were not taken into account. This simplification is possible if the inner load distribution is clearly defined, e.g. when there is only one component for load transfer of the tension force.

Further research

An interdisciplinary collaboration of the Institute of Structural Design and the Institute of Construction Materials at the University of Stuttgart aims at a common design method for steel to concrete joints bringing together the different types of approaches for fastenings and

steel design. So the joint modelling between steel columns and concrete elements like foundations as an integrative system of frame and foundation considering the joint stiffness is topic of this ongoing research.

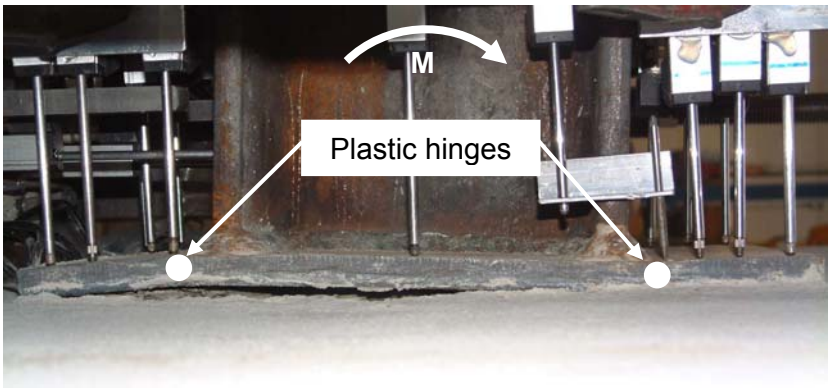

Figure 2 Anchor plate with headed studs avoiding brittle concrete failure by plastic hinges in tension and compression zone

Another current research project aims at gaining more knowledge about the structural behaviour of anchor plates with short edge distances. Within a test series with variation of different parameters like load angle, reinforcement and concrete quality and accompanying FE calculations the first mechanical model will be improved and the assumptions of the first design model for stiff anchor plates will be verified.

Conclusions

The load transfer of shear or tension forces by anchor plates with welded studs into concrete structures with reinforcement like in walls or columns is very relevant for practical applications. The proposed mechanical model may be a first step for solving this problem. It complies with the needs of an engineer for use in practice: transparency of the distribution of the forces and transferability to other situations. This model is based on the component method and therefore can easily be integrated in current European research work and code. More coordinated research work of steel und fastenings researchers is arranged for verification of the results and a higher acceptance of this method.

Markus Rybinski
University of Stuttgart
Institut of Structural Design
Pfaffenwaldring 7
70569 Stuttgart
Germany
markus.rybinski@ke.uni-stuttgart.de

Prof. Dr.-Ing. Ulrike Kuhlmann
University of Stuttgart
Institut of Structural Design
Pfaffenwaldring 7
70569 Stuttgart
Germany
u.kuhlmann@ke.uni-stuttgart.de

REPRODUCING ANCIENT MASONRY FOR IMPROVING DUCTILITY: A PRELIMINARY STUDY

Elisa Sala
University of Brescia, Brescia, Italy
Ezio Giuriani, Irene Giustina, Supervisors

Introduction

A previous study (Del Giorgio 1990-91) proved that, under uniaxial compression, the ductility of masonry could be increased through confinement.
The aim of this first part of the research was the design of a masonry specimen, suitably reproducing real historical masonries. To this end, an extensive number of mortar specimens were tested. Future development of this research will focus on the design of a method for confining masonry and for increasing ductility, in order to represent the actual behaviour of real masonry under seismic action.

Keywords

Masonry - mortar – ductility – seismic loading

Laboratory tests for choosing mortar

By testing some pieces of mortar, it is possible to choose the right mix of lime, lime putty, aggregates and water for the experimentation.
The method for selecting materials is based on a test procedure suggested by Felicetti and Gattesco (1998), which requires in-situ tests for measuring the mortar resistance. By using a sclerometer it is possible to obtain a relation between the number of hits and the rod embedded length in the mortar joint. Specimens of historical Italian masonries tested by means of sclerometer showed an average value of 5-6 hits/10 mm.
By considering the new European standard about limes (EN 459 2001), a natural moderately hydraulic lime, NHL 3.5, that well approximates historical mortar mechanical characteristics, was selected.(*Tab. 1-2)*.

Evaluation of crack-zone length

In order to assemble masonry specimens in the simplest way and in order to choose the most suitable test-loading machine it is necessary to know specimen crack length and inclination.
If one considers the masonry panel like a non-deformable block, it is simple to understand the resisting mechanism, which is based on the resisting moment due to the weight axial force. The axial force eccentricity is equal to the ratio of bending moment and axial load. At failure, the panel bottom section is cracked, provided that masonry does not offer any significant tensile strength. Cracks develop and extend until the reduced resisting section is able to support dead and over-loads.
In the paper an analytical formulation of the cracked-zone length and crack inclination is presented.

Table 1 Mortar mix

Test piece	Cod.	Lime [%]	Lime putty [%]	Water [%]	Aggregates [%]		
					3 mm	1.5 mm	0.5 mm
7	R2	8	5	15	36	36	--

Table 2 Test results

Test piece	hits/1st cm	hits/2nd cm	hits/3th cm	hits/4th cm	Average [hits/cm]
R2	5	5	5	--	5

Concluding remarks and future research

This first part of the experimentation gave important information about mortar characteristics and specimen geometry. Future studies will investigate the response of masonry panels subjected to seismic actions in order to design a method for confining masonry and increasing ductility.

Acknowledgments

The support of Eng. Fausto Minelli for his contribution in revising the paper, and of Mr. Pietro Mazzara in performing the experimental tests and in data reduction are gratefully acknowledged.

Reference

Del Giorgio, F., a.a. 1990-91, Valutazioni sperimentali degli effetti di un confinamento orizzontale sul comportamento di pareti in muratura, Tesi di Laurea, Relatori Macchi G. – Calvi M., Università degli Studi di Pavia

EN 459-1, 2001, Building Lime – Part 1: Definitions, Specification and conformity.

Felicetti G., Gattesco N., 1998, A penetration test to study the mechanical response of mortar in ancient masonry buildings, Material and structures, vol. 31

Elisa Sala
University of Brescia
DICATA
Via Branze, 43
25123 Brescia, Italy
elisa.sala@ing.unibs.it

Prof. Ezio Giuriani
University of Brescia
DICATA
Via Branze, 43
25123 Brescia, Italy
ezio.giuriani@ing.unibs.it

Prof. Irene Giustina
University of Brescia
DICATA
Via Branze, 43
25123 Brescia, Italy
irene.giustina@ing.unibs.it

IMPACT LOAD TESTS ON REINFORCED CONCRETE SLABS

Kristian Schellenberg
Institute of Structural Engineering, ETH Zurich, Switzerland
Thomas Vogel, Supervisor

A weight of 825 kg is dropped from 2 m on the reinforced concrete slab. This impact is then reproduced by a servo-controlled actuator in a second test and by the backstroke of blasted water in a third test. The suitability of these test setups to simulate the impact due to rockfall in the laboratory is evaluated. During the impacts, the support forces, strains and accelerations in the slabs are measured. The setup of the falling weight test is the most appropriate.

In mountainous countries like Switzerland, galleries are important structures regarding the reduction of risks due to rockfall. Together with avalanche galleries and tunnel entrances there are more than 350 structures endangered. The aim of this project is to develop a design method for new galleries and an evaluation procedure for existing ones. In preliminary tests three different setups were evaluated to suit for testing rockfall impacts on galleries under laboratory conditions.

An artificial boulder concrete with a diameter of 0.8 m and 825 kg weight is provided by the Swiss Federal Institute for Forest, Snow and Landscape Research (WLS) and dropped from a hook 2 m above the slab (Figure 1). The slab of 0.9 x 0.9 x 0.1 m is supported in the corners and is covered by a cushion layer, which is formed by a 0.19 m thick layer of sand in a textile bag. In the second setup the actions are simulated by a servo-controlled actuator. The applied actuator has an oil discharge of 120 l/min and a maximum load capacity of 1000 kN. The load is reproduced by enforcing a sudden displacement of 20 mm. In the third setup the impact is applied by blasting a water column inside a steel cylinder with an explosive charge. The explosive charge is implemented in a piston and displaces the water

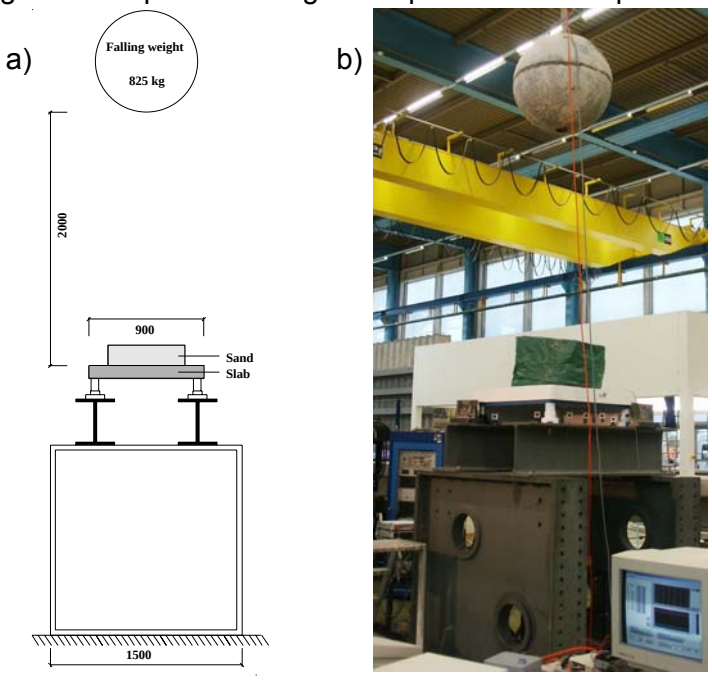

Figure 1 Falling weight test a) sketch, b) photo

a)  b) 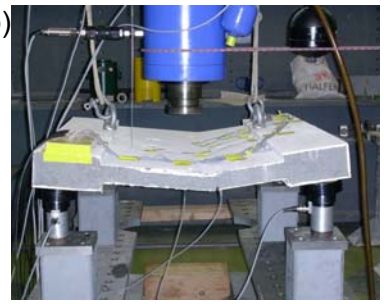 c) 

Figure 2 Specimens after the tests a) Falling weight , b) Actuator and c) Blasting test

after detonation. The reaction force of the accelerated water acts on the slab. The tube weights 20 kg and has a capacity of 1.5 litres water.

Support forces, accelerations in the slab, displacements and strains are measured with a sampling rate is 400 Hz. The supports are four load cells. The capacity of each cell is 300 kN. The accelerometers are attached to the specimen's soffit. The displacements are measured by an inductive displacement sensor and by a video extensometer. Eight gages of 20 mm length measure the strains at the upper surface of each specimen with a range of 4%. To enable a visual evaluation high speed cameras filmed the impact.

The stroke of the actuator test was too slow and reached the maximum after 45 ms. The water hammer had a loading time of 15 ms and is partially adequate to model a rockfall impact. However, the reached force is restricted by the equipment. The slabs after the tests are shown in Figure 2.

Concerning rockfall impacts, at least a sampling rate of 1 kHz should be applied. The most complex but also the most appropriated setup is the falling weight test. The applicability of actuator tests depends on the capacity of the oil valves. The velocity of the actuator should be at least 1 m/s. Although the water hammer has a short loading time, it shows a similar characteristic to the falling weight. With some adjustments in the water capacity or in the charge, the principle could be applied.

The contributions of C. Ebner, Dr. A. Volkwein, M. Baumann, S. Fricker, Dr. J. Laue, Prof. Dr. A. Dazio, Prof. Dr. M. H. Faber and Prof. T. Vogel are highly appreciated.

Kristian Schellenberg
ETH Zurich
Institute of Structural Engineering
HIL E 34.1
8093 Zurich, Switzerland
kristian.schellenberg@ethz.ch

Prof. Thomas Vogel
ETH Zurich
Institute of Structural Engineering
HIL E 33.3
8093 Zurich, Switzerland
vogel@ibk.baug.ethz.ch

Proceedings-CD file name:
125_Schleifer.pdf

SEPARATING FUNCTION OF LIGHT TIMBER FRAME ASSEMBLIES EXPOSED TO FIRE

Vanessa Schleifer
ETH Zurich, Zurich, Switzerland
Mario Fontana, Andrea Frangi, Supervisors

The main objective of the structural fire safety measures is to limit the fire spread to the room of origin by guaranteeing the load carrying capacity of the structure (requirement on mechanical resistance R) and the separating function of walls and floors (requirement on insulation I and integrity E) for the required period of time. The required period time is normally expressed in terms of fire resistance using the ISO standard fire exposure and is specified by the building regulations. While fire tests are still widely used for the verification of the fire resistance of assemblies of timber structures, calculation models become more and more common.
The research project studies the separating function of light timber frame assemblies consisting of solid timber studs or beams with linings of gypsum plasterboards, wood panels or combinations of it. The cavity is filled with insulation made of rock, glass or wood fibre or is void. To study the influence of different parameters on the fire performance of these assemblies fire tests have been performed on unloaded specimens at the Swiss Federal Laboratories for Materials Testing and Research (EMPA) in Dübendorf using ISO-fire exposure. Based on the test results and numerical simulations existing design methods for the verification of the separating function of wall and floor assemblies can be improved. The paper presents the test results and the first improvements of the model-coefficients for the verification of the separating function.
To calculate the fire resistance with regard to the separation function of assemblies, component additive methods are common. These methods are called component additive methods, since the fire resistance of a layered construction is obtained by adding the contribution to the fire resistance of the different layers.
According to EN 1995-1-2 2004 the time (t_{ins}) can be calculated as the sum of the contributions to fire resistance of the individual layers. For simplification, the contribution of each layer is calculated using the basic insulation value ($t_{ins,0,i}$), the position coefficient ($k_{pos,i}$) and the joint coefficient ($k_{j,i}$).

$$t_{ins} = \sum_i t_{ins,0,i} \cdot k_{pos,i} \cdot k_{j,i} \quad [min] \tag{1}$$

Based on the test results it could be shown that the temperature development is similar for gypsum plasterboards type A or F. That is also confirmed by König and Källsner 2000. Furthermore it could be observed that the temperature development of gypsum fibreboards is comparable to gypsum plasterboards. Therefore also the measured times of the separating function of the test with the gypsum fibreboard could be compared with the calculated values according EN 1995-1-2 2004. The measured times of the separating function of the tested assemblies with one layer of gypsum plasterboards or fibreboards are compared with the calculated times according EN 1995-1-2 2004. For separating constructions with only one layer, the position coefficient can be omitted. Furthermore the studied assemblies with gypsum plasterboards or fibreboards had no gaps. Therefore these constructions with one layer could be compared directly with basic insulation value. It could be shown that the basic

insulation value according to EN 1995-1-2 2004 is too conservative for thick boards. This could be also observed at wood panelling.

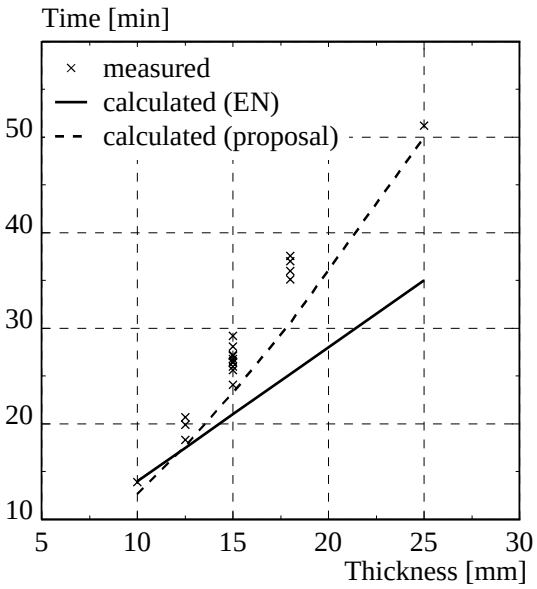

Figure 1 Times of separating function of assemblies with one layer of gypsum plasterboards or fibreboards

The large number of test results permit to improve the basic insulation value of gypsum plasterboards. For the basic insulation value of gypsum plasterboards with a panel thickness h_p [mm] the following equation is proposed:

$$t_{ins,0} = 0.4 \cdot h_p^{1.5} \quad [min] \qquad (2)$$

Figure 1 shows a good agreement between the calculated times according to equation (2) and the test results. Furthermore it can be seen that the basic insulation value is non linear proportional to the thickness. This observation could be also confirmed by finite element calculations using thermal material properties according to König and Källsner 2000 and Thomas 2002.

The basic insulation value for other materials can not be directly calculated from the test results, because of the small number of fire tests. To improve basic insulation values of these panels numerical simulations of heat transfer through the panels exposed to ISO-fire can be used. For these numerical simulations temperature related material properties are necessary. Some phenomena like the heat transfer by the evaporation of moisture and subsequent condensation further away from the heat source can not be taken into account in the finite element models. Therefore the input values of the thermal properties have to be calibrated to simulate these phenomena. The next steps are to calculate basic insulation values as well as position coefficients for different materials.

Vanessa Schleifer
ETH Zurich
Department of Civil, Environmental and Geomatic Engineering
Institute of Structural Engineering (IBK)
Wolfgang-Pauli-Str. 15
Zurich, Switzerland
schleifer@ibk.baug.ethz.ch

Prof. Dr. sc. techn. Mario Fontana
Dr. sc. techn. Andrea Frangi
ETH Zurich
Department of Civil, Environmental and Geomatic Engineering
Institute of Structural Engineering (IBK)
Wolfgang-Pauli-Str. 15
Zurich, Switzerland
fontana@ibk.baug.ethz.ch, frangi@ibk.baug.ethz.ch

PROBABILISTIC ASSESSMENT OF THE ROBUSTNESS OF STRUCTURAL SYSTEMS

Matthias Schubert
Institute of Structural Engineering, ETH Zurich, Zurich, Switzerland
Michael Havbro Faber, Supervisor

The present codes for the design of structural systems provide explicit design provisions for the individual members. The consistent assessment of the reliability of structural members is a well-developed research area. The codes provide requirements to member based design in terms of acceptable (target) failure probabilities. In general, the acceptable failure probability is associated with the expected direct consequences. Therefore these requirements are more related to the probability of failure or damage of components rather than to the reliability of the entire structural system. Even though the reliability of structural systems has been a subject receiving significant attention from structural engineers over the recent decades the design codes are less specific in terms of overall system requirements. To incorporate system performance, the stated requirement is that a system shall be robust. Most codes specify the property of robustness only in a qualitative manner, in the sense that, *the consequences of a structural failure should not be disproportional to the effect causing the failure*.

In the present paper a risk based framework for a quantitative assessment of robustness is outlined taking basis in previous works. The framework is then extended by considering the effects of possible determination effects as well as monitoring and maintenance activities. The robustness is a time dependent characteristic and depends strongly on the actions taken during the life cycle of a structure and on effects caused by its environment. Effects of aging and deterioration may have a strong influence on the robustness of a structure. Inspections and maintenance are necessary to keep a structure robust. The framework in the present paper is illustrated on an example concerning the time dependent performance of parallel systems.

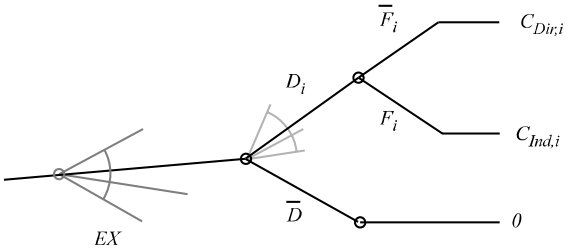

Figure 1: Event tree for the risk.

According to the generic risk assessment framework presently being written by the Joint Committee on Structural Safety a system can be represented as a spatial and temporal representation of all constituents required to describe the interrelations between all relevant exposures and their consequences. Direct consequences are related to damages on the individual constituents of the system whereas indirect consequences are understood as any

consequences beyond the direct consequences. This representation of a system can be modelled in an event tree (Figure 1).

First, an initial exposure (EX) occurs with a potential to cause damage in an undamaged system. The system maintains its initial condition if no damage $(\overline{D})$ occurs and no consequences are associated with this event. If a system is damaged several damage states (D_i) can result. All of the damage states which lead to failure (F_i) are associated with indirect consequences $(C_{Ind,i})$. In the cases where the system survives $(\overline{F}_i)$, only direct consequences $(C_{Dir,i})$ are associated.

By calculating the risk as the product of probability and consequences a corresponding index of robustness can be calculated through the ratio between the direct risks to the total risk. Introducing the time *t* allows for the calculation of the robustness of a structure over its lifetime.

As an example of the approach and to visualize the effects of time on the robustness of structural systems, a parallel system with ten members is investigated in detail. The annual probability of structural failure is calculated and the development of the robustness index over time in deteriorating structures is shown. Damage control such as inspection or repair of damaged components can be implemented in the analyses.

The presented framework is based on risk assessment and decision theory. It allows for the implementation of different mitigation measures over the life time of structural systems. It is shown that the proposed index reflects deterioration effects in structures consistently. By implementing repair and maintenance actions the robustness index can be kept above a certain level. The calculation of the ratio of the failure to the damage probability can also help to identify measures already in the decision phase that increases the robustness of a structural system.

Matthias Schubert
Institute of Structural Engineering
ETH Zurich
8093 Zürich, Switzerland
schubert@ibk.baug.ethz.ch

Prof. Dr. Michael Havbro Faber
Institute of Structural Engineering
ETH Zurich
8093 Zürich, Switzerland
faber@ibk.baug.ethz.ch

Proceedings-CD file name:
257_Schumacher.pdf

ROTATION CAPACITY OF STEEL FIBER REINFORCED CONCRETE BEAMS

Petra Schumacher
Delft University of Technology, Delft, The Netherlands
Joost Walraven, Supervisor
Joop den Uijl, Supervisor
Agnieszka Bigaj-van Vliet, Supervisor

Introduction

The use of nonlinear calculation models including the theory of plasticity can lead to cost savings in amount of concrete and steel. When using these approaches it has to be guaranteed that the deformation capacity provided by the structure exceeds the demand. The addition of fibers to concrete increases its ductility in compression and in tension. This suggests that it improves as well the rotation capacity of plastic hinges in reinforced concrete members. This research project aims at providing knowledge about if, and to what extent, the addition of fibers alters the rotation capacity of plastic hinges in concrete. The modeling steps that included the behavior in compression and tension, the bond of ribbed bars and the rotation capacity of plastic hinges in reinforced beams were supported by experiments.

Mechanical Properties of SFRC

The compressive strength and the axial tensile strength are not influenced by the amount of steel wire fibers used in this investigation. The ductility of the concrete in compression and tension is increased by the addition of the fibers. This increase depends on the effective amount of fibers, their geometry (fiber aspect ratio l_f/d_f, fiber length l_f), orientation, strength (pull-out or rupture) and bond properties in concrete (matrix quality, fiber shape). In this research project, the Compressive Damage Zone Model (Markeset 1993) was extended to different amounts of steel fibers with different aspect ratios.

Combined Reinforcement

In the scope of this research project, pull-out tests were performed on ribbed steel bars (d_s = 10 mm) in a self-compacting normal strength concrete without fibers and with 60 kg/m^3 hooked-end steel fibers (l_f = 30 mm, l_f/d_f = 80) varying the concrete cover (c = 15, 25, 35, 95 mm). The influence of the steel fibers in case of pull-out failure was very small. Considering the scatter of the test results, the influence of the steel fibers on the bond stress-slip relationship is neglected in the modeling in case of pull-out bond failure.
The concrete stresses at a crack in the steel fiber reinforced concrete (SFRC) have a value that is related to the crack width w. Contrary to plain concrete, the contribution of the concrete to the load transfer in the cracks cannot be neglected in modeling SFRC. The tensile strength is reached after a shorter transfer length in SFRC compared to plain concrete. Therefore, the crack spacing and the crack widths in the SLS are smaller for SFRC than for RC and the SFRC member is stiffer than a similar RC member.

Tests on the Rotation Capacity

In order to investigate the effect of steel fibers on the rotation capacity of reinforced concrete beams, beams (h = 300 mm, b = 150 mm, L = 3000 mm) were loaded at mid-span up to failure (rupture of a bar in case of steel failure or pronounced drop in load carrying capacity in case of concrete failure). The beams were reinforced with two ribbed bars with a diameter of

10 mm. Test variables were fiber content (no fibers and 60 kg/m^3 fibers with l_f = 30 mm, l_f/d_f = 80) and normal compressive force (N = 0 and N = 400 kN).
The addition of steel fibers in combination with the applied amount of reinforcing bars led to an increase in maximum moment of approximately 10% and to cracking but no spalling in the compressive zone. Remarkably the specimens tested with fibers had a smaller rotation capacity than those tested with fibers. This decrease in deformation capacity is explained with localization of the deformations in one large crack in case of the steel fiber reinforced specimens compared to several large cracks in case of the reinforced concrete specimens.

Localization of Deformations

To further investigate the phenomenon of localizations of the deformations in one large crack, a parameter study was carried out. The tensile member hardening was found to be proportional to the steel hardening ratio and inversely proportional to the fiber content.

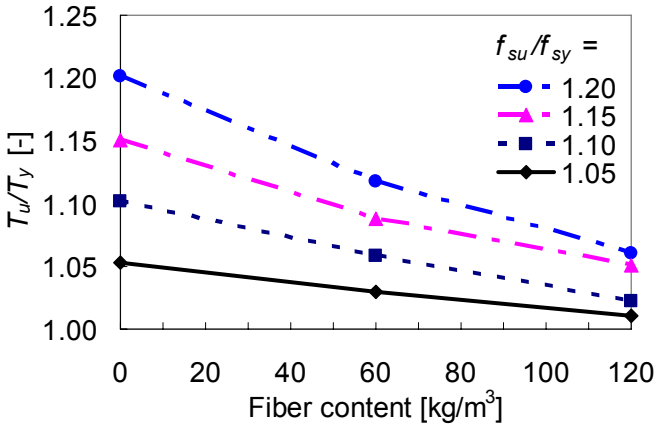

Figure 1 Tensile member hardening ratio for different f_{su}/f_{sy} and fiber contents

Keywords

Steel fiber reinforced concrete (SFRC), rotation capacity, bond, localization of deformations.

Petra Schumacher
Delft University of Technology
Civil Engineering and Geosciences
Section of Concrete Structures
P.O. Box 5048
2600 GA Delft
The Netherlands
P.Schumacher@citg.tudelft.nl

Prof. dr. ir. J.C. Walraven
Delft University of Technology
Civil Engineering and Geosciences
Section of Concrete Structures
P.O. Box 5048
2600 GA Delft
The Netherlands
J.C.Walraven@citg.tudelft.nl

Ir. J.A. den Uijl
Delft University of Technology
Civil Engineering and Geosciences
Section of Concrete Structures
P.O. Box 5048
2600 GA Delft
The Netherlands
J.A.denUijl@tudelft.nl

Dr. ir. A.J. Bigaj-van Vliet
TNO Built Environment and Geosciences
P.O. Box 49
2600 AA Delft
The Netherlands
Agnieszka.BigajvanVliet@TNO.nl

CONFINED REINFORCED CONCRETE COLUMNS: HISTORICAL DEVELOPMENT

Birgit Seelhofer
ETH Zürich, Zürich, Switzerland
Peter Marti, Supervisor

The structural behaviour of reinforced concrete columns has been investigated by many engineers and scientists and as a result, there is a wealth of experimental evidence and corresponding theoretical models, the historical development in this area has so far found only limited attention.

Before the development of confined reinforced concrete columns could be established, an intensive research of construction material science and technology and failure theory must precede.

The dimensioning of structural members necessitated the definition of limits for admissible stresses as well as characteristic material properties for the determination of the ultimate strength. Based on three different assumptions for determination of the ultimate strength, which were established in 1773 by Coulomb, see Figure 1 (a), in 1837 by St. Venant and in 1857 by Rankine, numerous scientists modified these failure criteria for several materials for better accordance with theirs test results. Particularly for plastic deformable materials, like steel, several assumptions were set up and with the implementation of the “yield potential” by von Mises in 1928, at last, the correlation between the yield condition and the associated deformation process could be established.

(a) (b)

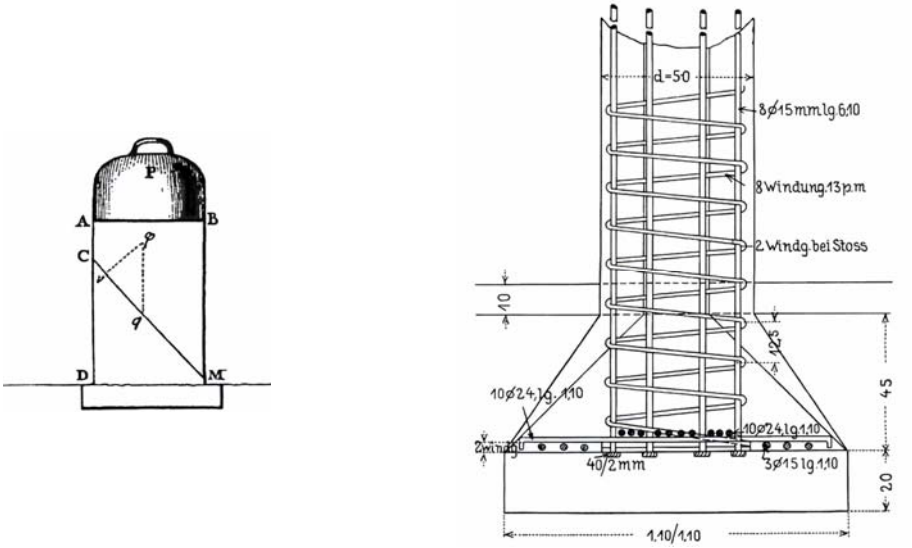

Figure 1 – (a) Coulomb 1773: Compressive strength of masonry;
(b) 1905: Column in the basement of the printing plant building at Brno.

In the 15th century, architectural theoreticians dealt with construction materials for the first time. Two centuries later, there was the beginning of the systematic investigation of construction materials. Only with the foundation of polytechnical schools in Europe in the 19th century, a general theory of elasticity and strength of materials emerged. Related to the investigation of the tectonic movements, at the end of the 19th century, numerous geological scientists subjected multiaxial compression tests with rock specimens to verify the different theories. These tests showed that in brittle materials plastic deformation can be generated. Inspired by the work of the geologist Heim, failure processes of different materials under multiaxial stress conditions were also examined within engineering and thereby the convenient effect of the confining pressure was discovered.

At the beginning of the 20th century the engineering tried to prevent the lateral deformation of pressed construction elements by different concepts of reinforcement. In 1901, Considère developed a confinement system for concrete elements for which he took out a patent in the same year. Besides, two years later, he documented the knowledge about the working principle of the confinement gained from the experiments and he proposed an empirical relationship for calculating the ultimate strength of confined reinforced concrete columns. At this time theoretical approaches to calculate the ultimate strength were hardly proposed. On the other hand the experimental research was rapidly expanded.

At the beginning of the 20th century, the confinement was individually used in the arch of concrete arch bridges but mainly in columns, see Figure 1 (b). The columns could be constructed more slender and thereby a better free space in the buildings was made possible.

Birgit Seelhofer
ETH Zürich
Department of Civil, Environmental and Geomatic Engineering
Institute of Structural Engineering
HIL E 41.1
Wolfgang-Pauli-Str. 15
CH-8093 Zürich, Switzerland
birgit.seelhofer@ibk.baug.ethz.ch

Peter Marti, Prof. Dr. sc. techn.
ETH Zürich
Department of Civil, Environmental and Geomatic Engineering
Institute of Structural Engineering
HIL E 41.2
Wolfgang-Pauli-Str. 15
CH-8093 Zürich, Switzerland
marti@ibk.baug.ethz.ch

MODELLING OF RC PLATE ELEMENTS AND FOLDED PLATE STRUCTURES

Hans Seelhofer
ETH Zürich, Zürich, Switzerland
Peter Marti, Supervisor

Many reinforced concrete structures such as bridge girders or cores of high-rise buildings act as folded plate structures and complex structures such as offshore-platforms can be treated as systems of folded plate structures. Based on well established models for panel elements a general treatment of plate elements and folded plate structures is presented.

To facilitate the discussion, a brief review of wall element models is given, emphasising the models' main assumptions. Usually, the behaviour of panel elements can be approximated by an uncracked elastic analysis, a cracked elastic analysis and a limit analysis based on the theory of plasticity. For the uncracked state the well-known relations for linear elastic solids in plane stress can be applied; in general, the contribution of the reinforcement can be neglected. The cracked elastic analysis can be based on the compression field theory. According to this theory one considers fictitious rotating, stress-free cracks with a vanishing spacing. The reinforcement is idealized by continuously distributed fibres with an infinitely small diameter, resisting only forces in their direction, and local stress variations in the concrete and in the reinforcement due to bond action are neglected.
For the limit analysis a rigid-plastic behaviour of concrete in compression is assumed, whereas its tensile strength is neglected. The reinforcement is idealized by continuously distributed fibres with a rigid-plastic behaviour and an infinitely small diameter, resisting only forces in their direction. The bond between the reinforcement and the surrounding concrete is assumed to be rigid. According to these assumptions one gets the yield locus and dimensioning rules for orthogonally reinforced concrete panel elements.

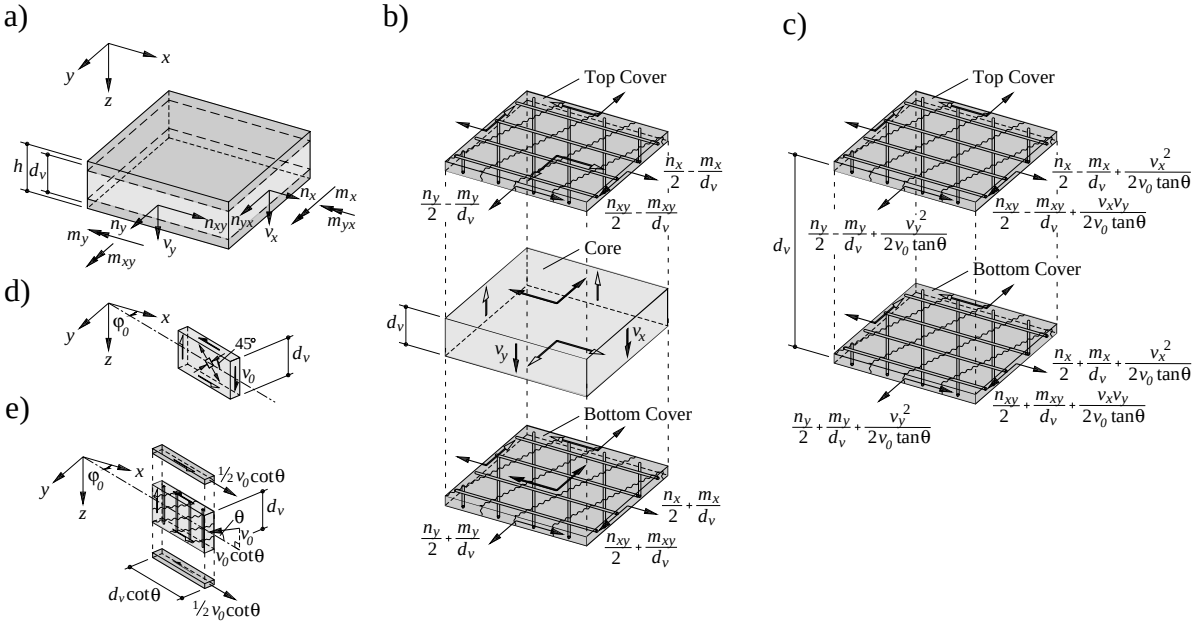

Figure 1 – Sandwich model: (a) stress resultants; (b) equivalent forces; (c) forces acting in cover elements in case of cracked core; (d) uncracked core; (e) cracked core.

An advanced modelling is provided by the cracked membrane model, which extends the classical compression field theory by assuming a rigid-plastic bond stress-slip relationship according to the tension chord model and by taking the compression softening in to account.

The introduction of a sandwich model enables a general treatment of plate elements by resolving the bending and twisting moments into equivalent forces acting on the top and bottom cover elements while the transverse shear forces are assigned to the core element, see Fig. 1. Thereby, the modelling is divided in cases with uncracked or cracked core. In the uncracked case, the cover forces are not affected by the transverse shear forces, see Fig. 1(b) and (d). For the cracked case, transverse reinforcement as well as additional equivalent forces in the top and bottom cover elements are required to equilibrate the diagonal compressive stress field in the core concrete, see Fig. 1(c) and (e). According to the lower-bound method of limit analysis, the sandwich model reduces the task of dimensioning a plate element for eight stress resultants to two membrane force dimensioning problems for the sandwich covers and, in the case of a cracked core, an additional web dimensioning problem. By combining the sandwich model with the cracked membrane model or the compression field theory the deformation and the deformation capacity of plate elements can be estimated.

Similar to the section-by-section design of reinforced concrete beams the modelling of folded plate structures with plate elements is restricted to regions without geometric and static discontinuities. In order to model entire folded plate structures the plate elements have to be supplemented with so-called generalized stringers, which combine two idealizations i.e. stringers of web-and-stringer models and shear lines in slabs. Future studies will concentrate on the further development of this model concerning the dimensioning and the estimation of both the deformation demand and the deformation capacity of folded plate structures.

In summary, the dimensioning of structural concrete folded plate structures can be carried out by subdividing the structure into plate elements and generalized stringers. Based on the sandwich model the modelling of plate elements can be traced back to that of panel elements. Apart from the dimensioning the sandwich model enables an approximate determination of the deformation capacity as well as the actual deformations.

Hans Seelhofer
ETH Zürich
Department of Civil, Environmental and Geomatic Engineering
Institute of Structural Engineering
HIL E 37.3
Wolfgang-Pauli-Str. 15
CH-8093 Zürich, Switzerland
seelhofer@ibk.baug.ethz.ch

Peter Marti, Prof. Dr. sc. techn.
ETH Zürich
Department of Civil, Environmental and Geomatic Engineering
Institute of Structural Engineering
HIL E 41.2
Wolfgang-Pauli-Str. 15
CH-8093 Zürich, Switzerland
marti@ibk.baug.ethz.ch

STRUCTURAL BEHAVIOR OF HIGH PERFORMANCE FIBER REINFORCED CONCRETE IN TENSION AND BENDING

Ryosuke Shionaga
Delft University of Technology, Delft, The Netherlands
J.C. Walraven, J.A. den Uijl, Y. Sato, Supervisors

Summary

This paper presents experimental results on the tensile and bending behavior of High Performance Fiber Reinforced Concrete (HPFRC). Axial tensile tests on concentrically reinforced prisms were performed in order to investigate the effect of steel fibers on the tension stiffening response. Furthermore, four-point bending tests on thin slab specimens with and without reinforcing bars were conducted in order to describe the interaction of steel fibers and conventional reinforcing bars in bending. Short straight fibers with a length of 13 mm and a diameter of 0.16 mm were applied, varying their orientation by the flow direction at casting in order to investigate the effect of the production method on the fiber orientation and the mechanical properties. The aim of these tests is to develop constitutive models for cracked HPFRC taking into account the fiber orientation.

Experimental program

Test parameters were two strength classes of concrete (B130 and B180) and the steel fiber content (V_f = 0, 0.8 and 1.6 Vol.%). The B130 mixture was self-compactable. In the specimens with this mixture the fiber orientation was either approximately aligned parallel or perpendicular to the principal load by varying the flow direction at casting. Fig. 1 shows the dimension of both the axial tensile and the four-point bending specimens. For the bending specimens the number of reinforcing bars was varied. The specimens were cast together as a large slab and sawn to the required size after hardening.

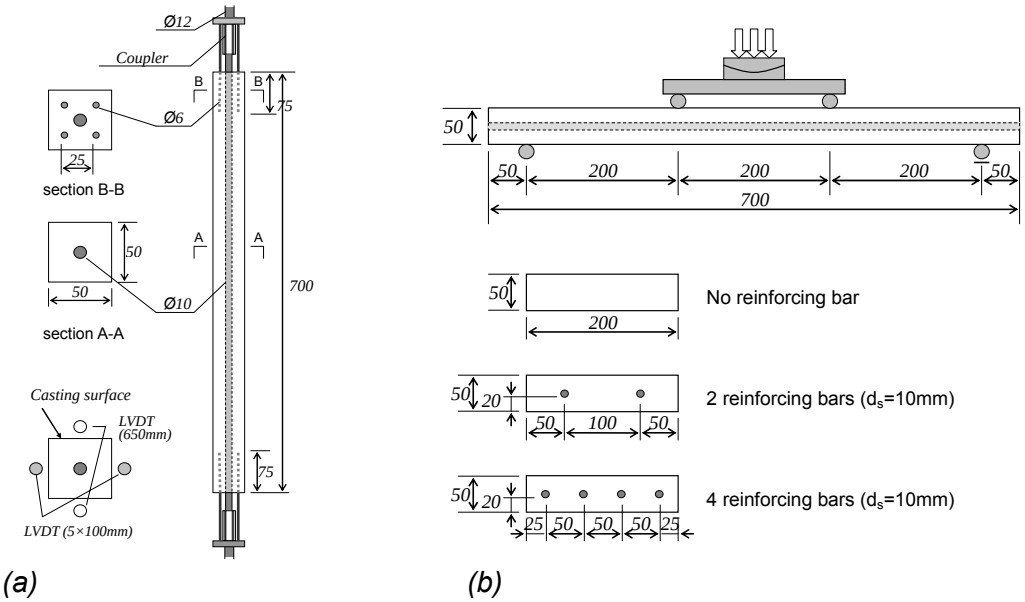

Figure 1 Specimen details of axial tensile test (a) and four-point bending test (b)

Test results and discussion

For the B130 series the tensile member responses are shown in Fig. 2 and the deflection responses of thin slab with 4 re-bars are shown in Fig. 3. These values were influenced by the fiber content and the casting direction (x; parallel to force, y; perpendicular to force). Similar tendencies were observed in the B180 series. From the results the following conclusions can be drawn:

- The addition of steel fibers to reinforced concrete members enhances the tension stiffening strain as well as the axial load at which the reinforcing bars start to yield. This resulted in more fine cracks, smaller crack spacing and less average crack width.
- Similar tendencies (influence of fibers, crack distribution) were observed in both the axial tensile tests and the four-point bending tests.
- The fiber orientation, which was aligned by varying the flow direction at casting, influenced both the tensile response and the bending response of HPFRC. The positive alignment (parallel to force) led to a reduction of the member deflections.

In order to relate the tension stiffening response to the fiber orientation and distribution, the actual fiber orientation should be quantified. To that end photographs of several sawn cross-sections will be subjected to image analyses.

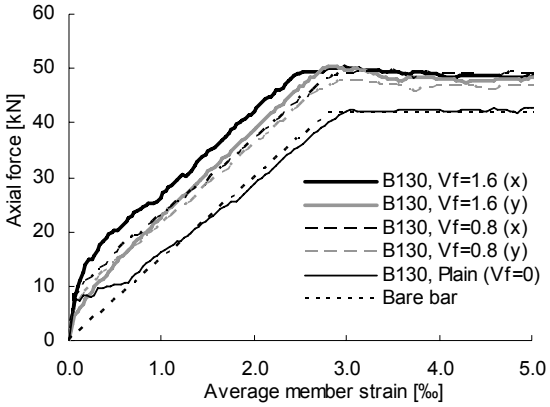

Figure 2 Elongation of axial tensile specimens on B130 series

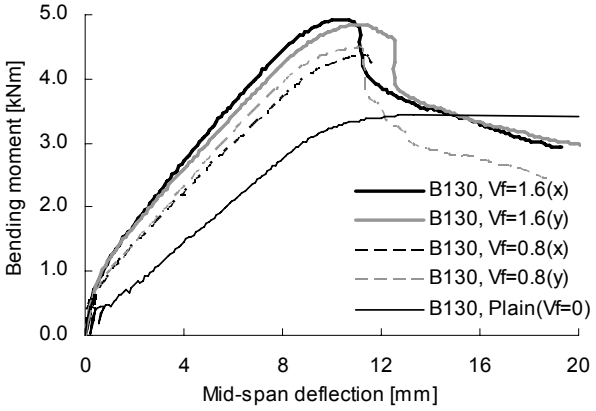

Figure 3 Mid-span deflection of four-point bending specimens on B130 series

Ryosuke Shionaga
Delft University of Technology
Civil Engineering and Geosciences
Section of Concrete Structures
Stevinweg 1, 2628CN Delft
The Netherlands
r.shionaga@tudelft.nl

Prof. dr. ir. J.C. Walraven
Delft University of Technology
Civil Engineering and Geosciences
Section of Concrete Structures
Stevinweg 1, 2628CN Delft
The Netherlands
j.c.walraven@tudelft.nl

Ir. J.A. den Uijl
Delft University of Technology
Civil Engineering and Geosciences
Section of Concrete Structures
Stevinweg 1, 2628CN Delft
The Netherlands
J.A.denUijl@tudelft.nl

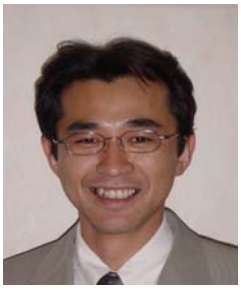

Dr. ir. Y. Sato
Hokkaido University
Division of Structural and Geotechnical Engineering
Hybrid and Concrete Structures
Kita-ku Kita13 Nishi8,
Sapporo
Japan
ysato@eng.hokudai.ac.jp

CHLORIDE TRANSPORT AND REINFORCEMENT CORROSION IN THE TRANSITION ZONE BETWEEN SUBSTRATE AND REPAIR CONCRETE

Pål Skoglund
Royal Institute of Technology in Stockholm / Swedish Cement and Concrete Research Institute
Jonas Holmgren, Supervisor

Abstract

The compatibility between concrete repair materials and old concrete is important for achieving a concrete repair with required durability. Bad experience of concrete repairs has been reported in several studies about concrete repairs. Enhanced knowledge and understanding of the repair material and the characteristics of the transition zone will increase the possibilities for optimal concrete repairs.

In this paper, results from a study of the transition zone between substrate concrete and repair concrete are presented. The investigation is focused on chloride transport and reinforcement corrosion. The results show that chlorides from a contaminated sound concrete migrate into a denser repair concrete. It is also observed that reinforcement corrosion may appear in the transition zone.

Methods

Reinforced concrete specimens, 250x100x55 mm, with concrete repairs were made in 1992 at CBI in Stockholm. In present investigation four of these specimens, 33R, 43R, 53R and 63R, were investigated. The concrete cover is 16 mm in all the specimens. The substrate concrete in the specimens had w/c ratio of 0.70 (33R and 53R) and 0.50 (43R and 63R). 1.0 wt% chlorides of cement weight were mixed into the substrate concrete for 33R and 43R. In specimens 53R and 63R 4.0 wt% chlorides were intermixed with the cement. The repair concrete had a w/c ratio of 0.40 in all the specimens. The specimens have been exposed to outdoor climate conditions without any external chloride ingress (CBI, Stockholm, Sweden) for 13 years.

The chloride profiles across the transition zone were analysed with SEM-EDS analysis. The reinforcements were ocullarly investigated and the corroded areas were studied

Results and Conclusions

Admixed chlorides of 1 and 4 wt% of cement weight in laboratory made concretes (w/c ratio 0.70 and 0.50) were found to migrate into a denser repair concrete (w/c ratio 0.40). The concentrations of chlorides reached relatively high levels in the repair concrete. In the case where the substrate concrete had a w/c ratio of 0.70, the chloride concentrations in the repair concrete reached higher values than the cases with w/c ratio of 0.50 in the substrate concrete.

Near the transition zone the substrate concretes have been carbonated due to a porous transition zone to about 2.3 mm (w/c ratio 0.70) and 1.6 mm (w/c ratio 0.50). The repair concrete showed little or no carbonation (0 – 0.2 mm depth).

The carbonated zone in the substrate concretes contains low concentrations of chlorides. Behind the carbonated zone the chloride concentrations reached high levels of 2 – 2.5 wt% for 33R and 43R and 3 – 5 wt% for 53R and 63R. High chloride concentrations behind carbonated concrete has earlier been reported in the literature and are caused by the carbonated concrete that has low capacity of binding chlorides. At greater depths the concentrations decreased to background values of about 1 wt% for 33R and 43R.

It was also observed that the corrosion products were located on either side of the transition zone.

The gathered data in this study suggest that differences in electrochemical potentials between concretes were established and that these differences have been the driving force for corrosion and chloride concentration at the transition zone.

It is the authors view that the potential for corrosion in the transition zone needs to be considered in patch repair work.

Pål Skoglund
Swedish Cement and Concrete Research Institute
SE-100 44 Stockholm, Sweden
pal.skoglund@cbi.se

Jonas Holmgren
Professor
Concrete Structures
Dept. of Civil and Architectural Engineering
Royal Institute of Technology (KTH)
SE-100 44 Stockholm
SWEDEN
jonas.holmgren@byv.kth.se

Proceedings-CD file name:
189_Spasojevic.pdf

POSSIBILITIES FOR STRUCTURAL IMPROVEMENTS IN THE DESIGN OF CONCRETE BRIDGES

Ana Spasojevic
Ecole Polytechnique Fédérale de Lausanne, Switzerland
Aurelio Muttoni, Supervisor

The improvement of the performance and efficiency of bridges is a constant task of engineering design. It is influenced by a variety of parameters, such as the structural concept (the shape and the type of material used), design approach, building abilities, construction method. In the context of this research, efficient structures are defined as structures that satisfy the design requirements with a minimum amount of materials, enabling easy construction. Recent developments in concrete material properties, as in the case of ultra high performance fibre reinforced concrete, have in particular renewed the research interest for this topic. The scope of the research are concrete road bridges of medium span.

The decrease in material consumption while keeping a sufficient strength and a suitable stiffness is observed as a constant driving force throughout the evolution of concrete bridges. Topological optimisation is thus applied as a procedure to find efficient structural shapes with respect to the maximum stiffness achieved for a given volume of material (fig. 1). This procedure led to the recognition of some existing structural shapes.

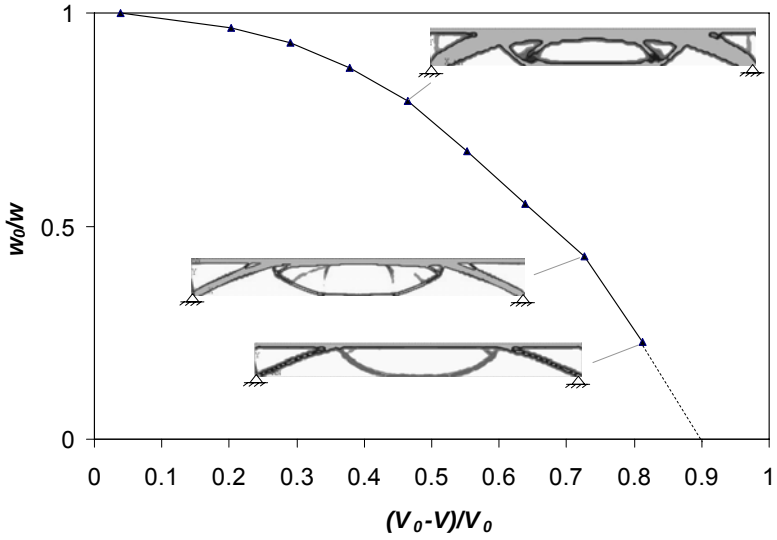

Figure 1 Change in structural stiffness (w_0/w) in function of the volume reduction with the corresponding optimised shapes

The resulting predefined shapes will be further optimised, including constrains of concrete bridge design, which required further development of numerical models. The final solution is controlled by the ultimate limit state, by the serviceability limit state requirements or by constructive constrains. An example of the application of this approach to the classical case of a continuous bridge girder with a box section is presented in the paper. This study has shown that classic concepts are low sensitive to material strength improvements in regard to material consumption (fig. 2).

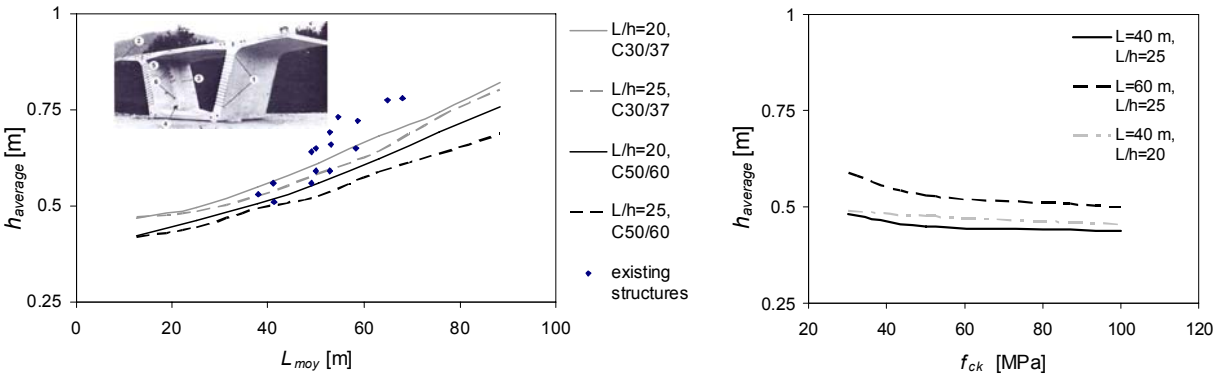

a) Influence of the span on the amount of concrete, compared to existing structures

b) Influence of the concrete strength on the amount of concrete

Figure 2 Parametric simulation of structural response

For a more competitive application of advanced properties of concrete, new structural concepts need to be investigated. A promising improvement is seen in the application of UHPFC, whose characteristics enable to avoid passive reinforcement, allowing an important decrease in dimensions. The new concept of a ribbed upper slab, with an equivalent thickness of less than 0.14 m, is currently under investigation. This system provides a significant decrease in weight in comparison to application of ordinary and high strength concrete, while keeping a sufficient stiffness and allowing an easy construction by prefabricated elements. To support this design, testing programme is currently under way at the Structural Concrete Laboratory at the EPFL. This experimental research should provide knowledge on particular structural responses and failure modes, leading to safe design approach enabling a better exploitation of this material's advanced properties.

Ana Spasojevic
EPFL – ENAC – IS-BETON
Bât. GC
Station 18
CH-1015
Lausanne
Switzerland
ana.spasojevic@epfl.ch

Prof. Dr. Aurelio Muttoni
EPFL – ENAC – IS-BETON
Bât. GC
Station 18
CH-1015
Lausanne
Switzerland
aurelio.muttoni@epfl.ch

STIFFNESS REQUIREMENTS FOR SLAB TRACK RAILWAY SYSTEMS FROM A DYNAMIC VIEWPOINT

Michaël J.M.M. Steenbergen
Delft University of Technology, Delft, the Netherlands
Coenraad Esveld, Supervisor
Andrei V. Metrikine, Supervisor

Nearly all designs of current slab-track railways are based on the principle of a relatively flexible concrete slab on top of a stiff substructure. The ballastless slab-track is applied on an increasing scale for high-speed lines, which are often built in delta areas with relatively weak subgrades. Therefore, often massive and cost-intensive soil improvements are necessary. A more economic possibility to meet stiffness requirements may be to increase the bending stiffness of the concrete slab-track itself, as can be achieved by applying an eccentric reinforcement. The present contribution compares both system stiffening methods from a dynamic viewpoint.
The model used to investigate the dynamic response of the slab track to a moving train load consists of a beam on visco-elastic half-space subject to a moving load. This model is described analytically, allowing for a derivation of the equivalent vertical dynamic stiffness of the half-space against the beam. With the help of this stiffness it is possible to reformulate the problem of the beam on half-space to a beam on a 1-D elastic foundation, with complex stiffness depending on frequency and wavenumber of flexural waves in the beam.
To determine the total vertical track stiffness under a moving train axle, also the bending behaviour of the beam itself is accounted for. In this way a quantity is derived which is designated as the total vertical generalised dynamic track stiffness, K_z. It is a function of both frequency and wavenumber, valid for any arbitrary loading in the time-space domain, and given by the summation of the vertical equivalent dynamic stiffness of the half-space under the beam and the dispersion characteristic of the free beam.

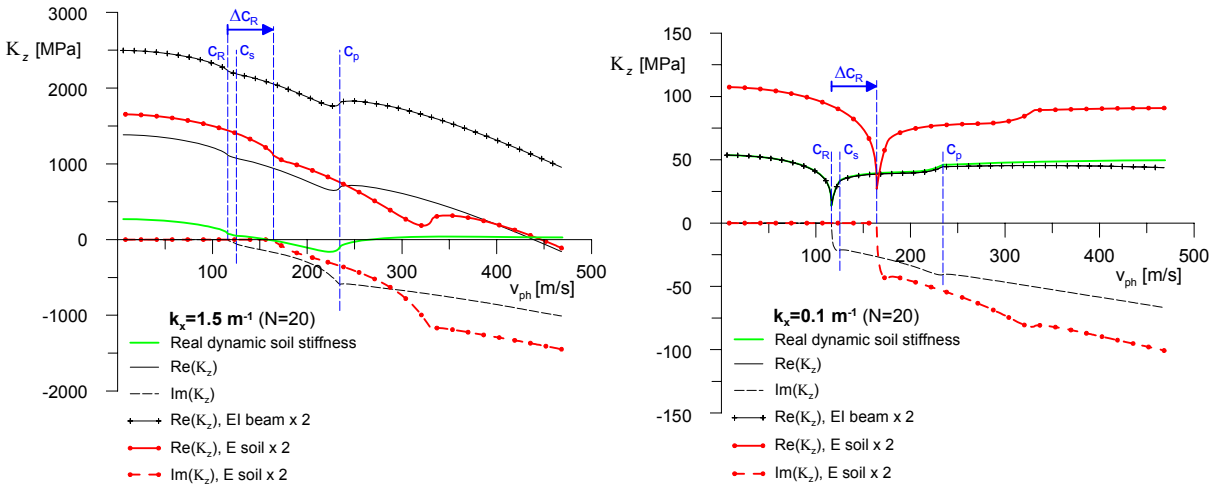

Figure 1 Effects of an increase of the beam flexural stiffness and a soil improvement on the generalised vertical dynamic track stiffness against arbitrary loading, for short waves (left) and long waves (right) relative to the track width (body and surface wave speeds are indicated for the reference situation).

In Figure 1, K_z is plotted as a function of the phase speed of longitudinal waves in the system, for relatively short waves and relatively long waves relative to the track width, and for a doubling of the soil Young's modulus and the slab bending stiffness respectively. The following conclusions can be drawn. An increase of the slab bending stiffness causes an *upward shift* of the stiffness function in the phase velocity domain, which is found to be proportional to the 4^{th} power of the wavenumber, indicating that the stiffness increase is much more significant for short waves than for long waves. The change of the total generalised track stiffness due to an increase of the soil Young's modulus on the contrary cannot be predicted unequivocally and depends on the actual magnitude of the equivalent soil stiffness. For an improved soil an increase of the Rayleigh wave speed (critical train speed) is found, which is most important for long waves. For long waves, the influence of slab stiffening appears to be negligible. Limiting considerations (for practice) to the sub-Rayleigh regime, it can be concluded that for long waves/low frequencies in the track soil improvement is a better solution, whereas for short waves/high frequencies increasing the slab stiffness is much more effective.
Figure 2 shows the effect of different track stiffening measures on the slab deflection amplitude under a uniformly moving harmonic load, as a function of the loading frequency (track with common parameter values). The above conclusions are confirmed. Therefore, in general the whole loading spectrum should be accounted for in an intelligent slab design.

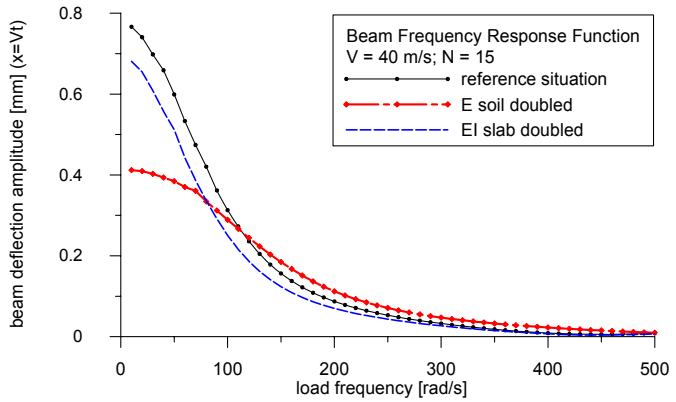

Figure 2 Effects of an increase of the beam bending stiffness and a soil improvement on the slab frequency response (at subcritical load velocities).

Michaël J.M.M. Steenbergen
Delft University of Technology
Faculty of Civil Engineering and Geosciences
Section of Road and Railway Engineering
Stevinweg 1
NL 2628 CN Delft, the Netherlands
M.J.M.M.Steenbergen@tudelft.nl

Coenraad Esveld
Delft University of Technology
Faculty of Civil Engineering and Geosciences
Section of Road and Railway Engineering
C.Esveld@tudelft.nl

Andrei V. Metrikine
Delft University of Technology
Faculty of Civil Engineering and Geosciences
Section of Structural Mechanics
A.V.Metrikine@tudelft.nl

RESPONSE OF ASYMMETRIC HIGH-RISE BUILDINGS UNDER WIND LOADING

Raphaël D.J.M. Steenbergen
Delft University of Technology, Delft, The Netherlands
Johan Blaauwendraad, Supervisor

Among the high-rise building design engineering community the ambition and necessity exist to build always higher and more slender buildings. Often, architects ask for freedom in design and propose building shapes with an asymmetric plan, which additionally can change along the height of the building. In this study, a calculation method has been developed to provide insight in the force flow in these types of structures. FEM programs are at disposal; however easy to use fast methods are not available, especially the in plane floor stiffnesses and the twisting stiffnesses are difficult to include. The new method is developed using a very small number of super elements; so, a fast calculation tool is obtained providing good insight in the behaviour of the building for preliminary design. We consider a high-rise building with an asymmetric floor plan (Fig. 1). Two slender tall walls and one shaft assure the stability of the building. One wing of the building has a reduced height as compared to the rest of the building, resulting in a discrete change in geometry in vertical direction.

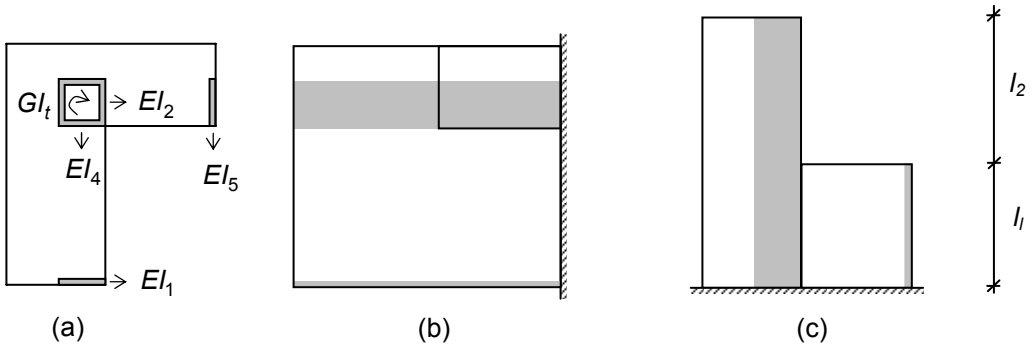

Figure 1 Ground plan (a), side view (b) and front view (c) of the asymmetric structure.

Closed-form solutions are presented for the response of the stability elements to static wind load, accounting for geometrical discontinuities. The in-plane stiffnesses of the floors are included and act as distributed coupling springs between the stability elements. The action of the stability elements and the distributed floors is of a parallel nature. Therefore the needed set of differential equations for each super element is an assemblage of the differential equations of the stability elements and the stiffness matrix of the distributed floors. For each super element a set of simultaneous differential equations is derived and closed-form solutions are obtained. For each super element the stiffness matrix is composed from the homogeneous solution and the load vector is composed from both the particular and the homogeneous solution. Foundation stiffness is accounted for. At each change of geometry (node) a marked disturbance in the moment and shear force diagram is found, attenuating along a number of storeys depending on the ratio of the characteristic length and the length of the building. For an example, see Fig. 2a for the shear force distribution in one direction of the shaft. The shear forces for the case of infinitely stiff floors and an infinite torsional rigidity of the shaft are indicated by a dashed line. Relative to this solution, we clearly observe disturbances in the moment and shear force distributions. Closed-form expressions for the influence lengths of these disturbances are obtained.

Including the rotational stiffness of the foundation may result in substantial disturbances in the stress state at the base of the building. To minimize the disturbances, the wall and shaft bending moments at the base of the building are the points of reference. The proportion between these base moments is the optimal proportion for the rotational stiffnesses of the wall foundation and shaft foundation; then no disturbance in the stress state will occur. In Fig. 2b the shear force distribution in stability wall 1 is shown for different realistic rotational stiffnesses of the foundation with respect to an infinitely clamped support (the solid line).

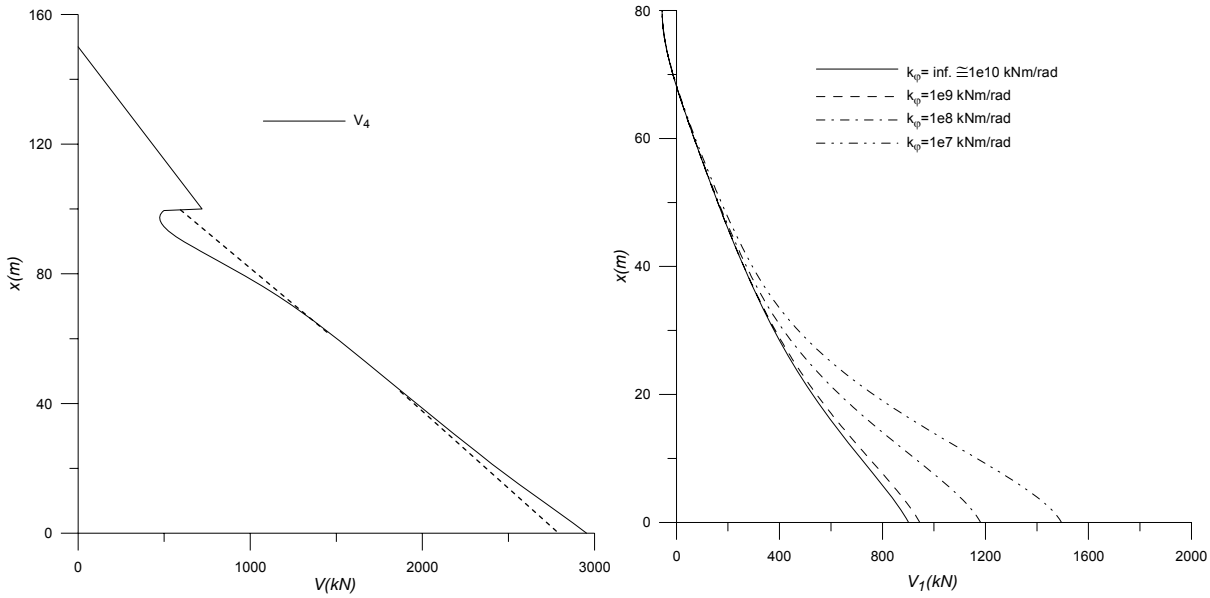

Figure 2 Disturbances in the shear force flow in stability wall 4 (a), Influence of the foundation stiffness on the shear force flow in stability wall 1 (b).

Because of the use of a very small number of super elements with closed-form solutions, the method contributes to the understanding of the behaviour of the considered tall buildings with a discrete change along the height. In a preliminary design stage a fast analysis can be made without spending much time in modelling. It is shown that the modelling and calculating time of the present method is reduced significantly in comparison with complete finite element analysis and accurate results are obtained.

R.D.J.M. Steenbergen
TU Delft
Civil Engineering
Structural Mechanics
Stevinweg 1
NL 2628 CN Delft
r.d.j.m.steenbergen@tudelft.nl

J. Blaauwendraad
Emeritus Professor
TU Delft
Structural Mechanics
Stevinweg 1
NL 2628 CN Delft
j.blaauwendraad@osbouw.nl

Proceedings-CD file name:
136_Teichmann.pdf

INFLUENCE OF CREEP AND MOISTURE ON THE LATERAL TORSIONAL BUCKLING OF TIMBER BEAMS

Gabriele Teichmann
University of Stuttgart, Stuttgart, Germany
Ulrike Kuhlmann, Supervisor

In addition to the stress calculation the stability analysis of slender laminated timber beams will become more important, because slender beams under bending may fail by lateral torsional buckling. The assessment of the lateral torsional buckling depends among others on the imperfection of the system; increasing imperfections decrease the safety against stability. In contrast to short term behaviour, stability behaviour concerned by changing and varied stiffness across section and length due to long-term effects has not yet been considered; creep and non-uniform swelling or shrinkage do not only increase the vertical but also the horizontal deflections. To obtain the influences of creep and shrinkage, the verification of lateral torsional buckling is extended by a rheological model of timber.
Wood shows a clear long-term behaviour. This long-term behaviour, resulting in with the time increasing deformations and a reduction of the strength, is verified also according to the new German and European standards only at the limit state of serviceability: Creep coefficients for middle moistening are given, which lead to an enlargement of the elastic deformations. However, creeping depends not only on the absolute moisture content of the wood, but also among others on moisture changes.

So far, the influence of long-term behaviour has only to be considered for the stability check at ultimate limit state, if the design value of the permanent load of structural members under compression in service class 2 and 3 is higher than 70% of the total load. Then, the stiffness is reduced by a factor $1/(1+k_{def})$ regardless whether the equivalent column method or a calculation according to the second-order-theory is applied.

However, the standards as well as preceding research work always assume temporally constant climatic conditions. If it comes to changes of moisture over the time, the mechano-sorptive effect arises, i.e. that the creep deformations become clearly larger with simultaneous mechanical load and moisture sorption than under constant load and constant dampness.
Furthermore, depending on the situation a cross section may be installed, so that it is protected from moisture as a whole or only partially. Thus a section may also be moistured only from two or three sides, so that there is a non-linear moisture content along the cross section which leads to an additional curvature resulting in an imperfection, see Fig. 1.
The imperfections due to three sided humidification increases the effect of lateral torsional buckling and thereby reduces the load carrying capacity of the beam.

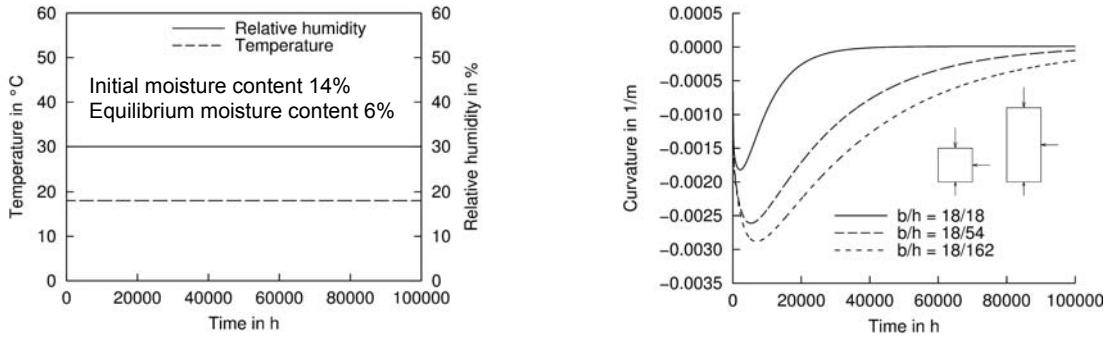

a) Climatic data *b) Curvature due to shrinking*

Figure 1 Curvature of construction units during three-sided moisture effect

The aim of this work is to analyse the influence of creeping as well as swelling and shrinking of wood during alternating climatic conditions in order to study the lateral torsional buckling safety of slender laminated timber beams computationally. Therefore, a program is developed based on differential equations according to second-order-theory.
These equations are extended by a term which considers the long-term behaviour of the timber. Here, it is assumed that the total deformations consist of an elastic portion and a portion from imperfection and/or creep deformations. These equations are implemented and solved in a computer program. The determination of the long-term behaviour is hereby carried out with a program, which has also been developed at the University of Stuttgart, Institute of Structural Design. With this calculation procedure the overall curvatures, the creep curvatures, as well as the stiffness of the cross section with respect to the current moisture content are determined for every time step, using different rheological models.

On the basis of this program, parameter studies are possible to identify the decisive factors of influence. The complex calculation model has to be simplified for an application in practice on the safe side. So the long-term behaviour might be considered e.g. by modified tilting factors and/or modified material indices or e.g. by reduced cross sections. By the evaluation of the simulation results a more exact and at the same time simpler analysis of the carrying and deformation behaviour will be possible for the design of slender laminated timber beams. The aim is to develop a model that allows a safe and economical design of all variables.

Gabriele Teichmann
University of Stuttgart
Institute of Structural Design
Pfaffenwaldring 7
70569 Stuttgart, Germany
Gabi.Teichmann@ke.uni-stuttgart.de

Prof. Dr.-Ing. Ulrike Kuhlmann
University of Stuttgart
Institute of Structural Design
Pfaffenwaldring 7
70569 Stuttgart, Germany
Ulrike.Kuhlmann@ke.uni-stuttgart.de

NUMERICAL SIMULATION OF THE FLOW BEHAVIOUR OF SELF-COMPACTING CONCRETES USING FLUID MECHANICAL METHODS

Stephan Uebachs
RWTH Aachen University, Germany
Wolfgang Brameshuber, Supervisor

The application of Self-Compacting Concrete (SCC) may lead to a poor quality of the building members when the concretes in the member feature no self-compacting properties, when the concretes segregate during the casting process or when there is a sedimentation of the coarse aggregate. These effects may even occur when the respective concretes show the required fresh concrete properties before casting. Thus, it is not always possible to ensure a problem-free application of SCC in a building member only on the basis of the fresh concrete tests. The reason therefore is that the characteristics from the fresh concrete tests, which have so far been applied for the assessment of SCC, do not completely describe the real mechanisms of the flowing and de-airing procedure.

A possible solution may be found in the numerical simulation of the flowing process by means of which any rheological property of the SCC and the geometry of the building components can be reproduced. When numerically modeling the fresh concrete properties of SCC, two approaches have been pursued: The Distinct Element Method (DEM) and the Dissipative Particle Dynamics (DPD). These methods are restricted because fresh concrete tests can only be simulated due to the enormous amount of necessary calculations. In this paper, examinations are presented which use numerical methods on the basis of fluid mechanical approaches, the Computional Fluid Dynamics (CFD).

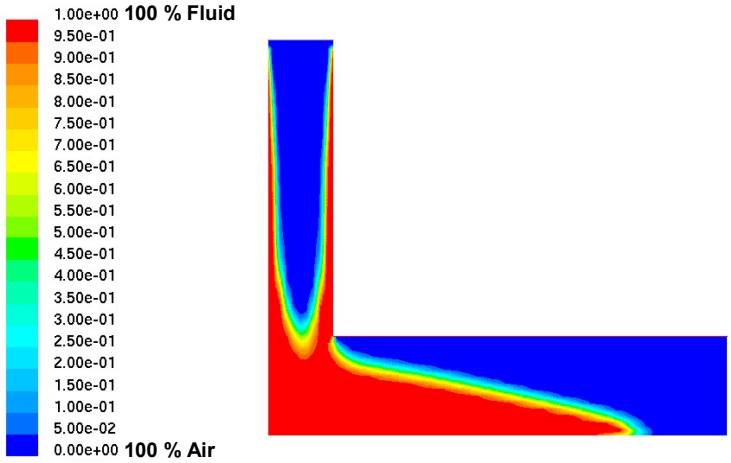

Figure 1: Computional Fluid Dynamics (CFD) calculation of the volume fraction of the self-compacting mortar and air within the L-Box test after 1,1 s (with fluid structure interaction)

The numerical modeling of the flowing process of self-compacting mortars and a Newtonian fluid with comparable viscosity was conducted using the L-Box test (see figure 1). To validate

the calculation results, these tests were evaluated using video recordings. It became obvious that the experiment delivered well reproducible results and that the chosen test setup and the evaluation by means of a special software were very well suited.

Despite a comparable viscosity, both fluids feature significantly different flow velocities. The flow velocity of a fluid is thus not determined by the viscosity alone. The numerical modeling with a commercial CFD-Code yielded good results for the Newtonian fluid. With respective modifications, also the flowing processes of the self-compacting mortar can be simulated. The next step will now be the expansion of the model by an additional phase, the coarse aggregate, in order to be able to simulate the flowing behavior of Self-Compacting Concretes.

Stephan Uebachs
RWTH Aachen University
Institute of Building Materials Research
Schinkelstrasse 3
D-52062 Aachen
Germany
uebachs@ibac.rwth-aachen.de

Wolfgang Brameshuber
RWTH Aachen University
Institute of Building Materials Research
Schinkelstrasse 3
D-52062 Aachen
Germany
brameshuber@ibac.rwth-aachen.de

BOND TEST CONCEPT FOR STRANDS IN POST-TENSIONED CONCRETE MEMBERS

Robert Ullner
ETH Zurich and Empa, Zurich, Switzerland
Peter Marti, Massoud Motavalli, Christoph Czaderski, Supervisors

So far, only limited research has been undertaken on the bond behaviour of strands in post-tensioned concrete members. New questions such as the need for temporary corrosion protection, the strength and stiffness evaluation of existing structures and the cutting of tendons require a more reliable knowledge of the bond behaviour. This contribution summarises experiences of a research project as part of which a series of 11 large-scale tests on post-tensioned concrete tension members with long embedment lengths was completed. The present paper provides an overview of the bond mechanics of strands, introduces the experimental concept and summarises the main results. Special emphasis is placed on a comparison of different experimental concepts such as bending tests, tension chord tests and pull-out tests, see Fig. 1.

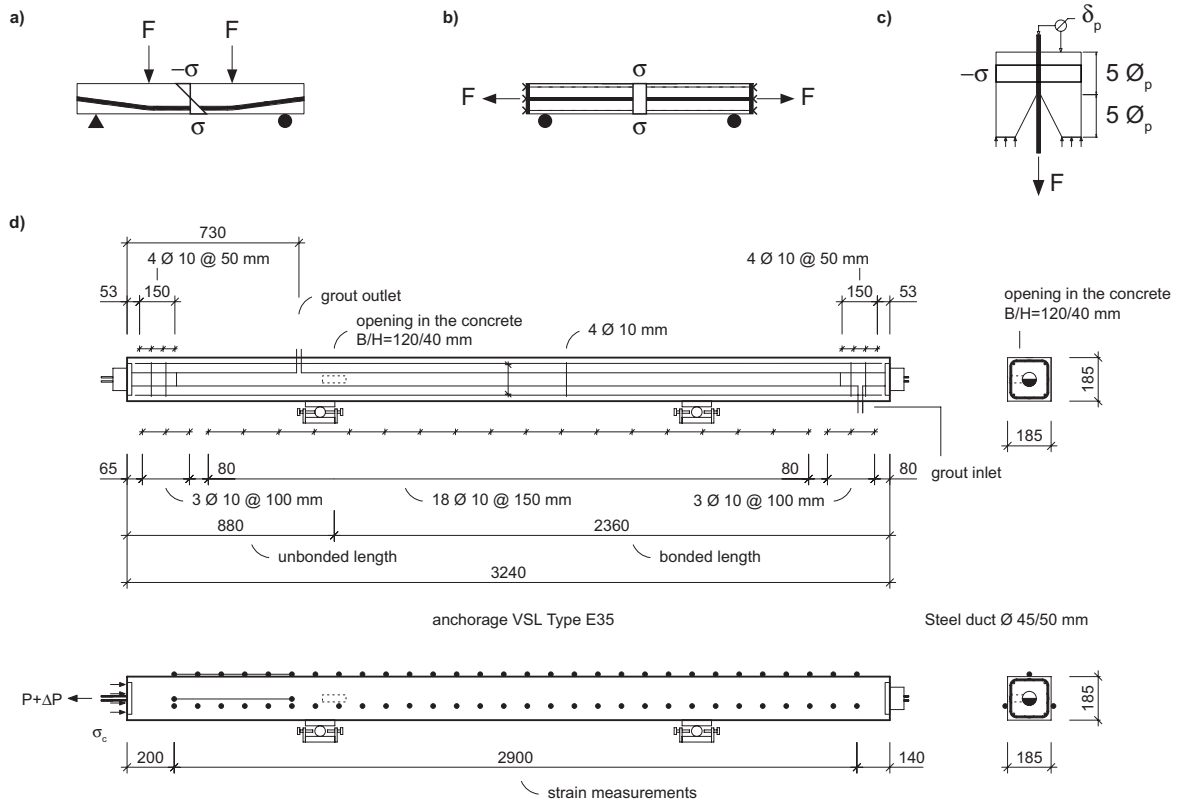

Figure 1 Experimental concepts for investigations of the bond behaviour of prestressing steel: (a) bending test; (b) tension chord member; (c) standard pull-out test; (d) new pull-out test specimen with long embedment length for the testing of tendons (example with three 0.6" strands)

Compared to non-prestressed and pre-tensioned steel the bond behaviour of post-tensioned steel is characterised by two additional components, i.e. the duct and the grout. This and the assembly of the wires of a strand result in a softer bond behaviour. For strand bundles the

bond mechanics are even more complex because the strands are interlocked and thus, higher bond shear stresses are activated, increasing the bond stiffness in comparison to single strands.

Different existing experimental methods, see Fig. 1(a), (b) and (c), were analysed to find an appropriate test concept for the testing of multi-strand tendons considering the bond mechanics of strands. A compromise between a cost-effective experiment, sophisticated bond mechanics and the identification of practical bond shear stress-slip relationships was found in a large-scale pull-out test with long embedment length, see Fig. 1(d).

The new test procedure was successfully applied for 11 experiments. The test procedure proved to be practical and could be further improved during the testing. The new pull-out test with long embedment length permits a direct determination of the bond length. The bond behaviour can be determined by measuring the concrete strains on the specimen surfaces and applying appropriate bond models. While standard pull-out tests are necessary they must be complemented by other tests to enable a comprehensive investigation of the structural behaviour.

Robert Ullner
ETH Zurich
Department of Civil, Environmental and Geomatic Engineering
Institute of Structural Engineering
Wolfgang-Pauli-Str. 15
CH-8093 Zurich, Zurich
ullner@ibk.baug.ethz.ch

Prof. Dr. Peter Marti
ETH Zurich
Department of Civil, Environmental and Geomatic Engineering
Institute of Structural Engineering
Wolfgang-Pauli-Str. 15
CH-8093 Zurich, Zurich
marti@ibk.baug.ethz.ch

Prof. Dr. Masoud Motavalli
Empa
Department Materials and Systems for Civil Engineering
Structural Engineering Research Laboratory
Ueberlandstr. 129
CH-8600 Duebendorf, Zurich
Masoud.Motavalli@empa.ch

Christoph Czaderski
Empa
Department Materials and Systems for Civil Engineering
Structural Engineering Research Laboratory
Ueberlandstr. 129
CH-8600 Duebendorf, Zurich
Christoph.Czaderski@empa.ch

CFRP STRENGTHENING OF TIMBER BEAMS

Ákos Varga
Budapest University of Technology and Economics, Budapest, Hungary
Zsuzsanna Józsa, Supervisor

Fibre reinforced polymer (FRP) composites can advantageously use to strengthen timber structures of historical monuments.
In the experimental program timber beams strengthened in flexure by CFRP (Carbon Fiber Reinforced Polymer) plates were tested. The beams were 1.0 m long spruce (Picea abies) elements with a cross-section of 73x75 mm. The specimens had a notch in the middle cross-section; the width of the notch was 4 mm, and height was 37.5 mm (half of the total height of the beam). With this notch a failure, a small deterioration, a local weak point was modelled. The main field of the experiment was whether the capacity of the original, full cross-section could be reached or eventually increased by FRP-strengthening.
The CFRP plates (cross section of 1.2 x 50 mm) were glued with epoxy resin on the bottom face of the beams. By six specimens the plates were longitudinally halved and were placed into longitudinal grooves made at both sides of the beam. These grooves were 25 mm wide and 4 mm thick and were placed 20 mm up from the bottom.
These two reinforcement types are shown in *Figure 1*. The bottom-face reinforcement (first type) was applied in 12 beams with three different lengths: 300, 600 and 800 mm. Unstrengthened control elements with notch in mid-spam and without any notch were also tested.

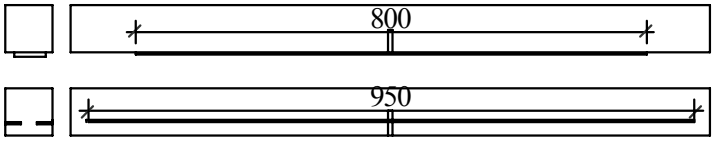

Figure 1 Reinforcement schemes

Four-point bending test was applied. The clear span was 900 mm; the loading points had a distance of 200 mm. (*Figure 2*) The deflection was measured at the middle cross-section. The load-deflection behaviour, the failure load and mode of failure were observed.

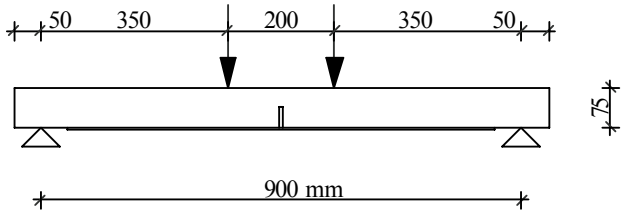

Figure 2 Test setup

Figure 3 Failure by the bending test

Table 1 presents a summary of the test results. Knots and local splits in the wood material influenced the ultimate load of the specimen and the place and mode of failure.
The strengthening with 800 mm long CFRP plate was the most effective solution: it has given an increase of 15% in ultimate load compared to the control element.
Figure 4 shows typical load-deflection curves for the different series. All specimens had a linear behaviour in the beginning. The failure occurred suddenly through a split in the wood and pealing-off of the CFRP plate by series 30K and 60K. The reinforcing could hold the beam together after the first local failure by series 80K and VK.

Table 1 Ultimate loads in kN, and the effect of strengthening

Mark	Reinforcement type	Min./Max. failure load	Average failure load	Effect
E	Control beam without notch	13.8 / 22.0	18.9	*100%*
EK	with notch in mid-spam	4.5 / 5.5	5.1	27%
30K	Bottom-faced, 300 mm	9.3 / 11.9	10.4	55%
60K	Bottom-faced, 600 mm	14.3 / 18.7	17.2	91%
80K	Bottom-faced, 800 mm	18.6 / 24.7	21.8	115%
VK	In grooves both side, 950 mm	14.6 / 19.0	16.9	89%

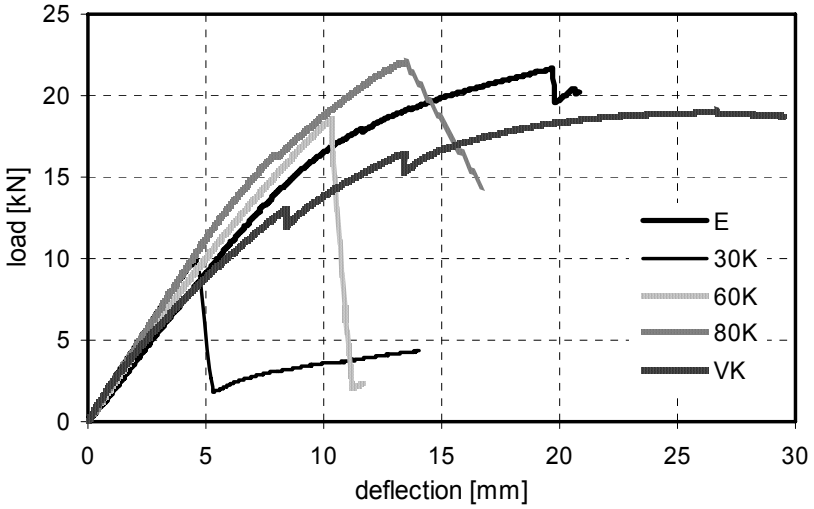

Figure 4 Typical load-deflection curves for the series

A model for the strengthened and unstrengthened beams was made with the AxisVM7 finite element software. The calculation of finite element model supported the results of the experiments. The highest tensile stresses could be observed at the ends of the CFRP strengthening.

The flexural CFRP strengthening has a bridging effect, the local failures cause no sudden failure, but the knots and splits also in case of CFRP plates influence the ultimate load of the specimen.

Ákos Varga
Budapest University of
Technology and Economics
Institute of Construction
Materials and Engineering
Geology
Műegyetem rkp. 3.
1111 Budapest, Hungary
v_akos@freemail.hu

Zsuzsanna Józsa PhD
Budapest University of
Technology and Economics
Institute of Construction
Materials and Engineering
Geology
Műegyetem rkp. 3.
1111 Budapest, Hungary
zsjozsa@epito.bme.hu

SHEAR STRENGTH OF RC BRIDGE DECK CANTILEVERS

Rui Vaz Rodrigues
Ecole Polytechnique Fédérale de Lausanne, Switzerland
Aurelio Muttoni, Supervisor

An experimental and theoretical investigation of the shear strength of reinforced concrete slabs without shear reinforcement is under way at the Ecole Polytechnique Fédérale de Lausanne. The first part of the program consists of 6 tests on two large scale bridge deck cantilevers (Figure 1). The specimens are tested under different configurations of concentrated forces simulating traffic loads. The observed failure mode is shear. The second part of the experimental program consists of shear tests on 12 slab strips, to investigate the influence of plastic hinge rotation on the shear strength. The test results show that the shear strength decreases with increasing plastic hinge rotation.

Figure 1: Full scale model of bridge deck cantilever (10.0 m length, 4.2 m width and 0.38 m maximal thickness)

The following conclusions can be made:

- Bridge cantilevers without shear reinforcement tend to fail in shear under concentrated loads.
- The ultimate flexural load predicted by the yield-line method was not reached for any of the six tests (Q_R/Q_{Flex} = 0.64 – 0.86).
- The measurements made of the slab thickness in the zone of shear failure indicate possible redistributions of the internal shear flow, with the progressive formation of shear cracks until equilibrium is no longer possible.
- The available results should contribute to a better understanding of shear and punching shear as similar phenomena.
- The tests on slab strips show that the shear strength of regions near plastic hinges decreases with increasing hinge rotation.

Detailed results are available at http://is-beton.epfl.ch/recherche/DalleRoulement/.

Rui Vaz Rodrigues
EPFL – ENAC –IS-BETON
Bât. GC
Station 18
CH-1015
Lausanne
Switzerland
rui.vazrodrigues@epfl.ch

Prof. Dr. Aurelio Muttoni
EPFL – ENAC –IS-BETON
Bât. GC
Station 18
CH-1015
Lausanne
Switzerland
aurelio.muttoni@epfl.ch

DESIGN METHODS FOR TEXTILE REINFORCED CONCRETE

Stefan Voss
RWTH Aachen University, Aachen, Germany
Josef Hegger, Supervisor

The use of high performance fibers as concrete reinforcement enables the production of thin lightweight elements with high durability and the possibility of economic savings. These advantages together with the high scope of design options given to the architects have made glassfiber-reinforced concrete (GFRC) a widespread building material around the world. A drawback of the reinforcement with chopped strands is the partial nondirectional distribution of the fibers over the total cross section, reducing their effectiveness. In contrast, Textile Reinforced Concrete (TRC) combines the advantages of both GFRC and ordinary steel reinforced concrete: no minimum concrete cover is required to protect the reinforcement against corrosion and the fiber material is placed only where necessary and in the direction of the tensile forces. This leads to a higher exploitation of the reinforcement material and better load-bearing properties of the component. The thickness of structural members primarily depends on the necessary concrete cover to ensure a proper anchorage of the reinforcement and to avoid a splitting failure.

A basic requirement for the successful application of a construction material is the availability of design methods. At RWTH Aachen University extensive test programs and theoretical investigations are currently being carried out with the objective of deriving design methods and improving the material properties. With the results of the investigations the production of first prototypes like only 25 mm thick façade elements and a diamond-lattice grid was possible, both demonstrating the enormous application potential of TRC.



Usually, the textile reinforcement is a two-dimensional fabric. The fabrics are made out of rovings which themselves consist of some hundreds to thousands of single fibers (filaments). At present alkali resistant glass (AR glass), carbon and aramid are the most favorable fiber materials. Depending on the mesh size, the stitching type and the roving thickness different fabric properties are arising. Specialized to certain applications other reinforcement geometries like spacer fabrics have already been produced.

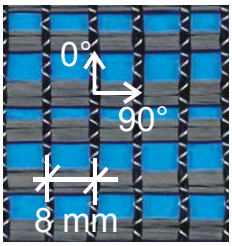

Carbon fabric

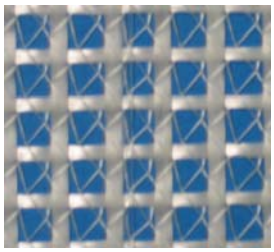

AR glass fabric

Spacer fabric

The load-bearing behavior of TRC is influenced by material properties, amount and alignment of the textile reinforcement. In particular the bond behavior of the textiles is important. The fiber material as well as the binding and the cross section of the roving have significant influence on the bond performance. Deviations between the direction of the tension forces and the rovings cause loss of strength mainly initiated by the actions on the filaments at the crack edges. Assuming that the loss of strength grows linearly with increasing angle between loading and roving direction results in good accordance with test results. The design models known from steel reinforced concrete cannot be applied without additional considerations. However, design models for the tension, bending and shear strength of TRC-elements have been derived by analogy with known models for steel reinforced concrete. The bending capacity of TRC-elements can be calculated by analogy with steel reinforced concrete with an additional factor considering the effects of the curvature of the beam. The shear capacity of beams made of TRC cannot be described by a pure truss model. An additional concrete contribution exists which is the capacity of the concrete compression zone. For the calculation of the truss contribution the angular change of the shear reinforcement has to be considered. Furthermore, if AR glass is used the deterioration of the fibers in the alkaline milieu has to be considered.

The author thanks the Deutsche Forschungsgemeinschaft (DFG) in context of the Collaborative Research Center 532 “Textile Reinforced Concrete - Development of a new technology” for its financial support.

Dipl.-Ing. Stefan Voss
RWTH Aachen University
Faculty of Civil Engineering
Institute of Structural Concrete
Mies-van-der-Rohe-Str. 1
D-52074 Aachen, Germany
svoss@imb.rwth-aachen.de

Univ.-Prof. Dr.-Ing. Josef Hegger
RWTH Aachen University
Faculty of Civil Engineering
Institute of Structural Concrete
Mies-van-der-Rohe-Str. 1
D-52074 Aachen, Germany
heg@imb.rwth-aachen.de

Proceedings-CD file name:
200_Wuest.pdf

STRUCTURAL BEHAVIOUR OF REINFORCED CONCRETE ELEMENTS IMPROVED BY LAYERS OF ULTRA HIGH PERFORMANCE REINFORCED CONCRETE

John Wuest
Ecole Polytechnique Fédérale de Lausanne(EPFL), Lausanne, Switzerland
Emmanuel Denarié, Eugen Brühwiler, Supervisors

Introduction

An increasing number of civil structures are in need of rehabilitation to address durability problems and to increase the load carrying capacity. Ultra-High Performance Fibre Reinforced Concretes (UHPFRC) are being used to rehabilitate existing structures because of their ease of on-site casting combined with their excellent strength and durability properties. The goal of this study was to investigate (1) the composite UHPFRC-concrete element early age deformational behaviour under a high degree of restraint and (2) the composite element structural response up to the ultimate force. The tested elements were 300 cm long, 100 cm high, and the UHPFRC layer thickness varied between 2.25 and 3.25 cm.

Conceptual approach

The conceptual approach is to use the UHPFRC locally to “harden” the existing concrete element where it is subjected to high mechanical and severe environmental actions.
The goal is thus to combine an existing (or also a newly constructed) reinforced concrete structure with UHPFRC layers located at high-stress zones rather than constructing a complete structure with only UHPFRC.

Material properties

Two UHPFRC compositions were tested. Two different materials, CM0 and CM11, each contained steel fibres with aspect ratios (length/diameter) of 50 and 33.3 respectively. CM11 has a higher fibre volume (10%) in comparison to CM0 6%. The uniaxial tensile tests on dog-bone shaped specimens showed that CM0 (value at peak ε = 0.073 %, σ = 9.7 MPa) has a pronounced strain hardening behaviour while CM11 (value at peak ε = 0.052%, σ = 8.4 MPa) exhibited an elastic-plastic yielding behaviour.

Early age measurements

The UHPFRC layers were cast in the vertical direction as if the elements were wall elements. During the early age, they were simply-supported with a 220 cm central span and 40 cm cantilevers and thus cured in a vertical position. The early age UHPFRC deformation was attributed to autogenous shrinkage. The measured values in four elements varied between –635 [μm/m] (at day 73) and –400 [μm/m] (at day 68). The appearance of fine microcracks (smaller than 0.1 mm), correlated with the deformational rate, was observed in the UHPFRC layers during the first 28 days. Thereafter, only a small number of microcracks formed. The microcracks tended to form at the wall upper edge or in the middle of wall, at the casting joint, and with only a few occurring in the wall bottom.

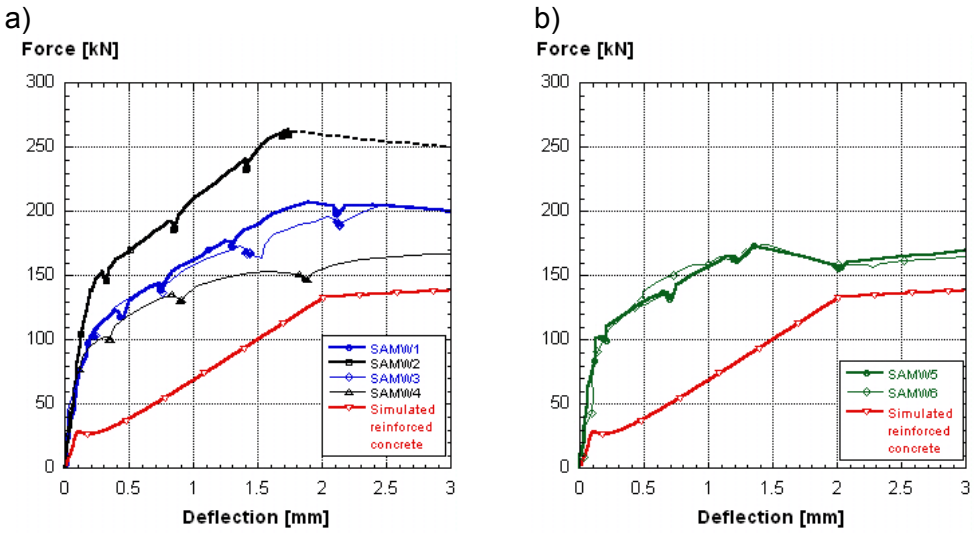

Figure 1 Detailed presentation of the wall element linear and non linear structural response a) SAMW1 to SAMW4 and b) SAMW5 and SAMW6.

Fracture testing

The composite elements were tested as a beam under bending rather than a wall under predominant normal force. A four point simply-supported bending system was employed inducing a constant negative bending moment in the element mid-span

The comparison (Figure 1a) and b)) between plain reinforced concrete element and UHPFRC-reinforced element shows that by adding the UHPFRC layers the resistance in the linear and non-linear pre-peak domain and the linear domain stiffness is significantly improved. The use of UHPFRC with short fibres offers an improved structural behaviour as compared to conventional reinforced concrete, but results show that the improvement is much smaller as compared to the elements reinforced with long fibres.

John Wuest
Ecole Polytechnique Fédérale
de Lausanne (EPFL)
Structural Institute – MCS
Station 18
Lausanne, Switzerland
john.wuest@epfl.ch

Eugen Brühwiler
Ecole Polytechnique Fédérale
de Lausanne (EPFL)
Structural Institute – MCS
Station 18
Lausanne, Switzerland
eugen.bruehwiler@epfl.ch

Proceedings-CD file name:
177_Ye.pdf

PROGRESSIVE FAILURE PROCESS OF ADHESIVELY BONDED JOINTS COMPOSED OF PULTRUDED GFRP

Ye Zhang
Ecole Polytecnique Fédérale de Lausanne, Lausanne, Switzerland
Thomas Keller, Supervisor

Adhesively bonded joints are being used increasingly in civil engineering, especially joints composed of pultruded GFRP laminates. Due to the complicated material architecture of pultruded composites, it is important to understand the failure mechanism of the joints under both static and cyclic loading, as well as the progressive failure process considering crack initiation and propagation.

In this paper, two types of specimens were investigated: balanced double lap joints (DLJ) and stepped lap joints (SLJ), both composed of pultruded GFRP laminates of 50 mm width and 6 or 12 mm thickness. The adhesive layer thickness was 2 mm. In each specimen, two back face strain gages were placed above the locations where crack initiation was expected to influence the strain response and two more strain gages were used to measure the axial strains outside the joint where the stresses were expected to remain uniformly distributed (see Fig. 1 (left)). Furthermore, two displacement transducers were employed to measure the elongation of the joint over the gage lengths. An Instron Universal 8800 hydraulic machine was used to apply the axial force with a displacement rate of 0.5 mm/min for the SLJs and of 1 mm/min for the DLJs. The specimens were loaded up to failure.

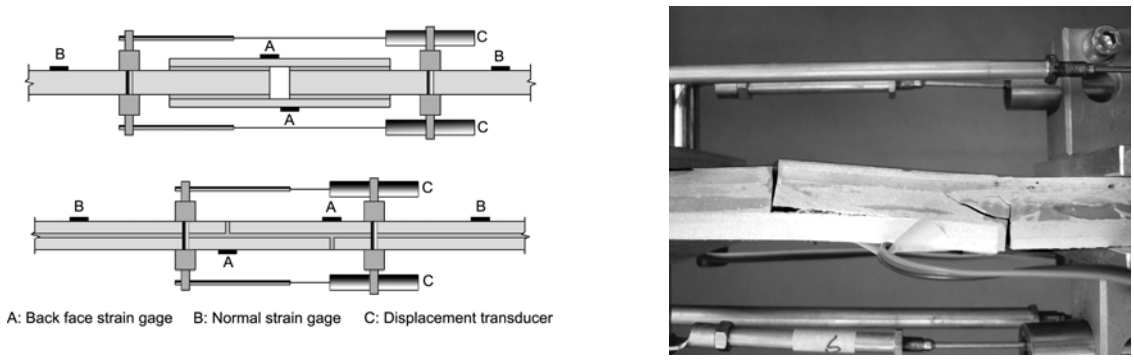

Figure 1 Experimental instrumentation (left) and failure mode (right) of SLJ joints.

The double lap joints had an almost linear load-elongation response up to the failure, which was very brittle. In contrast, the stepped lap joints exhibited a discontinuous two stage behavior, although the final failure was also brittle. For the SLJs, when the load reached 7.0 kN on average, a failure in the adhesive in the two small gaps perpendicular to the longitudinal adhesive layer occurred (see Fig. 1), which was followed by a steep decrease of the load. After this first failure, however, the joints continued to sustain an increase in load, although the crack initiation and propagation led to a decrease in overall stiffness. The average static ultimate loads of DLJs and SLJs were 45.6 kN and 10.5 kN respectively.

For both types of joints, the dominant failure mode was a fiber-tear-off failure in the GFRP laminates. Failure initiation occurred in the two outer mat layers of the 12 mm laminates below the ends of the outer 6 mm laminates in the DLJs, and in the 6 mm laminates below the (already cracked) small gaps in the SLJs. Failure propagation then occurred in the same

mat layers up to final joint failure. In some cases, cracks were observed even below the mat layers in the roving layer. Failures were brittle and sudden and their initiation and propagation were normally not observable by the naked eye, with the exception of some SLJs where approximately the first 20 mm of crack growth could be observed (see Fig.1).

Though the dominant failure mode of both types of joints was considered as very brittle it was still possible to observe the crack initiation using back face strain gages. Fig. 2 shows typical measured strains with increasing load for a DLJ and SLJ. While the normal strains in the DLJ remained almost linear up to ultimate load, the back face strains showed an offset at 30 kN due to stress redistribution after crack initiation. The back face strains for the SLJ were first influenced by the adhesive failure in the small joint gaps. After adhesive failure in the small gaps, the much higher eccentricity of the axial load in the new single lap joint configuration provoked bending moments that changed the sign of the back face strains from tension to compression. Subsequently, small offsets in the again increasing strain curves were measured, the first offset evidently being caused by the stress redistribution due to crack initiation in the laminate. Furthermore, the back face strains showed a high sensitivity to the initial stage of crack propagation up to approximately 6 mm crack length. Subsequently, the curves leveled off and approached an almost constant value when the crack started to propagate unstably.

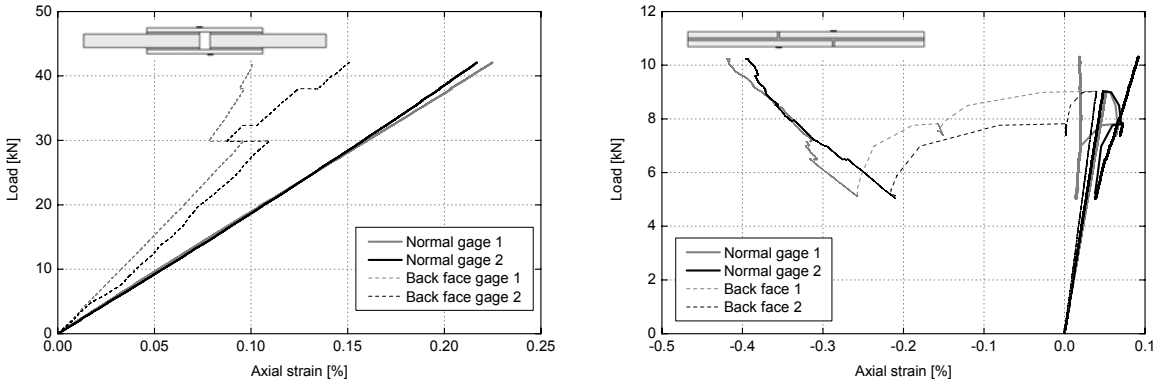

Figure 2 Measured back face strain versus load of typical DLJ (left) and SLJ (right).

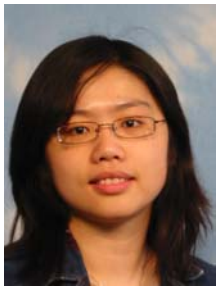

Ye Zhang
Ecole Polytecnique Fédérale de Lausanne
ENAC-IS Institute
Composite Construction Laboratory
BP Ecublens Station 16
Lausanne, Switzerland
ye.zhang@epfl.ch

Thomas Keller
Ecole Polytecnique Fédérale de Lausanne
ENAC-IS Institute
Composite Construction Laboratory
BP Ecublens Station 16
Lausanne, Switzerland
thomas.keller@epfl.ch

Authors index